

Synthesis and characterisation of chitosan based sponges for wound

dressings

by

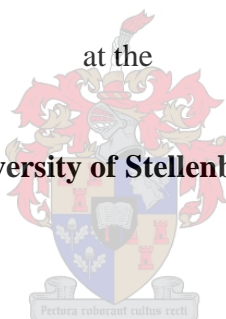
Taguma Matsvaire

Thesis presented in partial fulfilment of the requirements for the degree of

Master of Science

at the

University of Stellenbosch



Supervisor: Dr M Lutz

March 2017

Department of Chemistry and Polymer Science

DECLARATION

By submitting this thesis electronically, I declare that the entirety of the work contained therein is my own, original work, that I am the sole author thereof (save to the extent explicitly otherwise stated), that reproduction and publication thereof by Stellenbosch University will not infringe any third party rights and that I have not previously in its entirety or in part submitted it for obtaining any qualification.

Taguma Matsvaire

March 2017

Copyright © 2017 Stellenbosch University
All rights reserved

Abstract

The work presented in this study focused on the development of chitosan based sponges for the possible use as wound dressings. The sponges were to be modified to try and overcome some of the flaws associated with the use of natural polymers, that is, the poor mechanical properties. The important parameters that had to be met were a continuously porous morphology, to have a good absorption capability, good thermal properties, increase the mechanical strength and to maintain and/or increase the antimicrobial properties inherently in the chitosan.

The two crosslinking agents that were used in this study to crosslink the chitosan sponges were genipin and tannic acid (TA). These are both natural crosslinking agents as this provided a platform to create a possible non-toxic wound dressing. The mechanical properties of the chitosan sponges resulting from these two crosslinking agents were compared to that when a synthetic crosslinking agent, namely glutaraldehyde (glut), was used. In an attempt to further enhance the mechanical properties, microcrystalline cellulose (MCC) was incorporated into the sponges as a reinforcing agent.

The antimicrobial nature of a wound dressing is of high importance as it aids the healing processes in wounds. Certain properties that were imparted on the sponges by the different synthesis parameters were analysed in order to determine how to best enhance these properties as they play a vital role in the wound healing process.

The sponges were synthesized using the bubbling technique and freeze-drying. The temperature used during the synthesis was of importance as the interaction between the chitosan and the crosslinking agents differs at different temperatures. The time taken to crosslinking time allowed during synthesis of the sponges was also of significance as this variable also had an important influence on the resultant properties of the sponges.

The crosslinking of the sponges was confirmed using FTIR spectroscopy where the characteristic shifts and peaks that have occurred due to the crosslinking could be seen. These shifts are due to the chemical reactions that occur when the chitosan and the crosslinking agents react. The morphology of the sponges was determined using SEM where the porosity of the sponges could then be analysed and gave better understanding of some of certain other properties. The

homogeneous distribution of MCC in the chitosan sponges was confirmed using confocal microscopy. The thermal properties of all the sponges were investigated using TGA and DSC. The TGA and DSC results showed that the crosslinking using either genipin or TA improved the thermal properties of the sponges. Absorbance tests were done to determine the absorption properties of the sponges which were also improved by the crosslinking when using either one of the involved crosslinking agents. For testing of the mechanical strength, compressional tests were done and these showed that there was an increase in the strain percentage in comparison to the uncrosslinked sponges but was, however, less than those for the sponges crosslinked with glutaraldehyde.

The antimicrobial properties of the samples were analysed using the alamar assay technique. This assay showed that the antimicrobial properties were sensitive to crosslinking temperature, MCC loadings, Gramicidin S treatment and the crosslinking agent used. The samples crosslinked with genipin at 0.5 weight percent concentrations showed the greatest enhancement in antimicrobial properties.

Opsomming

Hierdie studie fokus op die ontwikkeling van chitosan gebaseerde sponse vir die moontlike gebruik as wondbedekkings. Die sponse is aangepas om te probeer om sommige van die tekortkominge wat verband hou met die gebruik van natuurlike polimere te oorkom, dit wil sê die swak meganiese eienskappe. Die belangrikste eienskappe waaraan voldoen moes word was 'n deurlopende poreuse morfologie, 'n goeie absorpsie vermoë, goeie termiese eienskappe, verhoogde die meganiese sterkte en handhawing en of verhoging van die antimikrobiese eienskappe inherent tot die chitosan.

Die twee kruisbindingsagente wat in hierdie studie gebruik was om die chitosan sponse te kruisbind, is genipin en tanniensuur (TA). Beide kruisbindingsagente is natuurlike verbindings aangesien dit 'n platform voorsien om 'n moontlike nie-toksiese wondbedekking te skep. Die meganiese eienskappe van die sponse wat met behulp van die twee kruisbindingsagente gesintetiseer is, is vergelyk met dié wat met behulp van 'n sintetiese kruisbindingsagent, naamlik glutaraldehyd (glut), gesintetiseer is. Om die meganiese eienskappe van die sponse verder te

versterk, is mikrokristallyne sellulose (MCC) in die sponse geïnkorporeer as 'n versterking van die agent.

Die antimikrobiese aard van 'n wondbedekking is van groot belang, aangesien dit die helende prosesse in wonde aanhelp. Sekere eienskappe wat aan die sponse oorgedra is deur middel van die verskillende sintese parameters is geanaliseer om sodoende te bepaal hoe om hierdie eienskappe die beste te verbeter, aangesien dit 'n belangrike rol speel in wondgenesing.

Die sponse is gesintetiseer deur middel van 'n borreltegniek en vries-droging. Die temperatuur tydens die sintese was van belang aangesien die interaksie tussen die chitosan en die kruisbindingsagente verskil by verskillende temperature. Die tyd wat dit neem om die monsters te kruisbind was ook van belang, aangesien dit ook 'n invloed het op die resulterende eienskappe van die sponse.

Die kruisbinding van die sponse is bevestig met behulp van FTIR spektroskopie waartydens die karakteristieke verskuiwings en pieke wat plaasgevind het as gevolg van die kruisbinding sigbaar geword het. Hierdie verskuiwings is die gevolg van die chemiese reaksies wat plaasvind wanneer die chitosan en die kruisbinding agente reageer. Die morfologie van die sponse is bepaal met behulp van SEM waartydens die porositeit van die sponse ontleed is en dit het 'n beter begrip van sommige van die ander eienskappe gebied. Die MCC is homogeen in die spons versprei en dit is bevestig met behulp van konfokale mikroskopie. Die termiese eienskappe is ondersoek met behulp van TGA en DSC. Die TGA en DSC resultate het getoon dat kruisbinding wat met behulp van genipin of TA plaasgevind het hierdie eienskappe verbeter het. Daar is absorpsie toetse gedoen om die absorberingseienskappe van die sponse wat ook verbeter word deur die kruisbinding te bepaal. Vir die meganiese sterkte, was saamdrukbaarheidsweerstand toetse gedoen en dit het getoon dat daar 'n toename was in die druk persentasie in vergelyking met die kruisgebinde sponse, maar was egter minder as dié van die sponse wat kruisgebind was met glutaraldehyde.

Die antimikrobiese eienskappe van die monsters is ontleed met behulp van die alamar toets tegniek. Hierdie toets het getoon dat die antimikrobiese eienskappe was sensitief vir temperatuur, MCC beladings, gramisidien S behandeling en die kruisbinding agent gebruik. Die kruisgebind met genipin monsters het die grootste toename in die antimikrobiese eienskappe op 0,5 gewig persent konsentrasies.

Acknowledgements

First and foremost, I would like to thank God for meticulously guiding me through this study and through life.

My utmost gratitude and appreciation goes to my supervisor, Dr. Maretjie Lutz, for your support, your encouragement, guidance and belief in me cannot fully be expressed in words.

I would like to thank my parents and my siblings, for making my being here possible and for the love, the continuous encouragement and the prayers.

I would also like to thank the staff members of the Department of Chemistry and Polymer Science especially Calvin Maart, Jim Motshweni, Deon Koen, Erinda Cooper and Aneli Fourie for their undying support during this study.

I would also like to thank the following people:

Wilma van Rensburg for her assistance with the antimicrobial tests, Dr Angelique Laurie for the SEM analysis, Dumisile Lumkwana for Confocal microscopy analysis and Roediger Agencies for the TGA analysis.

Prof Albert Van Reenen and the olefins family for the group meetings and the flurry of ideas that was shared throughout the study.

Friends, family and Katleho Bookholane for the support through the good and the bad times.

Table of contents

Abstract	iii
Opsomming.....	iv
Acknowledgements.....	vii
Table of contents.....	viii
List of figures.....	xii
List of tables.....	xv
List of abbreviations	xvi
Chapter 1: Introduction.....	1
1.1 Introduction	1
1.2 Aim and objectives.....	2
1.3 Layout of thesis	3
1.3.1 Chapter 1: Introduction.....	3
1.3.2 Chapter 2: History and theoretical background	3
1.3.3 Chapter 3: Experimental	3
1.3.4 Chapter 4: Chitosan and Chitosan-MCC based sponges	3
1.3.5 Chapter 5: Absorption and mechanical properties.....	3
1.3.6 Chapter 6: Antimicrobial results and analysis	4
1.3.7 Chapter 7: Conclusions and recommendations.....	4
1.4 References	5
2 Chapter 2: Theoretical background.....	6
2.1 Wound healing	6
2.2 Wound dressing.....	8
2.3 Polymeric materials used	10
2.3.1 Chitosan	11

2.3.2	Crosslinking	14
2.3.3	Genipin.....	15
2.3.4	Tannic acid.....	18
2.4	References	21
3	Chapter 3: Experimental	26
3.1	Introduction	26
3.2	Materials.....	26
3.3	Preparation of chitosan sponges	27
3.4	Preparation of genipin crosslinked sponges	27
3.5	Synthesis of tannic acid crosslinked sponges.....	28
3.6	Synthesis of Glutaraldehyde crosslinked sponges	28
3.7	Synthesis of microcrystalline cellulose (MCC) loaded sponges.....	28
3.8	Labelling of MCC	29
3.9	Characterization methods.....	29
3.9.1	Attenuated total reflectance – Fourier transform infrared (ATR-FTIR).....	29
3.9.2	Scanning electron microscopy (SEM)	29
3.9.3	Thermogravimetric analysis (TGA).....	30
3.9.4	Differential scanning calorimetry (DSC).....	30
3.9.5	Confocal fluorescence microscopy.....	30
3.9.6	Compressional tests	31
3.9.7	Absorption tests	31
3.9.8	Treatment of polymers with Gramicidin S	31
3.9.9	Alamar blue assay.....	32
3.9.9.1	Preparation of <i>Micrococcus luteus</i> :	32
3.9.9.2	Dose response	32

3.10	References	33
4	Chapter 4: Chitosan and chitosan-MCC sponges	33
4.1	Introduction	33
4.2	The effect of crosslinking time and temperature.....	34
4.3	Fourier Transform Infra-Red spectroscopy analysis.....	40
4.4	Scanning electron microscopy (SEM) analysis.....	44
4.5	Confocal microscopy results	48
4.6	Thermal gravimetric analysis results.....	50
4.7	Differential scanning calorimetry results	55
4.8	Conclusion.....	60
4.9	References	62
5	Chapter 5: Absorption and mechanical results	64
5.1	Introduction	64
5.2	Absorbance results analysis	64
5.3	Mechanical properties	67
5.4	Conclusions	70
5.5	References	71
6	Chapter 6: Antimicrobial results.....	72
6.1	Introduction	72
6.2	Antimicrobial results	72
6.3	Conclusions	84
6.4	References	86
7	Chapter 7: Conclusions and recommendations.....	87
7.1	Conclusions	87
7.1.1	Synthesis of chitosan based sponges and modifications.....	87

7.1.2	Morphological properties	87
7.1.3	Sponge characteristics.....	88
7.1.4	Antimicrobial properties	88
7.2	Recommendations	89

List of figures

Figure 2.1: Illustration of the key procedures in the healing process showing the fibrin clot that has inflammatory cells, fibroblasts and a dense capillary network of granulation. Epidermal reconstructions occur at the edge of the wound [1].	7
Figure 2.2: Structures of chitin (top) and chitosan (bottom) illustrating the difference being the amine group on the chitosan in place of an N-acetyl group in the chitin due to the deacetylation to form chitosan.	12
Figure 2.3: The different types of crosslinking possible with chitosan based structures. The first is based on electrostatic interactions or non-covalent crosslinking, the second based on coordination complex crosslinking with metals and the third based on covalent bonds [21].	15
Figure 2.4: The molecular structure of genipin	16
Scheme 2.1: Reaction between genipin and primary amine group [39]	17
Scheme 2.2: Second reaction of genipin with amine group [39]	17
Figure 2.5: Outline of the reaction between genipin and chitosan [58]	18
Figure 2.6: Molecular structure for tannic acid	19
Figure 4.1: Colour of genipin crosslinked sample left at room temperature for 4 hours on the left and 12 hours on the right	35
Figure 4.2: Migration of the bubbles from a) the tannic acid matrix and b) the genipin matrix ..	36
Figure 4.3: The effect of absence of air on the colour change of genipin crosslinking	37
Figure 4.4: Colour change after a) 1 hour, b) two hours and c) three hours in the oven for the genipin crosslinked samples	38
Figure 4.5: The deep blue colour obtained after 5 hours in the oven	39
Figure 4.6: Genipin crosslinked samples; a) which was left at room temperature for 11 hours and b) which was in the oven for 2 hours	39
Figure 4.7: FTIR spectra for the neat uncrosslinked chitosan and genipin crosslinked samples .	41
Figure 4.8: FTIR spectra of uncrosslinked and tannic acid crosslinked chitosan samples namely, Neat and TA respectively.....	43
Figure 4.9: Comparison of the morphologies for A, the uncrosslinked sample, B, genipin crosslinked sample and C, tannic acid crosslinked sample.....	45

Figure 4.10: SEM images for uncrosslinked samples with A no thermal treatment and B is thermally treated	46
Figure 4.11: SEM images for tannic acid crosslinked samples A, synthesized at room temperature and B synthesized at 60°C.	47
Figure 4.12: SEM images for genipin crosslinked samples A, before peptide treatment and B, after peptide treatment and oven drying.....	48
Figure 4.13: Confocal microscopy image showing A; Neat sample without labelled MCC, B; Chi/MCC sample with labelled MCC, C; Gen/MCC sample with labelled MCC and D; TA/MCC sample with labelled MCC	49
Figure 4.14: TGA graph above shows the neat uncrosslinked sample and the samples crosslinked with 5, 7.5 and 10mg of genipin.	50
Figure 4.15: TGA thermogram of the neat uncrosslinked sample and the samples crosslinked with 20, 50 and 80 mg of tannic acid labelled TA20, TA50 and TA80 respectively.	51
Figure 4.16: TGA thermogram of the neat uncrosslinked sample, uncrosslinked sample loaded with MCC, the genipin crosslinked sample loaded with MCC and the tannic acid crosslinked sample loaded with MCC labelled Neat, Chi/MCC, Gen/MCC and TA/MCC respectively.	53
Figure 4.17: TGA thermogram comparing the neat uncrosslinked sample, glut; the glutaraldehyde crosslinked sample, TA; the tannic acid crosslinked sample and the genipin crosslinked sample.	54
Figure 4.18: DSC thermograms of a) un-crosslinked chitosan sponge, b) 3 mg genipin crosslinked sample, c) 7.5 mg genipin crosslinked sample, d) 8 mg genipin crosslinked sample and e) 10 mg genipin crosslinked sample	56
Figure 4.19: DSC thermogram of a) neat un-crosslinked chitosan sponge, b) 20mg tannic acid (TA20) crosslinked sample, c) 50mg (TA50) crosslinked sample and d) 80mg (TA80) crosslinked sample	58
Figure 4.20: DSC thermogram of MCC loaded samples with a) neat uncrosslinked sample with no MCC, b) Chi/MCC sample, c) the TA/MCC sample and d) the Gen/MCC sample.....	59
Figure 6.1: Antimicrobial activity for the control and GS treated genipin crosslinked sponges..	74
Figure 6.2: Antimicrobial activity for the genipin crosslinked samples, MCC loaded samples and the neat uncrosslinked samples	75

Figure 6.3: Graph of the antimicrobial properties for the tannic acid crosslinked samples	77
Figure 6.4: Graph of antimicrobial properties of tannic acid crosslinked samples	78
Figure 6.6: Graph of antimicrobial activity of freeze-dried genipin crosslinked samples.....	82
Figure A. 1: FTIR spectra of chitosan sponges crosslinked with 3,5 and 8mg genipin	91
Figure A. 2: FTIR spectrum of chitosan sponges crosslinked with 20, 50 and 80mg TA.....	92
Figure B. 1: SEM images of glutaraldehyde crosslinked sponges at two magnifications	93
Figure B. 2: SEM images of genipin crosslinked samples with A and A1 – 3mg genipin sample; B and B1 – 5mg sample; and C and C1 – 10mg sample at different magnifications.....	94
Figure B. 3: SEM images of TA crosslinked sponges with A and A1 – TA80 sample; B and B1 – TA50 sample; and C and C1 – TA20 sample at different magnifications.....	95
Figure B. 4: SEM images of MCC loaded samples	96
Figure C. 1: Confocal Microscopy images of A – chitosan sponges without fluorescent MCC; B – uncrosslinked sample with fluorescent MCC; C – genipin crosslinked sample with fluorescent MCC; and D – TA crosslinked sample with fluorescent MCC	97
Figure C. 2: Confocal microscopy images showing the depth profile of fluorescent MCC loaded TA crosslinked chitosan sponges.....	98
Figure C. 3: Confocal microscopy images showing the depth profile of MCC loaded uncrosslinked chitosan sponges	99
Figure C. 4: Confocal microscopy images showing the depth profile of genipin crosslinked sample loaded with fluorescent MCC	100
Figure C. 5: Confocal microscopy images showing the depth profile of chitosan samples without labelled MCC	101
Figure E. 1: Comparison of the antimicrobial properties for the genipin crosslinked samples with A) the freeze – dried samples and B) the oven dried samples	104
Figure E. 2: Comparison of the antimicrobial properties for the TA crosslinked samples with A) the freeze – dried samples and B) the oven dried samples.	105

List of tables

Table 5.1: Absorbance results.....	65
Table D 1: Absorbance results.....	102
Table D 2: Mechanical properties results	103

List of abbreviations

A	Absorbance
ATR – FTIR	Attenuated total reflectance – Fourier transform infrared
Ca ²⁺	Calcium (II) ions
Chi/MCC	Chitosan – microcrystalline cellulose
CM	Confocal microscopy
CO ₂	Carbon dioxide
DSC	Differential scanning calorimetry
ECM	Extracellular matrix
FITC	Fluorescein isothiocyanate
Gen/MCC	Genipin – microcrystalline cellulose
Glut	Glutaraldehyde
GS	Gramicidin S
MCC	Microcrystalline cellulose
MTP	Microtitre plate
NaCl	Sodium chloride
NaHCO ₃	Sodium hydrogen carbonate
NaOH	Sodium hydroxide
PBS	Phosphate buffered saline
PGA	Poly (glycolic acid)
PLA	Poly (lactic acid)
rpm	Revolutions per minute
SEM	Scanning electron microscopy
TA	Tannic acid
TA/MCC	Tannic acid – microcrystalline cellulose
T _g	Glass transition temperature
TGA	Thermogravimetric analysis
W _i	Initial weight
W _f	Final weight
wt%	Weight percent

Chapter 1: Introduction

1.1 Introduction

The interest in the synthesis and characterisation of naturally occurring polymers has increased enormously in the last years, particularly in the biomedical field. This has been largely due to the unique properties that come with the use of these naturally occurring polymers when applied in biological systems. Naturally occurring polymers that are abundant, like cellulose and chitin, have been the targeted polymers for many studies due to their structures and their ability to be used in biological systems without causing any foreign body reactions [1, 2]. This is also important for the synthesis of materials that will interact in a positive way with tissue to allow for the regeneration of lost and/or injured tissue [3]. Some other naturally occurring polymers that have also been exploited for their desirable qualities due to their suitability in their representation of a structural cellular environment [3], include hyaluronic acid [4], silk fibroin [5], starch, collagen [6] and chitosan [7-9]. Chitosan is a derivative of chitin, the second most abundant naturally occurring polymer after cellulose, and has sparked a lot of interest due to it being capable of degrading in the body to form the building blocks of the body's tissues [8]. This biodegradability and the general structure of chitosan make it suitable for use and manipulation during the manufacturing process that allows for a wide range of end uses.

In this study, chitosan based sponges were prepared. These sponges may possibly serve as a stepping stone towards forming wound dressings for use in severe injuries that result in the loss of most and/or the whole skin layer and tissue. Chitosan was the backbone of the sponges and crosslinking agents were used to enhance the mechanical properties of the synthesized sponges as chitosan is known to be mechanically weak [10]. The resultant properties imparted from this crosslinking, using genipin and tannic acid as the crosslinking agents, were to be analysed and characterised to investigate their effect on the properties that are inherent to chitosan.

The production of the sponge was carried out using the freeze-drying method, which is a relatively simple method for the synthesis of the sponges.

1.2 Aim and objectives

The main aim of this study was to prepare sponges for the possible use as wound dressings in injuries where the whole layer of skin and/or some flesh has been lost. Chitosan was chosen as the polymer to synthesize these sponges and to be modified by means of crosslinking with agents that were selected based on their properties that would possibly enhance those inherent in chitosan. Chitosan is derived from nature and as such, the crosslinking agents selected were also obtained from natural sources, namely genipin and tannic acid. Once the sponges had been synthesized, their properties were to be analysed, that is, the effect the use of genipin and tannic acid as crosslinking agents, had on the inherent properties of chitosan and to determine how the parameters used during synthesis affected the end products. An antimicrobial peptide, namely Gramicidin S, was also incorporated into the sponges to determine if the properties of the sponges could be enhanced in terms of their antimicrobial efficacy.

The objectives of the project are therefore stated as follows:

- To synthesize chitosan based sponges with a porous structure obtained using the bubbling technique.
- To reinforce the chitosan based sponges using crosslinking agents, namely genipin and tannic acid (TA), and to compare their mechanical properties to those of glutaraldehyde crosslinked sponges.
- To determine the effect the crosslinking agents and the subsequent crosslinking would have on the antimicrobial, morphological, water absorption, mechanical and thermal properties of the chitosan sponges.
- To determine the effect of the time and temperature used during the synthesis of the sponges
- To evaluate the effect of introducing an antimicrobial peptide, namely Gramicidin S (GS), on the antimicrobial efficacy of the sponges.
- To examine the effect of incorporating microcrystalline cellulose (MCC) into the sponges, regarding the resultant properties of both the crosslinked and none crosslinked chitosan sponges.

1.3 Layout of thesis

1.3.1 Chapter 1: Introduction

Chapter 1 introduces the problem and identifies the aim and ultimately the suggested solutions in the form of objectives.

1.3.2 Chapter 2: History and theoretical background

This chapter is aimed at reviewing currently available literature and elucidating the reasons for this study. It contains an overview of the parent polymer, chitosan, and the crosslinking agents used in the synthesis of the sponges namely genipin and tannic acid.

1.3.3 Chapter 3: Experimental

In this chapter, the materials that were used for the synthesis of the uncrosslinked and crosslinked sponges are given. The procedures followed for the synthesis, incorporation of the MCC and the GS are also given in this chapter. The techniques that were used in the analysis and characterisation of the resultant sponges are also given in this chapter.

1.3.4 Chapter 4: Chitosan and Chitosan-MCC based sponges

This chapter focuses on the results that were observed during the synthesis of the various sponges using the two crosslinking agents, genipin and TA. This chapter also focuses on the characterisation of the resultant sponges.

1.3.5 Chapter 5: Absorption and mechanical properties

This chapter was focused on the physical properties of the sponges and looked at the absorbance and the compressional properties of the sponges. The effect the synthesis parameters had on these properties was analysed and reported.

1.3.6 Chapter 6: Antimicrobial results and analysis

The antimicrobial properties of the sponges are analysed in this chapter. The effect the synthesis parameters had as well as the effect of incorporating MCC and GS are also evaluated in this chapter.

1.3.7 Chapter 7: Conclusions and recommendations

In this chapter, the conclusions that were obtained from the study are summarised. Recommendations and suggested future work can also be found in this chapter.

1.4 References

1. Croisier F, Jerome C. Chitosan-based biomaterials for tissue engineering. *Eur Polym J* [Internet]. **2013**;49(4):780–92.
2. Jayakumar R, Prabakaran M, Kumar PTS, Nair S V, Tamura H. Biomaterials based on chitin and chitosan in wound dressing applications. *Biotechnol Adv* [Internet]. Elsevier Inc.; **2011**;29(3):322–37.
3. Silva SS, Motta A, Rodrigues MT, Pinheiro AFM, Gomes ME, Mano JF, et al. Novel genipin-cross-linked chitosan/silk fibroin sponges for cartilage engineering strategies. *Biomacromolecules*. **2008**;9(10):2764–74.
4. Liao E, Yaszemski M, Krebsbach P, Hollister S. Tissue-Engineered Cartilage Constructs Using Composite Hyaluronic Acid/Collagen I Hydrogels and Designed Poly(Propylene Fumarate) Scaffolds. *Tissue Eng* [Internet]. **2007**;13(3):537–50.
5. Vepari C, Kaplan DL. Silk as a biomaterial. *Prog Polym Sci*. **2007**;32(8):991–1007.
6. Aigner T, Stöve J. Collagens—major component of the physiological cartilage matrix, major target of cartilage degeneration, major tool in cartilage repair. *Adv Drug Deliv Rev*. **2003**;55(12):1569–93.
7. Francis Suh J-K, Matthew HW. Application of chitosan-based polysaccharide biomaterials in cartilage tissue engineering: a review. *Biomaterials*. **2000**;21(24):2589–98.
8. Griffon DJ, Sedighi MR, Schaeffer D V., Eurell JA, Johnson AL. Chitosan scaffolds: Interconnective pore size and cartilage engineering. *Acta Biomater*. **2006**;2(3):313–20.
9. Dash M, Chiellini F, Ottenbrite RM, Chiellini E. Progress in Polymer Science Chitosan — A versatile semi-synthetic polymer in biomedical applications. *Prog Polym Sci* [Internet]. Elsevier Ltd; **2011**;36(8):981–1014.
10. Muzzarelli R, El Mehtedi M, Bottegoni C, Aquili A, Gigante A. Genipin-Crosslinked Chitosan Gels and Scaffolds for Tissue Engineering and Regeneration of Cartilage and Bone. *Mar Drugs* [Internet]. Multidisciplinary Digital Publishing Institute; **2015** Dec 11 [cited 2016 Sep 25];13(12):7314–38.

2 Chapter 2: Theoretical background

2.1 Wound healing

The skin comprises of two main tissue layers namely, the keratinised stratified epidermis and the underlying layer of collagen rich dermal connective tissue that provides support and nourishment. The skin provides the body with a protective layer and therefore any damage to this layer needs immediate and effective reparation to protect the body from environmental elements [1]. The main reason for wound treatment is to close off the wound and to create a working, that is, capable of restoring the original functionality, and aesthetically appealing scar [2]. The temporary closure of the wound is achieved by the formation of a clot [1]. This closure is an attempt by the body to create a pseudo-skin layer to prevent microorganisms from affecting the healing processes at the wound site [3]. If the wound is infected by bacteria, the bacteria will retard the healing processes that take place at the wound site and results in sepsis [4]. Skin lesions usually take a couple of weeks to heal and when they do, they are usually not aesthetically appealing due to the collagen in the dermal layer being poorly reconstituted [1].

Severe wounds are those in the range of bedsores, ulcers and burn wounds and in these cases, a variety of steps have to be taken into consideration to treat them [4]. The wound healing process has been analysed and is said to go through an inflammation stage, a cell migration stage, an angiogenesis stage, a provisional matrix synthesis stage, a collagen deposition stage and a re-epithelialisation stage [5]. The image in Figure 2.1 illustrates the major processes involved in the healing of a wound and how a wound is ideally temporarily plugged by a fibrin clot.

Aoyagi *et al* also mentioned that the healing process constitutes multiple stages namely, an infectious stage, a necrosis stage, an agglutination stage, a proliferation stage and an epidermal formation stage [4]. The above processes define similar processes and state the procedures that should occur undeterred to result in the healing of the wound in short periods of time. The above processes and the desire to protect the wound from external organisms that slow down the healing process has resulted in the need for wound dressings whose purpose is to protect the wound from these organisms.

The need for an impeccable wound dressing is of great importance as this will aid the wound healing processes by quickening the healing as they can provide closure and protection from bacteria that retards healing. Wound dressings are also needed to reduce pain and irritation during the healing process as well as to help in the restoration of the damaged tissue [6, 7]. There is currently an abundance of wound dressings and this is largely due to the differences in the wounds and the methods in which they heal [6, 8, 9].

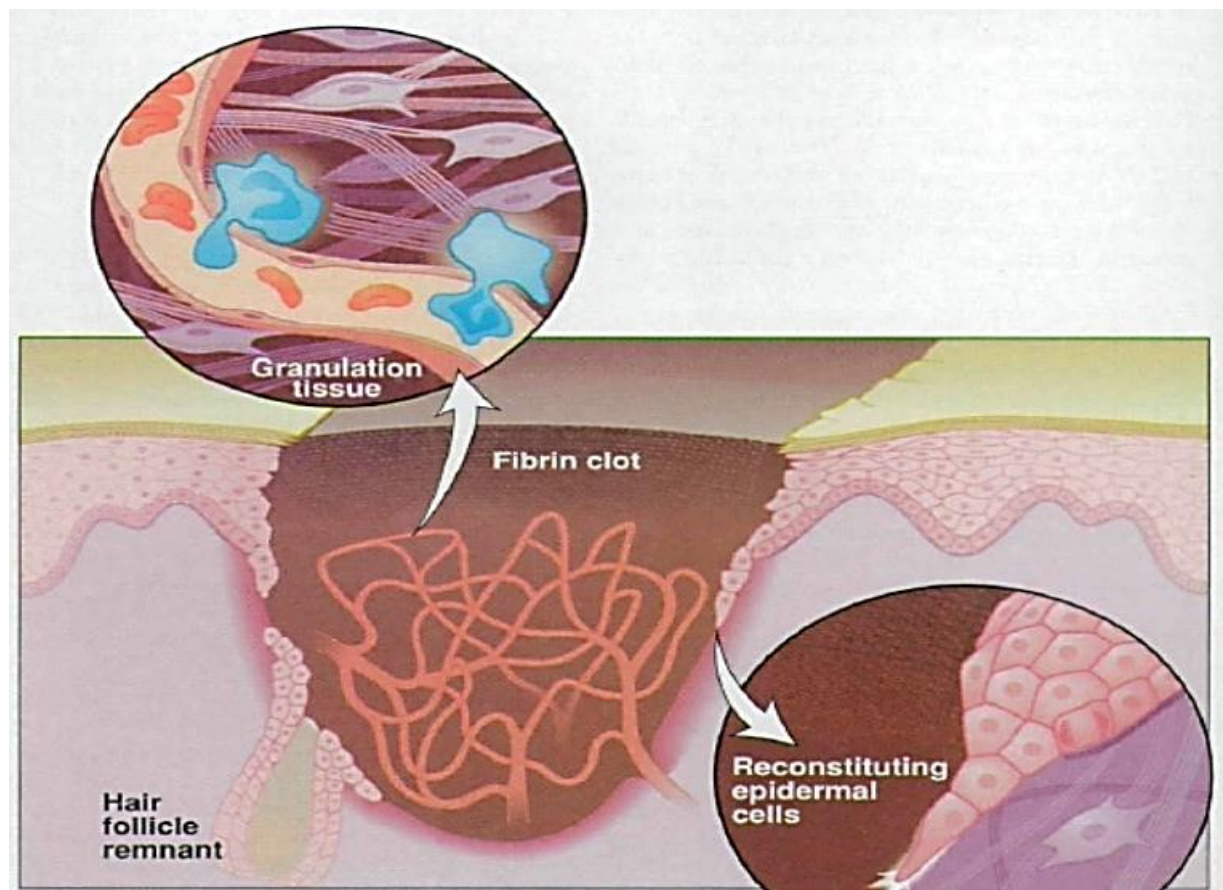


Figure 2.1: Illustration of the key procedures in the healing process showing the fibrin clot that has inflammatory cells, fibroblasts and a dense capillary network of granulation. Epidermal reconstructions occur at the edge of the wound [1].

An ideal wound dressing should be able to maintain desirable moisture levels at the wound boundary to prevent the surface from drying out. Oxygen permeation is required in the healing process and as such the wound dressing should have a good gaseous permeability. A good wound dressing should be able to prevent the penetration of microorganism and can remove the excess

exudates as the build-up of exudate can cause bacterial growth that ultimately slows down healing [3, 5]. Jayakumar *et al* also states that a wound dressing should be non-toxic, non-allergenic, non-adherent and easy to remove from the wound site without causing trauma and must be easily synthesizable from materials that are readily available and are bio-based and have antimicrobial properties [3]. The antimicrobial properties can enhance the healing process as well as to prevent bacterial proliferation and to kill bacteria that may have been present on the wound surface. The nontoxicity is of importance in that it prevents any secondary damage to the neonatal tissues and the body rejecting the materials used [5].

2.2 Wound dressing

The healing process is complex and as such several procedures can be carried out to assist the body in the reparation of damaged bodily tissues. This has sparked a lot of interest due to the complexity of these processes which has resulted in a lot of research on the improvement of the healing process being done. The processes involved in wound treatments have gone from the ancient methods which were based on the closure of the wound to prevent bleeding and environmental irritants from coming into contact with the wound, which is still the foundation of treatment, to the enhancement of the healing processes as the understanding of the processes involved has improved with time [3]. The management of wounds has generally been separated into different categories which are the loss of partial skin and the larger and more severe wounds where the full thickness of the skin and/or flesh has been lost or damaged. Membranes and thin films are then used for injuries where there is partial skin damage. For the larger and more severe wounds where the full thickness of the skin and/or flesh has been lost or damaged, scaffolds and spongy materials are more sought after for the treatment of these wounds [10]. This is largely due to the ability of the cells that are responsible for proliferation being able to organise their extracellular matrix in a three-dimensional structure which acts as a support. This is the main driving force in designing a structure that is capable of supporting this cellular behaviour [11].

A number of biopolymers can be synthesized into high water content absorbing and low interfacial tension compounds, namely, gels [12]. Gels have the capability of reducing the number of times a dressing is applied to the affected area as well as reduce the application and/or the amount of drugs to be administered [13]. When the gels are synthesized from biocompatible polymers, they also

possess the advantage of being able to be assimilated by the body [12, 14]. This has the benefit of improving the patients' reception of the wound treatments. Chitosan based gels have been used as mucosal delivery systems due to their ability to improve retention times on oral mucosa as well as the controlled release of drugs [13]. The release of drugs from gels and other microparticles synthesized from chitosan is largely dependent on the pH as this has an effect on the solubility of the gels [15]. The ease at which chitosan forms gels has also been exploited in the use to block the absorption of cholesterol and lipids in the intestines as it can form gels that traps the lipids and cholesterol [16].

Nanofibrous materials have also been showing remarkable possibilities in the synthesis of sensors, membranes and biomedical applications, biosensing, tissue engineering and wound dressings [17]. The nanofibers can be used as wound dressings and are of key importance in that they provide high surface to volume ratio, an oxygen permeable structure and a morphology similar to that of the extracellular matrix (ECM) in the skin [3, 17]. There are a large number of techniques used in the synthesis of these nanofibers such as electrospinning, phase separation and self-assembly method which result in multiple and unique properties [3]. The field has attracted a lot of attention with new organic and inorganic materials being synthesized as nanocomposites [18]. These composites usually comprise of nanofillers that aid in the end use functionality of the products [18].

Films based on biopolymers have also gained interest due to their potential to replace the conventional petrochemical and/or other non-biodegradable materials in a variety of applications [19]. Polysaccharides, proteins and lipids have thus been the main focus for this replacement as they occur naturally. Of these possible alternatives, polysaccharides are in abundance and are capable of forming films in an easy manner [19]. These films have been studied for the use as wound dressings with the primary focus being their barrier and mechanical properties as polysaccharides are known to have poor mechanical and barrier properties in film form [19, 20]. The use of films and porous membranes is generally for the use in wounds that have the skin tissue damaged and require a more two-dimensional shape [21].

Scaffolds and sponges, when synthesized from biomaterials, have been used for a variety of applications but have particularly been used in tissue engineering where they are needed to replace

the skin and/or hard tissue [22, 23]. These materials are required to meet set parameters for the application as wound dressings. These parameters include the maintenance of a moist wound surface, to conform to the surface and to cover the surface of the wound well. This coverage is important as it prevents air pockets from forming due to this ultimately resulting in a build-up of exudate that causes bacterial growth at the wound surface [24]. In the case of replacing hard tissue, the material should be able to support osteogenic tissue and have osteoconductive properties [23]. Chitosan has been a candidate for these materials as it is known to accelerate the healing of wounds and the regeneration and bone formation [22].

The synthesis of biopolymer based sponges is brought about by ice crystal growth in the matrix upon freezing and the subsequent removal of the water in the matrix by lyophilisation [25]. The structure can also be brought about by adding bubbles to the matrix, using reagents that react with the media in the matrix and freezing the bubbles within the structure and subsequent lyophilisation [10]. The microstructure of the resultant product, along with the crystallinity and mechanical strength, can be altered to suit specific end uses by adjusting the freezing rate, the amount of the bubbling agent and changing the concentrations of the matrices used [10, 25].

2.3 Polymeric materials used

Recent years have seen a rise in the interest for naturally occurring products and this has trickled to the polymeric world particularly to replace petrochemical products which aren't renewable. The likes of starch, collagen, gelatin, cellulose and chitin, to mention a few, are in their abundance and are naturally occurring which makes them candidates for the replacement of fossil based polymers [21, 26]. There is however, a challenge when it comes to obtaining the same properties that are attainable using synthetic polymers when using biomaterials from a functional point of view [21]. The mechanical properties of the synthetic materials produced from petrochemicals are significantly higher than those of the biopolymers [27]. This has led to researchers investing time towards trying to develop methods to try and synthesize materials that resemble their synthetic counterparts as this would result in much "greener" products.

It has been shown that the structures that are present in many biological organisms are those that make up matrices that are held together by fibrous biopolymers and this was found to be an

exploitable property [27]. The addition of fillers to these matrices would add some stability to these matrices as reinforcement and as such research has been focused on the reinforcement with several fillers.

2.3.1 Chitosan

The meteoric rise in biomaterial studies for the use in biomedical applications led to the interest in chitin and its derivatives as they are derived from nature and increase the metabolic processes during healing [3]. A variety of other polymers have been tested for use in wound dressings such as polylactic (PLA) and polyglycolic acids (PGA). These however, showed undesirable results in that they induced a foreign body reaction when they degraded into their by-products [11]. PGA was also unable to integrate with neighbouring tissue [11]. Chitosan on the other hand is a natural aminopolysaccharide and degrades to form neutral and weak sugars that are the building blocks of glycosaminoglycan's [3, 11, 28-31].

Chitosan stands out in that its intrinsic properties are unique and are valuable due to its properties that are not found in petrochemicals. These inherent properties are the reason behind chitosan being used directly for biological applications [21]. Chitosan is derived from the second most abundant natural polymer, chitin, is of low cost and has been used for a large number of applications that include solids, compressible materials and haemostatic agents since 2003 [32]. Chitosan is mucoadhesive, has haemostatic properties, is antimicrobial, bioabsorbable, biodegradable, antifungal, analgesic and nontoxic [3, 5, 10, 14, 18, 28, 33-40]

The structure of chitin, poly (β -(1-4)-N-acetyl-D-glucosamine, is similar to that of cellulose with the difference being the acetamido (-NHCOCH₃) at the C-2 position and not the hydroxyl group which is present in cellulose [24, 38, 41, 42]. Chitosan, which can also be referred to as 2-amino-2-deoxy- β -glucans, is produced by the deacetylation of chitin in alkaline conditions and at high temperatures [24, 41, 42]. The deacetylation procedure however, does not reach completion and as such the deacetylation degrees vary from anything between 30 and 95% [24, 30].

Upon deacetylation, the ratio of the glucosamine and the N-acetyl glucosamine will give the degree of deacetylation [30]. Figure 2.2 shows the structures of chitin and chitosan and from these structures the difference and the origin of the deacetylation degree is clear. Chitosan and chitin

can also be synthesized from the fermenting of fungi [24, 43, 44]. The molecular weight of the resultant chitosan, depending on its origin as it highly dependent on the source and ranges from 300 to 1000 kD [30].

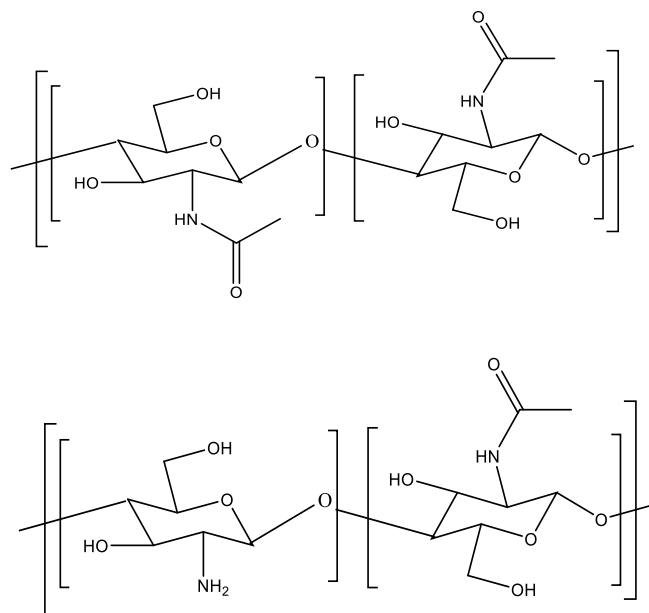


Figure 2.2: Structures of chitin (top) and chitosan (bottom) illustrating the difference being the amine group on the chitosan in place of an N-acetyl group in the chitin due to the deacetylation to form chitosan.

The biocompatibility and enzymatic degradation of chitosan has resulted in the extensive use of chitosan in the biomedical field [12]. The N-acetyl glucosamine present in chitosan is of value as it is responsible for tissue repair due to it the N-acetyl being a major component of dermal tissue. When chitosan is dissolved in acidic media, the free amine groups present on the surface of the polymer are protonated ($-\text{NH}_3^+$) and gives it a cationic nature [24, 25, 29, 45, 46]. This cationic nature gives chitosan the ability to support cell growth and assists in the coagulation of blood so as to induce blood clotting at the surface of the wound [5]. This is largely due to the cationic amine groups forming polyelectrolyte complexes with the acidic groups in blood [5, 21, 29].

The chemical nature of the chitosan, that is, the tertiary structure of the surface, is responsible for the necessary properties which allow it to bind with plasma proteins and specific subsets of platelet surfaces and proteins that are responsible for the accelerated fibrin gel formation when the platelet integrin's come into contact with plasma protein saturated chitosan surfaces [41]. Research has

also shown that the use of chitosan is capable of reducing the serum cholesterol levels in the body and can also boost the immune system [24].

The use of chitosan shows an increment in the healing processes at a molecular and cellular level. Chitosan is capable of providing a three dimensional matrix that allows tissue to grow and activates macrophages and the killing of tumor cells [3]. The use of chitosan also results in the red blood cell cohesion, thrombin production and fibrin mesh synthesis in the environment immediately around the chitosan [41]. The haemostatic properties allow blood clot formation and the blockage of nerve endings which results in less pain. Cell growth and the histoarchetectural tissue organisation have been shown to be stimulated by chitosan [3].

The cationic nature of the chitosan is also responsible for the interference with anionic residues of macromolecules at the cell surface by presumably competing for calcium ions (Ca^{2+}) for electronegative locations on the surface of the membranes without causing stability which then causes the membranes to become leaky [40]. Chitosan has also been shown to prevent the growth of various fungi, yeasts and bacteria [40]. The depolymerisation of the chitosan within the wound also results in the release of N-acetyl- β -D-glucosamine, which is the initiator of fibroblast proliferation. This subsequently leads to organised collagen deposition which ultimately stimulates the production of natural hyaluronic acid which helps in the prevention of scarring and contributes to faster recovery [3].

When chitosan is used in the wound environment, it is known that it undergoes some deacetylation which is due to enzymatic action which affects cell adhesion. Research has however shown that this does not result in a foreign body reaction and there is accelerated angiogenesis and the tissue granulation is normal [30]. Chitosan has an antimicrobial nature and this is further enhanced by its ability to cause neutrophil migration and activity [11]. These properties result in an immunomodulatory influence, which is the modification of the immune systems response, which in turn causes the material and the host to integrate [30].

A variety of naturally occurring polymers, the likes of agarose, gelatine, collagen, alginate and chitosan, to name a few, have been given a lot of attention due to their functionality and their desirable biological application properties. The aforementioned polymers are highly sought after due to their advantageous properties that are being biocompatible and biodegradable but, however,

these polymers all tend to be mechanically weak and have to be altered for end use purposes. Various efforts by researchers have shown that the physicochemical properties of chitosan can be modified by crosslinking or by combining with other polymers to attain a functional end product [47]

2.3.2 Crosslinking

Crosslinking is achieved when a crosslinking agent successfully bonds to two ends of polymeric chains, usually from two different polymer chains or the same chain depending on its orientation in space. In biological systems, the crosslinking process has been done by using formaldehyde, glutaraldehyde, dialdehyde starch and epoxy compounds [48]. Crosslinking can also be attained physically, that is, without forming a chemical link but by having interactions between the polymer chains and the crosslinking agent. This is possible due to the formation of hydrogen bonds and hydrophobic interactions to name a few [21]. These are relatively highly cytotoxic and as a result, the use of naturally occurring crosslinking agents so as to produce biocompatible materials has been of primary importance in the biomedical field [48]. The most widely used crosslinking agent has been glutaraldehyde particularly in the fixation of biological tissue. Due to its toxic properties that causes the stiffening of biological tissues, fibrosis and calcification, there has been a shift to other options [49].

The crosslinking of chitosan has been achieved using both physical and chemical associations [21]. The physical interactions are those that are generally reversible due to them not being connected covalently and these include hydrogen bonding, electrostatic interactions and hydrophobic interactions [21, 50, 51]. This is whereby a metal ion is used to form these coordination bonds between the chitosan polymeric chains thereby giving it a more stable structure. Electrostatic interactions have also been used to crosslink chitosan based materials along with physical methods that involve heating, but this has been avoided due to the possibility of degrading the polymer systems at high temperatures [21]. The following image, Figure 2.3, is a simplistic illustration of some of the interactions that are possible between chitosan polymeric chains and the crosslinking material used.

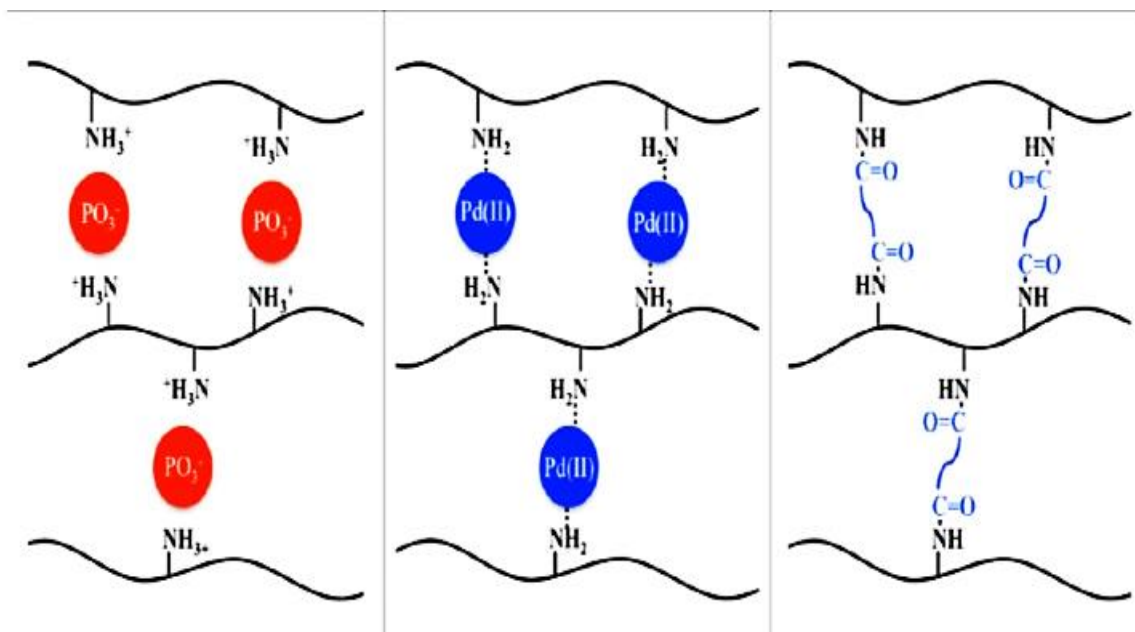


Figure 2.3: The different types of crosslinking possible with chitosan based structures. The first is based on electrostatic interactions or non-covalent crosslinking, the second based on coordination complex crosslinking with metals and the third based on covalent bonds [21].

There is an abundance of materials that have been applied in the crosslinking of chitosan based materials and this has been due to the presence of the primary amine groups that are found on the chitosan structure. These amine groups are very reactive and as such make it possible for a variety of crosslinking agents to react with the chitosan by either a Schiff base reaction or a Michael addition reaction [20, 29, 47, 52-54].

2.3.3 Genipin

The need for a non-toxic and biocompatible crosslinking agent resulted in research going in the direction of applying and using biocompatible crosslinking agents [48]. As such, interest for the naturally occurring crosslinking agent, genipin, was sought after due to its known reactivity with natural polymeric materials that have free amino groups present in their structures [12]. Genipin is also capable of forming stable structures and materials when reacted with chitosan and as such was seen as a valid alternative for toxic crosslinking agents such as glutaraldehyde and formed a biocompatible material after their reaction [48]. The use of genipin, as shown in literature, resulted in a much lower calcium content and less inflammation in comparison to glutaraldehyde and this suggested the formation of products with biocompatibility [12, 49].

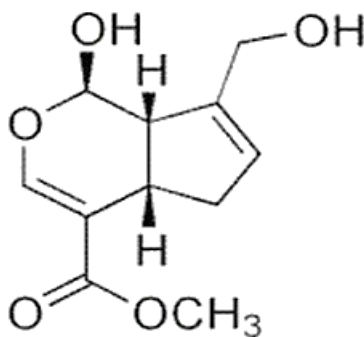


Figure 2.4 : The molecular structure of genipin

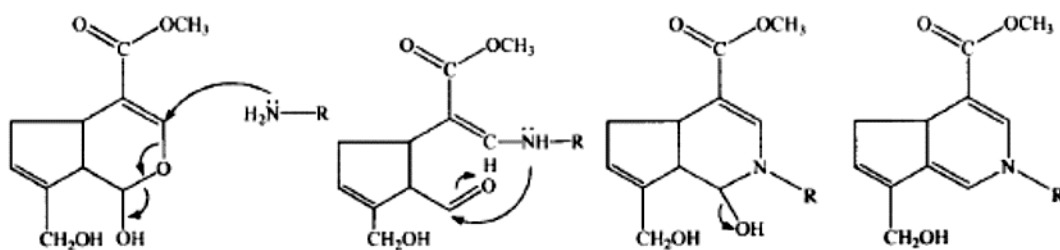
Genipin is obtained from geniposide which is a parent compound obtained from *Gardenia Jasminoides* Ellis and has been used for numerous years in the treatment of inflammation, jaundice, headaches, edema, fevers, hepatic disorders and hypertension [48, 55]. These properties have provoked interest in the use of genipin as it is also capable of crosslinking chitosan and other proteins that contain primary amine groups particularly gelatine and soya [39]. The extracts from the *Gardenia Jasminoides* have been known to react with primary amines in the presence of oxygen and form brilliant blue pigmented products which have been used as food colouring [39].

Early observations of the dimerization of genipin in the presence of glycine led to the idea that genipin could be used to react with proteins with residual primary amine groups thereby crosslinking by means of the formation of covalent bonds [39]. Further research has also shown that genipin crosslinked tissue was capable of resisting enzymatic degradation to the same extent that glutaraldehyde was capable of [48]. Genipin has since been used for the fixation of tissue, drug delivery systems and in foodstuff due to its crosslinking properties [39]. The research done on the toxicity of genipin has shown that the toxicity of glutaraldehyde is 5000 to 10000 times more toxic and this markedly lower toxicity make it the better choice in the synthesis of biocompatible materials [39, 56].

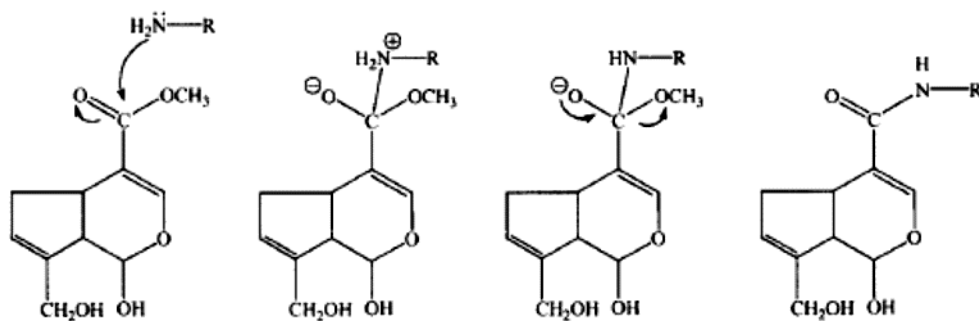
Genipin has the capacity to relieve, and in some instances, prevent, inflammation when applied to a wounded area and has been used as cholagogues, that is, as an agent to promote the discharge of bile from the system, usually by ingesting it as a herbal medicine [55, 56]. Pharmacological activity that includes the prevention of oxidative damage and fibrolytic and cytotoxic behaviour has been confirmed in past research [55]. Furthermore, the prevention of apoptosis after being absorbed and

transforming the growth factors responsible by interfering with their mitochondrial permeability transitions, their anti-inflammatory properties and the protection of hippocampal neurons [55].

The reactivity of the genipin with the chitosan has been studied and the reactions that take place in the presence of primary amine groups containing materials, show that the reaction results in the formation of covalent bonds [36, 38, 39, 57]. The formation of the covalent bonds with chitosan and other primary amine containing compounds is believed to occur via two reactions that occur on two positions of the genipin molecule and is illustrated in the schemes illustrated below.



Scheme 2.1 : Reaction between genipin and primary amine group [39]



Scheme 2.2 : Second reaction of genipin with amine group [39]

The resultant of the two reactions illustrated in Scheme 2.1 and in Scheme 2.2 above, when used to crosslink chitosan results in the genipin crosslinked chitosan structure that is shown in Figure 2.5. This will result in a much more mechanically apt material due to the covalent bond created.

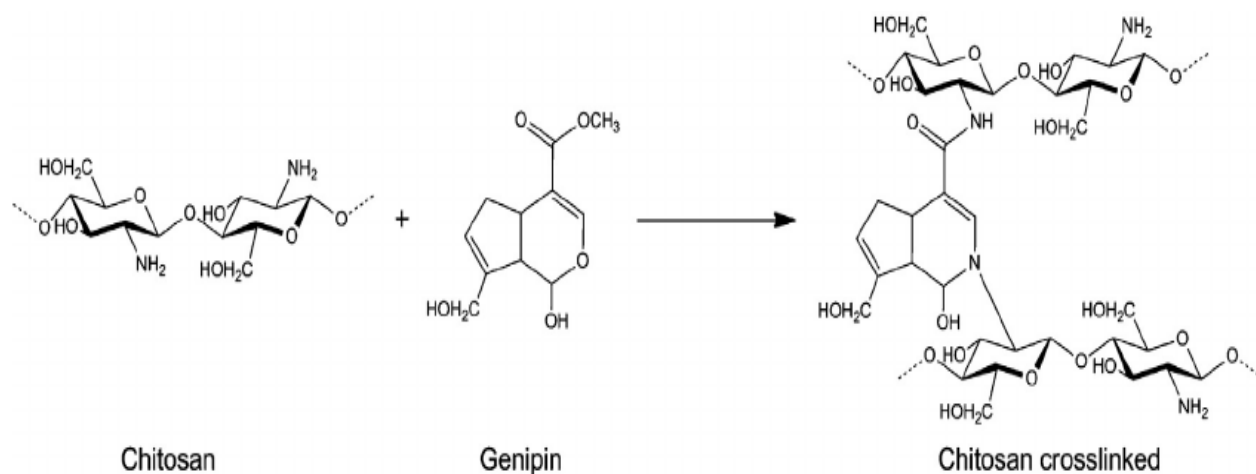


Figure 2.5: Outline of the reaction between genipin and chitosan [58]

The above properties are the main reasons genipin was studied for the crosslinking of the chitosan sponges as it is biocompatible and biodegradable. However, there was need to compare the properties of genipin as a crosslinking agent with another biocompatible and biodegradable crosslinking agent and in this study, we focused on the use of tannic acid as it has been used for many years in the medicinal field and more importantly in wound treatment.

2.3.4 Tannic acid

Tannic acid is a collective name for the materials responsible for turning putrefiable skin into leather that is not liable to degradation [59]. Tannic acid is common in vegetables and is mostly found in the barks of trees. Polyphenols that are between 500 and 3000 D Mw are considered to be a part of the vegetable tannins [18, 59]. The tanning process is largely based on the crosslinking between collagen fibrils in their matrices and is the same process that occurs in denatured protein in burnt skin [59]. Tannic acid is also responsible for the crosslinking that occurs between lipids and protein complexes thereby coagulating the remainder of the dermis resulting in the formation of a leather like painless eschar [59].

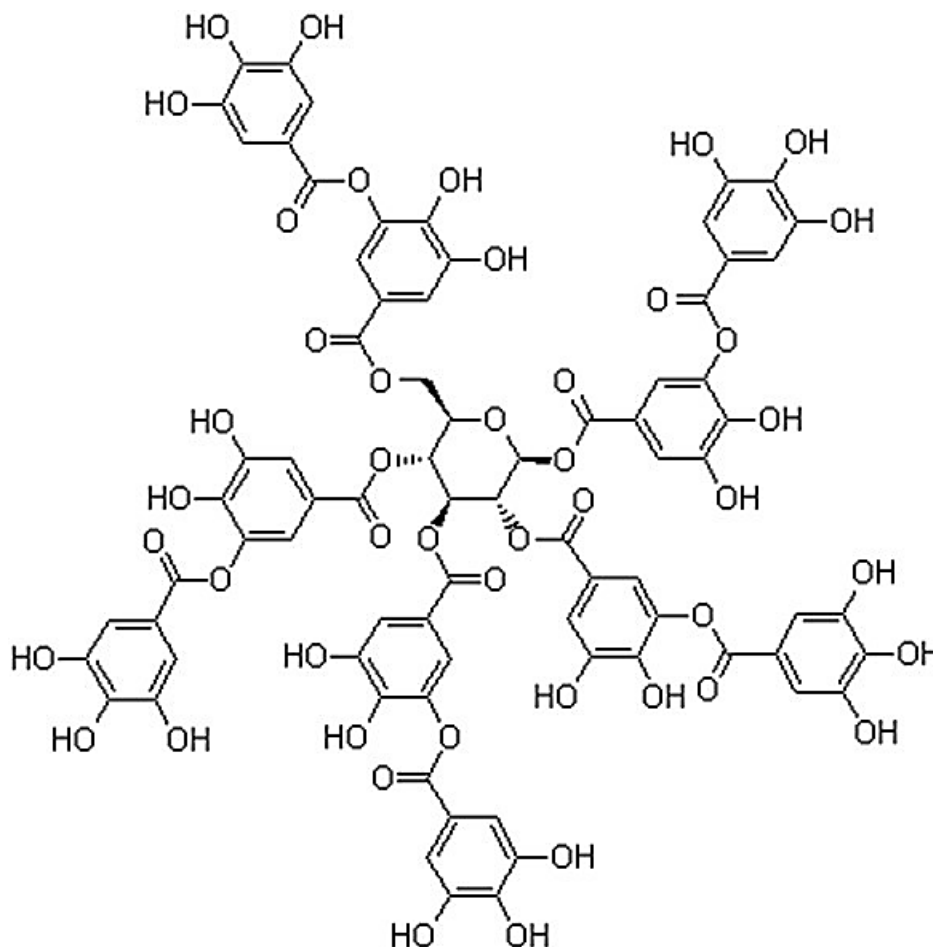


Figure 2.6: Molecular structure for tannic acid

The use of tannic acid dates back to the Neanderthal era where burn wounds were treated with plant extracts and over the years Chinese medicine has perfected its use in this regard [60]. Davidson's publication in 1925 resulted in the widespread use of tannic acid in western medicine in the subsequent years to follow [59]. During the years of the second world war, the use of the tannic acid was thought to be causing infection as it was leading to necrosis of the liver [59, 60]. These findings resulted in a drop in the use of tannic acid in the years that followed due to fears of this necrosis. Research that was done in later years showed that the reason the tannic acid that was used was causing necrosis was because it was impure and was mainly due to gallic acid [59, 60].

Tannic acid is found in the galls of *Rhus* and *Quercus* species and can be considered as an antioxidant, antimicrobial, antiviral, anti-inflammatory agent and causes the contraction of skin cells and other body tissues [60]. The family to which it belongs is the galloyl-glucose family and these are polyphenols [18, 60]. Plant polyphenols have been sought after as viable substitutes for

the use as crosslinking agents to replace toxic aldehyde crosslinking agents. Tannic acid comprises of a glucose backbone with the hydroxyl groups usually on the glucose substituted with five di-gallic acid groups [60]. These polyphenols are known to contain hydroxyl and /or other groups with one or two appearing every 100D and thus makes them capable of crosslinking. The classification of tannic acid that is used in medicinal applications is Gallotannin and specifically the Chinese tannin [18]. It has also been shown that tannic acid is capable of forming multiple bonds with proteins that are rich in α -amino acids [61].

Due to a significant rise in the interest and attention to three dimensional structures for the use in the medical field, there has also been a rise in the interest for the use of biopolymeric systems in this field. However, biopolymers are known to be unstable in biological systems as they can be degraded by enzymatic action on them and hence the use of crosslinking agents is the go to in order to circumvent this enzymatic attack. Work done trying to synthesize these three dimensional structures has shown that in the absence of a crosslinking agent, the resultant materials were unable to maintain the moisture at the surface that is required for healing processes [60]. Tannic acid became classified as an active biological molecule after research on the enhancements it had attributed to collagen and elastin had been researched from the category of vegetable tanning agents in the leather industry [60]. As such tannic acid was a viable option for this study for monitoring how it would affect the properties of the resultant chitosan sponges that were to be synthesised.

2.4 References

1. Martin P, Martin P. Wound Healing — Aiming for Perfect Skin Regeneration. **2014**;75(1997):75–82.
2. a, Dam, S J, Inger, M.D., and, et al. Inter- Leukin-1, Transforming Growth Factor. *N Engl J Med.* **1999**;341:738–46.
3. Jayakumar R, Prabakaran M, Kumar PTS, Nair S V, Tamura H. Biomaterials based on chitin and chitosan in wound dressing applications. *Biotechnol Adv . Elsevier Inc.;* **2011**;29(3):322–37.
4. Aoyagi S, Onishi H, Machida Y. Novel chitosan wound dressing loaded with minocycline for the treatment of severe burn wounds. *Int J Pharm.* **2007**;330(1–2):138–45.
5. Archana D, Dutta J, Dutta PK. Evaluation of chitosan nano dressing for wound healing: Characterization, in vitro and in vivo studies. *Int J Biol Macromol . Elsevier B.V.;* **2013**;57:193–203.
6. Morgado PI, Lisboa PF, Ribeiro MP, Miguel SP, Simões PC, Correia IJ, et al. Poly(vinyl alcohol)/chitosan asymmetrical membranes: Highly controlled morphology toward the ideal wound dressing. *J Memb Sci . Elsevier;* **2014**;469:262–71.
7. Ribeiro MP, Espiga A, Silva D, Baptista P, Henriques J, Ferreira C, et al. Development of a new chitosan hydrogel for wound dressing. *Wound Repair Regen . Blackwell Publishing Inc;* **2009** ;17(6):817–24.
8. Weller C, Sussman G. Wound Dressings Update. *J Pharm Pract Res.* **2006** ;36(4):318–24.
9. Alves A, Pinho ED, Neves NM, Sousa RA, Reis RL. Processing ulvan into 2D structures: Cross-linked ulvan membranes as new biomaterials for drug delivery applications. *Int J Pharm.* **2012**;426(1):76–81.
10. Chen C, Liu L, Huang T, Wang Q, Fang Y. Bubble template fabrication of chitosan/poly(vinyl alcohol) sponges for wound dressing applications. *Int J Biol Macromol . Elsevier B.V.;* **2013**;62:188–93.
11. Griffon DJ, Sedighi MR, Schaeffer D V., Eurell JA, Johnson AL. Chitosan scaffolds: Interconnective pore size and cartilage engineering. *Acta Biomater.* **2006**;2(3):313–20.
12. Mi FL, Shyu SS, Peng CK. Characterization of ring-opening polymerization of genipin and pH-dependent cross-linking reactions between chitosan and genipin. *J Polym Sci Part A Polym Chem.* **2005**;43(10):1985–2000.
13. Şenel S, İkinci G, Kaş S, Yousefi-Rad A, Sargon MF, Hincal AA. Chitosan films and

- hydrogels of chlorhexidine gluconate for oral mucosal delivery. *Int J Pharm.* **2000**;193(2):197–203.
14. Muzzarelli R, El Mehtedi M, Bottegoni C, Aquili A, Gigante A. Genipin-Crosslinked Chitosan Gels and Scaffolds for Tissue Engineering and Regeneration of Cartilage and Bone. *Mar Drugs* . Multidisciplinary Digital Publishing Institute; **2015** ;13(12):7314–38.
 15. Oungbho K, Müller BW. Chitosan sponges as sustained release drug carriers. *Int J Pharm.* **1997**;156(2):229–37.
 16. Koide SS. Chitin-chitosan: Properties, benefits and risks. *Nutr Res.* **1998**;18(6):1091–101.
 17. Mirzaei E, Faridi-majidi R, Shokrgozar MA, Asghari F. Genipin cross-linked electrospun chitosan-based nanofibrous mat as tissue engineering scaffold. **2014**;1(3):137–46.
 18. Liu BS, Huang TB. Nanocomposites of genipin-crosslinked chitosan/silver nanoparticles - Structural reinforcement and antimicrobial properties. *Macromol Biosci.* **2008**;8(10):932–41.
 19. Rubentheren V, Ward TA, Chee CY, Nair P, Salami E, Fearday C. Effects of heat treatment on chitosan nanocomposite film reinforced with nanocrystalline cellulose and tannic acid. *Carbohydr Polym.* **2016**;140:202–8.
 20. Rivero S, García MA, Pinotti A. Crosslinking capacity of tannic acid in plasticized chitosan films. *Carbohydr Polym.* **2010**;82(2):270–6.
 21. Croisier F, Jerome C. Chitosan-based biomaterials for tissue engineering. *Eur Polym J* . **2013**;49(4):780–92.
 22. Park YJ, Lee YM, Lee JY, Seol YJ, Chung CP, Lee SJ. Controlled release of platelet-derived growth factor-BB from chondroitin sulfate-chitosan sponge for guided bone regeneration. *J Control Release.* **2000**;67(2–3):385–94.
 23. Seol Y-J, Lee J-Y, Park Y-J, Lee Y-M, Young-Ku, Rhyu I-C, et al. Chitosan sponges as tissue engineering scaffolds for bone formation. *Biotechnol Lett.* **2004**;26:1037–41.
 24. Denkbas EB. Perspectives on: Chitosan Drug Delivery Systems Based on their Geometries. *J Bioact Compat Polym.* **2006**;21(4):351–68.
 25. Nettles DL, Elder SH, Gilbert JA. Potential Use of Chitosan as a Cell Scaffold Material for Cartilage Tissue Engineering*. *TISSUE Eng.* **2002**;8(6).
 26. Liu X, Ma L, Mao Z, Gao C. Chitosan-Based Biomaterials for Tissue Repair and Regeneration. In Springer Berlin Heidelberg; **2011**p. 81–127.
 27. Rubentheren V, Ward TA, Chee CY, Tang CK. Processing and analysis of chitosan nanocomposites reinforced with chitin whiskers and tannic acid as a crosslinker. *Carbohydr Polym.* **2015**;115:379–87.

28. Ravi Kumar MN. A review of chitin and chitosan applications. *React Funct Polym* . **2000**;46(1):1–27.
29. Dash M, Chiellini F, Ottenbrite RM, Chiellini E. Progress in Polymer Science Chitosan — A versatile semi-synthetic polymer in biomedical applications. *Prog Polym Sci* . Elsevier Ltd; **2011**;36(8):981–1014.
30. Di Martino A, Sittinger M, Risbud M V. Chitosan: A versatile biopolymer for orthopaedic tissue-engineering. *Biomaterials*. **2005**;26(30):5983–90.
31. Kreuter J. Nanoparticles and microparticles for drug and vaccine delivery. *J Anat*. **1996**;189 (Pt 3:503–5.
32. Dowling MB, Smith W, Balogh P, Duggan MJ, MacIntire IC, Harris E, et al. Hydrophobically-modified chitosan foam: Description and hemostatic efficacy. *J Surg Res* . Elsevier Inc; **2015**;193(1):316–23.
33. Portero A, Teijeiro-Osorio D, Alonso MJ, Remun-Lopez C. Development of chitosan sponges for buccal administration of insulin. *Carbohydr Polym*. **2007**;68(4):617–25.
34. Xu Y, Du Y. Effect of molecular structure of chitosan on protein delivery properties of chitosan nanoparticles. *Int J Pharm* . **2003** ;250(1):215–26.
35. Moura LIF, Dias AMA, Leal EC, Carvalho L, Sousa HC De, Carvalho E. Acta Biomaterialia Chitosan-based dressings loaded with neurotensin — an efficient strategy to improve early diabetic wound healing. *Acta Biomater. Acta Materialia Inc.*; **2014**;10(2):843–57.
36. Harris R, Lecumberri E, Heras A. Chitosan-genipin microspheres for the controlled release of drugs: Clarithromycin, tramadol and heparin. *Mar Drugs*. **2010**;8(6):1750–62.
37. Rinaudo M. Chitin and chitosan: Properties and applications. *Prog Polym Sci* . **2006**;31(7):603–32.
38. Dimida S, Demitri C, De Benedictis VM, Scalera F, Gervaso F, Sannino A. Genipin-cross-linked chitosan-based hydrogels: Reaction kinetics and structure-related characteristics. *J Appl Polym Sci* . **2015**;132(28)
39. Butler MF, Ng YF, Pudney PDA. Mechanism and kinetics of the crosslinking reaction between biopolymers containing primary amine groups and genipin. *J Polym Sci Part A Polym Chem*. **2003**;41(24):3941–53.
40. Bégin A, Van Calsteren MR. Antimicrobial films produced from chitosan. *Int J Biol Macromol*. **1999**;26(1):63–7.
41. Busilacchi A, Gigante A, Mattioli-Belmonte M, Manzotti S, Muzzarelli RAA. Chitosan stabilizes platelet growth factors and modulates stem cell differentiation toward tissue regeneration. *Carbohydr Polym* . Elsevier Ltd.; **2013**;98(1):665–76.

42. Jayakumar R, Menon D, Manzoor K, Nair S V., Tamura H. Biomedical applications of chitin and chitosan based nanomaterials - A short review. *Carbohydr Polym* . Elsevier Ltd.; **2010**;82(2):227–32.
43. Suntornsuk W, Pochanavanich P, Suntornsuk L. Fungal chitosan production on food processing by-products. *Process Biochem*. **2002**;37(7):727–9.
44. Nwe N, Chandkrachang S, Stevens WF, Maw T, Tan TK, Khor E, et al. Production of fungal chitosan by solid state and submerged fermentation. *Carbohydr Polym*. **2002**;49(2):235–7.
45. Allouche FN, Guibal E, Mameri N. Preparation of a new chitosan-based material and its application for mercury sorption. *Colloids Surfaces A Physicochem Eng Asp* . Elsevier B.V.; **2014**;446:224–32.
46. Silva MC, Andrade CT. Evaluating conditions for the formation of chitosan/gelatin microparticles. *Polímeros* ; **2009** ;19(2):133–7.
47. Garnica-Palafox IM, Sánchez-Arévalo FM. Influence of natural and synthetic crosslinking reagents on the structural and mechanical properties of chitosan-based hybrid hydrogels. *Carbohydr Polym*. **2016**;151.
48. Tsai CC, Huang RN, Sung HW, Liang HC. In vitro evaluation of the genotoxicity of a naturally occurring crosslinking agent (genipin) for biologic tissue fixation. *J Biomed Mater Res* . **2000**;52(1):58–65.
49. Sung HW, Liang IL, Chen CN, Huang RN, Liang HF. Stability of a biological tissue fixed with a naturally occurring crosslinking agent (genipin). *J Biomed Mater Res*. **2001**;55(4):538–46.
50. Nadège Boucard, Christophe Viton and, Domard* A. New Aspects of the Formation of Physical Hydrogels of Chitosan in a Hydroalcoholic Medium. *American Chemical Society* ; **2005**;
51. Berger J, Reist M, Mayer J., Felt O, Gurny R. Structure and interactions in chitosan hydrogels formed by complexation or aggregation for biomedical applications. *Eur J Pharm Biopharm*. **2004**;57(1):35–52.
52. Monteiro OA., Airoidi C. Some studies of crosslinking chitosan–glutaraldehyde interaction in a homogeneous system. *Int J Biol Macromol*. **1999**;26(2):119–28.
53. Zhang ZQ, Pan CH, Chung D. Tannic acid cross-linked gelatin-gum arabic coacervate microspheres for sustained release of allyl isothiocyanate: Characterization and in vitro release study. *Food Res Int* . Elsevier Ltd; **2011**;44(4):1000–7.
54. Muzzarelli RAA. Chitins and chitosans for the repair of wounded skin , nerve , cartilage and bone. *Carbohydr Polym* . Elsevier Ltd; **2009**;76(2):167–82.

55. Koo H-J, Lim K-H, Jung H-J, Park E-H. Anti-inflammatory evaluation of gardenia extract, geniposide and genipin. *J Ethnopharmacol* . **2006**;103(3):496–500.
56. Mi F-L, Shyu S-S, Peng C-K. Characterization of ring-opening polymerization of genipin and pH-dependent cross-linking reactions between chitosan and genipin. *J Polym Sci Part A Polym Chem* . Wiley Subscription Services, Inc., A Wiley Company; **2005**;43(10):1985–2000.
57. Delmar K, Bianco-Peled H. The dramatic effect of small pH changes on the properties of chitosan hydrogels crosslinked with genipin. *Carbohydr Polym*. **2015**;127:28–37.
58. Kondejewski LH, Farmer SW, Wishart DS, Kay CM, Hancock REW, Hodges RS. Modulation of Structure and Antibacterial and Hemolytic Activity by Ring Size in Cyclic Gramicidin S Analogs *. **1996**;271(41):25261–8.
59. Hupkens P, Boxma H, Dokter J. Tannic acid as a topical agent in burns: historical considerations and implications for new developments. *Burns*. **1995**;21(1):57–61.
60. Natarajan V, Krithica N, Madhan B, Sehgal PK. Preparation and properties of tannic acid cross-linked collagen scaffold and its application in wound healing. *J Biomed Mater Res - Part B Appl Biomater*. **2013**;101(4):560–7.
61. Isenburg JC, Simionescu DT, Vyavahare NR. Tannic acid treatment enhances biostability and reduces calcification of glutaraldehyde fixed aortic wall. *Biomaterials*. **2005**;26(11):1237–45.

3 Chapter 3: Experimental

3.1 Introduction

Chitosan is a biopolymer that has gained a lot of attention due to its admirable properties for the use in biological systems that range from ingestion, wound dressings and for organ regeneration [1-3]. Chitosan is biocompatible, biodegradable and has antimicrobial properties that makes it an interesting option for the use as a medical material. Chitosan is also a low cost polymer and is abundant as it is derived from the second most abundant natural polymer, chitin, which only comes in second after cellulose [4]. The study of polysaccharide based materials is of significance in that the by-products of their degradation have the possibility of bioresorption [5].

It is known that the mechanical properties of chitosan are not as good as synthetic polymers and as such there is need to crosslink the polymer to give it better strength during its application [3]. As such, glutaraldehyde has been used in past papers to crosslink chitosan based materials along with other aldehyde based materials and epoxy crosslinking agents [6]. The shift to using naturally occurring crosslinking agents saw a surge in the last couple of years and as such more and more focus is given to natural products [7].

This study is focused on the synthesis of chitosan based sponges for the use as wound dressings for wounds where the full thickness of the skin and/or some flesh is lost. The sponges will comprise of varying concentrations of crosslinking agents and their properties as a result of this variation in the crosslinking agent concentration analysed. Three crosslinking agents were compared in this study, namely glutaraldehyde, genipin and tannic acid and were used as will be shown in this chapter.

3.2 Materials

The materials used in this study were used as received from the manufacturers and were of a high grade.

- Chitosan – medium molecular weight, deacetylated chitin; Poly D(glucosamine), deacetylation degree: 75 – 85%

- Sodium hydrogen carbonate (NaHCO_3) ACS reagent, Merck
- Genipin $\geq 98\%$ (HPLC) powder, SIGMA ALDRICH
- Tannic acid (Gallotannin, Tannin) ACS reagent, SIGMA ALDRICH
- Glutaraldehyde solution – assay $\sim 50\%$ in water (5.6M), SIGMA ALDRICH
- Microcrystalline cellulose (MCC) - VIVAPUR101, JRS Pharma

3.3 Preparation of chitosan sponges

The synthesis of the chitosan sponges was carried out using 3 main procedures namely:

1. Dissolution
2. Bubbling
3. Freeze drying

The dissolution of the chitosan was carried out by dissolving 2 g of chitosan powder in 1% acetic acid (v/v) solution to form a 2% (w/v) chitosan solution. The solution was then left stirring for 24 hours at room temperature at a stirring speed of 250 rpm. After 24 hours, sodium hydrogen carbonate was added to the solution to form bubbles within the matrix and was further stirred for an hour. Once the sodium hydrogen carbonate (NaHCO_3) had formed uniform bubbles, the solution was then frozen using liquid nitrogen in order to maintain the porous structure that is as a result of the bubbles and then dried on a VirTis Sentry 2.0 freeze drier. The chitosan sponges that were formed after the freeze-drying step were white in colour.

3.4 Preparation of genipin crosslinked sponges

For the synthesis of genipin crosslinked sponges, the dissolution and bubbling steps were carried out as stated above, however, after the bubbling step, the resultant mixture was then crosslinked. This was achieved by adding varying amounts of genipin, that is, 1 mg, 2 mg, 3 mg, 5 mg, 8 mg and 10 mg to each individual solution. The solution was then further stirred for 10 minutes to allow distribution of the crosslinking agent within the matrix. The solution was allowed to crosslink at room temperature or at 60 °C with the two temperatures crosslinking after different time intervals. The sample that were left to crosslink at room temperature took 10 hours or more to crosslink and the samples placed in an oven at 60 °C took 5 hours. This was done so as to aid the crosslinking

process as leaving the matrix at room temperature would take too long and result in the bubbles escaping from the matrix. After 5 hours, the samples were taken out of the oven and allowed to cool to room temperature before being frozen in liquid nitrogen and subsequently freeze dried.

3.5 Synthesis of tannic acid crosslinked sponges

The synthesis of the tannic acid crosslinked samples was carried out by dissolution, bubbling followed by the addition of tannic acid in concentrations of 20 mg, 40 mg, 50 mg, 60 mg, 80 mg, 125 mg and 200 mg. These were then stirred for a further 15 minutes to allow for dispersion of the tannic acid within the matrix. The samples were then left to crosslink at room temperature or placed in the oven for 5 hours at 60°C to allow crosslinking to take place. After the 5 hours the samples were taken out of the oven allowed to cool to room temperature and then frozen in liquid nitrogen and subsequently freeze dried.

3.6 Synthesis of Glutaraldehyde crosslinked sponges

The synthesis for the glutaraldehyde crosslinked sponges was carried out by dissolution, bubbling followed by the addition of the glutaraldehyde. The glutaraldehyde was initially reduced to a 25% in water solution and 0.37 ml were added as this was an ideal concentration obtained from previous work done in the group. The solution was then stirred vigorously as the crosslinking procedure when glutaraldehyde is used was rapid and would result in clumping at lower stirring speeds. The samples were left to crosslink at room temperature for an hour as the glutaraldehyde was capable of crosslinking much faster than the genipin and TA. The samples were then frozen in liquid nitrogen and then lyophilized.

3.7 Synthesis of microcrystalline cellulose (MCC) loaded sponges

For the synthesis of MCC loaded sponges, the MCC was sonicated for 10 minutes to insure that there were no agglomerations as the MCC tends to agglomerate when placed in water. The chitosan was weighed out and dissolved for 24 hours in a 1% acetic acid solution and the MCC was added to the solution at 10 wt % concentration and further stirred for an hour to allow for dispersion of

the MCC in the matrix. The bubbling step was then carried out and for the crosslinked samples, the crosslinking agents are added as mention in 3.4 and 3.5 for genipin and TA crosslinked samples respectively. The samples are then frozen in liquid nitrogen and then freeze dried.

3.8 Labelling of MCC

In order to show the dispersion of the MCC within the matrix, the MCC was labelled using fluorescein isothiocyanate (FITC). FITC (4.3 mg) was dissolved in 9.95 ml of a 0.1 M NaOH solution and then 99.0 mg of MCC was added to the solution. This was then followed by stirring with a magnetic stirrer for 72 hours in darkness. After stirring for 72 hours, the solution was centrifuged for 10 minutes. The excess solution was then decanted, 0.1 M NaOH added to the labelled MCC and the centrifugation process repeated until the yellow colour was not visible anymore. Once the solution was clear, 50ml NaOH was added to the labelled MCC and then decanted into a dialysis tube. Dialysis was then carried out for one week changing the water three times a day. After seven days, the MCC was then frozen using liquid nitrogen and thereafter lyophilised. The resultant labelled MCC was then loaded into the chitosan sponges as was mentioned above and the dispersion of the MCC analysed using fluorescent microscopy.

3.9 Characterization methods

3.9.1 Attenuated total reflectance – Fourier transform infrared (ATR-FTIR)

The chitosan based sponges that were synthesized were analysed using a Thermo Fisher Nicolet iS10 attenuated total reflectance-Fourier transform infrared spectrometer. The samples were solid pieces that had been cut from various areas on the sponges and then analysed. The parameters for the runs was 64 scans for each of the samples and was run from 650 to 4000 wavenumbers with a resolution of 4 cm^{-1} . The runs were carried out in the transmittance mode with the background subtracted for each run.

3.9.2 Scanning electron microscopy (SEM)

The scanning electron microscopy for the sponges was carried out at the Central Analytical Facility of Stellenbosch University. This was done to determine the morphological properties of the

sponges and to see if the structure was porous. The samples were placed on a stub using double sided tape and then gold coated in order to enhance the image. The images obtained were at high magnification so as to see the morphological properties. The beam conditions during the analysis were altered for each of the samples to obtain the best possible images.

3.9.3 Thermogravimetric analysis (TGA)

The thermogravimetric analysis was carried out at Roediger Agencies at Stellenbosch University. TGA is a technique that measures the thermal stability of the samples by gradually raising the temperature at a set rate and measuring the weight lost by a material due to the increment in temperature under a controlled atmosphere. The TGA was carried out to gain a broad image of the thermal properties that were imparted on the sponges by the various reactions and incorporations that had been done in the synthesis procedures. The samples were weighed for each run and then subjected to a heating rate of 10°C/min from room temperature to 600°C in a nitrogen atmosphere.

3.9.4 Differential scanning calorimetry (DSC)

The thermal properties and the changes brought about by altering the temperature were then monitored using a TA Instruments Q100 differential scanning calorimeter. The measurements were carried out at a heating rate of 10 °C/min over a temperature programme that went from 25 °C to 160 °C and then back down to -20 °C without being isothermal at 160°C. The range then went from -20 to 200 °C. The temperature was left constant at -20 °C for 5 minutes.

3.9.5 Confocal fluorescence microscopy

The chitosan sponges, both crosslinked and uncrosslinked, that contained the MCC which was labelled with the FITC were then analysed using a Carl Zeiss LSM 780 Elyra S1 microscope. The samples were cut and then placed on a microscope slide. The microscope can detect fluorescent components in samples and can obtain images that show the cross section of a sample being analysed. This provides a three-dimensional view of the sample and thus a clear depiction of the dispersion and homogeneity of the dispersion for the sample being analysed. The samples were then analysed using lasers of wavelengths 488 nm and the 561 nm respectively [8].

3.9.6 Compressional tests

The compressional tests were carried out by measuring the same dimensions for the sponges, that is, 1 cm height, 1 cm length and 1 cm width. The samples were then placed on a flat surface with a ruler on the background and as they were compressed by the weight, the compression/depression of the samples was measured as a function of time. The length the samples were compressed as a function of the starting length, was used to obtain the percentage strain. This was then used to calculate the mechanical properties. After a set amount of time, the weight was removed and the recovery was also measured as a function of time. This set up was used to get a perception of the mechanical properties imparted by the crosslinking. The tests were done three times.

3.9.7 Absorption tests

The water absorption test was done to determine the amount of water a material is capable of absorbing at set conditions. In this study, 100 mg samples were weighed for each of the sponges with varying crosslinking agent concentrations. The samples were then placed in a desiccator for 72 hours in order to condition the samples. The samples were then submerged in phosphate buffered saline (PBS) for 24 hours at room temperature. After the 24 hours had elapsed, the samples were carefully removed and the excess PBS solution was removed using filter paper and then weighed again to obtain the weight of the samples with the solution absorbed. The initial weight of the dry samples was denoted as W_i and the final weight after absorbing the PBS solution was denoted as W_f . These values were then used in the following equation to obtain the water absorption rate;

$$A = (W_f - W_i)/W_i \quad [9]$$

3.9.8 Treatment of polymers with Gramicidin S

Stock solution of MilliQ water was used to prepare a 2 mg/ml gramicidin S solution. Peptide solution was then prepared to 50 $\mu\text{g/ml}$ by using 25 μL of the peptide solution and 975 μL of water. Once diluted, 200 μL was then added to the samples and adjusted until the samples were completely covered with peptide solution. This was then incubated for an hour at room

temperature. After the hour, the excess peptide solution was removed and the samples rinsed with MilliQ water. The samples were then dried over night at 30 °C in an oven or dried by lyophilisation.

3.9.9 Alamar blue assay

3.9.9.1 *Preparation of Micrococcus luteus:*

Freezer stocks were streaked out and incubated at 37 °C for 48 hours. Media comprising of 15 Tryptone, 0.5% yeast extract, 1% NaCl; adjust pH to 7.5; add 1.5% agar for plates, was prepared. Three to five colonies were then selected and grown overnight for 16 hours in 20 ml optimum media (LB) to an OD₆₂₀ = 0.8 – 1.2, slanted at 150 rpm. The cultures were then diluted to an OD₆₂₀ = 0.2. After the assay, 100 times serial dilutions were made and plated out onto an agar plate – cell counts to be used to calculate initial cell concentration.

3.9.9.2 *Dose response*

1. Sterilised polymers were added to the wells in the black microtitre plates (MTP) leaving two rows in the plates for organism growth control and alamar control. The polymers were sterilised by placing them in a desiccator with a small amount of chloroform for at least 30 minutes.
2. The cell suspension was then added to MTP and covered and incubated for an hour at 37 °C.
3. 10 µL of Alamar blue solution (0.3 mg/mL resazurin salt in PBS) were added into the MTP wells, covered with foil and incubated for 2 hours at 37 °C.
4. The plate was then read at Ex530-560: Em590.
5. The results were then analysed and growth inhibition thereof determined.

$$\%Growth\ inhibition = \frac{100(A_{595}\ of\ well - Mean\ A_{595}\ of\ total)}{Mean\ A_{595}\ of\ growth\ control - Mean\ A_{595}\ of\ total\ inhibition}$$

3.10 References

1. Sionkowska A, Płanecka A. Preparation and characterization of silk fibroin/chitosan composite sponges for tissue engineering. *J Mol Liq.* **2013**;178:5–14.
2. Aoyagi S, Onishi H, Machida Y. Novel chitosan wound dressing loaded with minocycline for the treatment of severe burn wounds. *Int J Pharm.* **2007**;330(1–2):138–45.
3. Wang X, Yan Y, Lin F, Xiong Z, Wu R, Zhang R, et al. Preparation and characterization of a collagen/chitosan/heparin matrix for an implantable bioartificial liver. *J Biomater Sci Polym Ed.* **2005**;16(9):1063–80.
4. Morgado PI, Lisboa PF, Ribeiro MP, Miguel SP, Simões PC, Correia IJ, et al. Poly(vinyl alcohol)/chitosan asymmetrical membranes: Highly controlled morphology toward the ideal wound dressing. *J Memb Sci . Elsevier*; **2014**;469:262–71.
5. Lai HL, Abu’Khalil A, Craig DQM. The preparation and characterisation of drug-loaded alginate and chitosan sponges. *Int J Pharm.* **2003**;251(1–2):175–81.
6. Sung HW, Liang IL, Chen CN, Huang RN, Liang HF. Stability of a biological tissue fixed with a naturally occurring crosslinking agent (genipin). *J Biomed Mater Res.* **2001**;55(4):538–46.
7. Croisier F, Jerome C. Chitosan-based biomaterials for tissue engineering. *Eur Polym J .* **2013**;49(4):780–92.
8. Grange M. The use of fluorescence to probe the morphology changes in complex polymers Marehette le Grange. **2015**;(March).
9. Water Absorption ASTM D570 .

4 Chapter 4: Chitosan and chitosan-MCC sponges

4.1 Introduction

Chitosan is a biodegradable material and as such, there are advantages and disadvantages that come with such a property. The advantages are that it can be used in a variety of biomedical

applications due to its degradability and the disadvantages being that the products synthesized from chitosan are mechanically weaker than their synthetic counterparts and have a generally shorter shelf life [1, 2]. These disadvantages can be averted by crosslinking the materials that are synthesized using chitosan and/or by combining with other polymers to help improve the mechanical properties [1-6]. The use of synthetic crosslinking agents was the go to, with glutaraldehyde being the most studied in the previous years, however, further research showed that the use of these synthetic crosslinking agents is dwindling due to the cytotoxicity imparted on the materials produced after reacting with biocompatible polymers [1, 2, 4, 7-9].

The use of crosslinking agents with lower cytotoxicity has become the substitute to the synthetic ones with genipin being the most used in combination with chitosan [1]. The reaction between chitosan and genipin has been researched and the processes that occur during the reaction are well understood for a number of reaction conditions [1]. The reaction of chitosan and genipin is a bi-functional one and results in the formation of a blue coloured material [1, 10-12]. The crosslinking density for the samples crosslinked with genipin was reported to be highest when the crosslinking reaction was carried out in neutral conditions [9] thus the use of sodium hydrogen carbonate for the formation of the bubbles in the structure as the acid-base reaction would raise the pH from acidic to values closer to neutral without going too high as this would result in the chitosan becoming insoluble.

4.2 The effect of crosslinking time and temperature

The following section will focus on the results and observations that were taken during the synthesis of the sponges and brief explanations on the appearances and how the optimum conditions for the sponges were obtained for the different crosslinking agents used in the synthesis.

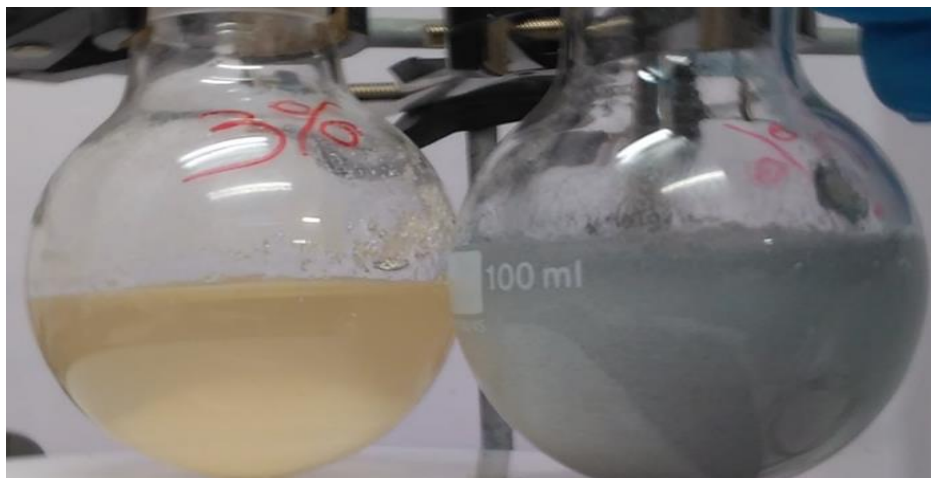


Figure 4.1: Colour of genipin crosslinked sample left at room temperature for 4 hours on the left and 12 hours on the right

The crosslinking of chitosan with genipin results in a blue colour being seen in the resultant material. The image above, Figure 4.1, shows the colour difference of a sample that was left to crosslink for 4 hours at room temperature, on the left, and a sample that was left for 12 hours to crosslink on the right. From the image, it is clear that the sample left for 12 hours did not get to as deep a blue as the samples that were eventually put in the oven for 5 hours as is shown in Figure 4.5. The image also shows that the samples did not contain any bubbles and as such an increase in the genipin concentration was warranted in order to keep the bubbles in the sample. Figure 4.2 shows the effect of increasing the genipin concentration to try and maintain the bubbles in the structure.

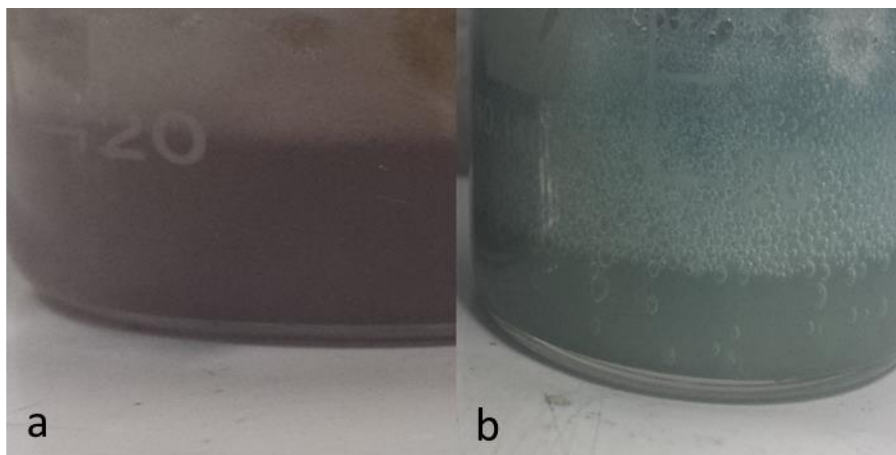


Figure 4.2: Migration of the bubbles from a) the tannic acid matrix and b) the genipin matrix

Figure 4.2 above shows two of the samples that were left to crosslink at room temperature with a) being the tannic acid crosslinked sample and b) the genipin crosslinked sample. The images show the absence of bubbles in the bottom half of the samples as the bubbles had escaped before the crosslinking had taken place and was sufficient enough to hold them within the matrix. This was as a result of the crosslinking process, which leads to the blue colour, only occurring after extended periods of time in excess of 10 hours at genipin masses less than 10 mg. This meant that the porosity of the sponge could not be maintained if the crosslinking took this long. For the samples being crosslinked with tannic acid this was overcome by sealing the vessel in which the sponges synthesized. This made it possible to maintain the porous structure of the tannic acid crosslinked samples as the crosslinking took place at a faster rate than the genipin samples at room temperature. The tannic acid crosslinking procedure took place in 5 – 7 hours whereas the genipin samples took more than 10 hours. To counter the long synthesis times, the samples were then placed in an oven at 60°C due to the chain flexibility being independent of any intermolecular interactions and thus would result in accelerated interactions between the crosslinking agents and the chitosan [13]. This would then result in the prevention of the bubbles from escaping the matrix before the crosslinking had taken place and would take less time.



Figure 4.3: The effect of absence of air on the colour change of genipin crosslinking

The blue colour in the samples above was only visible at the surface when the beakers were covered as seen in Figure 4.3 above. Due to the beakers being sealed with the foil, a layer of water accumulated at the surface of the sponges due to condensation of the evaporating water and this blocked the interaction of the matrix with air and the coloration of the rest of the sample did not occur. This goes to show that the presence of air was influential in the blue coloration of the samples. This blue coloration is presumed to be due to the crosslinking process, that is, the oxygen radical induced polymerisation of the intermediate genipin compounds [11]. These polymerisations of the genipin compounds are known to have distinct properties that are dependent on the pH and are due to the reaction mechanisms which involves the nucleophilic attack of the genipin [9]. In acidic conditions, the genipin crosslink-bridges between the carbohydrate polymer chains are shorter than when the crosslinking is in alkaline conditions as the bridges are longer due to a tendency to self-polymerise [11]. The synthesis of the sponges was carried out in acidic conditions to ensure the formation of short crosslink – bridges as this would result in a more stable structure.

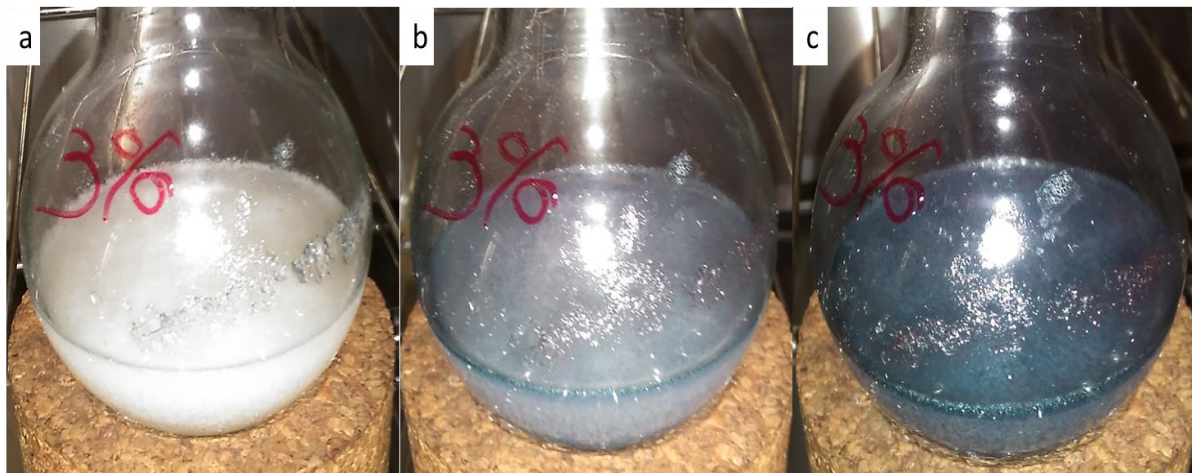


Figure 4.4: Colour change after a) 1 hour, b) two hours and c) three hours in the oven for the genipin crosslinked samples

The figure above, Figure 4.4, shows the coloration process as a function of time for the genipin crosslinked samples placed in the oven. After the first hour, with the samples exposed to air, no significant colour change was observed and the matrix was white as seen in a). After two hours in the oven, the sample had turned to a light blue colour as is seen in b) above. After three hours in the oven, the sample had turned into a darker blue colour than that seen at two hours. This clearly showed the progression in the crosslinking as the deeper blue colour would indicate that more of the genipin had reacted with the chitosan and the genipin bridges had formed. This was then evidence of the pivotal role air played in the crosslinking process and the subsequent coloration of the resultant material.



Figure 4.5: The deep blue colour obtained after 5 hours in the oven

After the fifth hour in the oven, the sponges had a deep blue colour as is seen in Figure 4.5 above. The deep blue colour was constant throughout the samples from the fourth hour to the fifth hour. After taking the samples from the oven they were cooled down to room temperature and then quenched by freezing them in liquid nitrogen to prevent the bubbles escaping from the matrix and to prevent the growth of water crystals within the structure as this would affect the porosity of the sponges. This was to prevent inconsistent results as *Lai et al* had reported that the size of water crystals during the freezing process had an effect on the porosity [6]. The porosity for the sponges was only supposed to be due to the bubble formation that resulted from the CO_2 emitted during the acid-base reaction when NaHCO_3 was added to the acetic acid containing matrix.

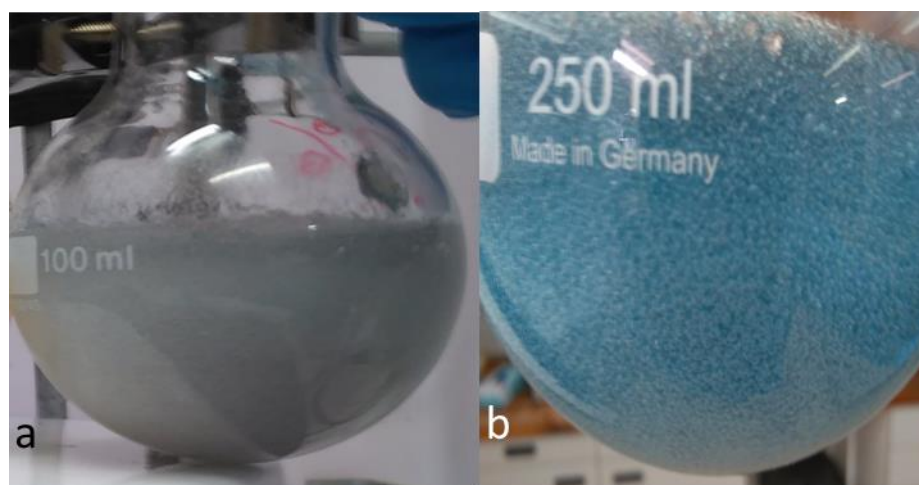


Figure 4.6: Genipin crosslinked samples; a) which was left at room temperature for 11 hours and b) which was in the oven for 2 hours

Figure 4.6 shows the absence of bubbles in sample a) and the presence in sample b) which was possible due to the use of the oven which allowed the samples to crosslink at an accelerated pace and consequently prevent the migration of the bubbles from the sponge matrix. Sample a) shows that the matrix did turn blue but only after about 10 hours and at this point, the bubbles had already escaped from the matrix. The blue colour that was produced at room temperature over the longer period of time was not as deep as that obtained by the same concentration of genipin and placed in the oven as is seen in Figure 4.1 and Figure 4.5. The distribution of the bubbles in the matrix of the sample labelled b) was also homogeneous which is essential in the synthesis of a sponge to be used in wounds as this will provide a stable and uniform structure for cell proliferation [14-17]. The method of putting the sample in the oven was clearly of importance as this resulted in faster crosslinking as well as better porosity as the bubbles were lost in the samples left at room temperature.

4.3 Fourier Transform Infra-Red spectroscopy analysis

The chemical properties of the samples were analysed using Fourier transform infrared spectroscopy as described in Section 3.7.1. The focus was on distinct peaks that have been reported in literature that correspond to the various interactions that occur during the crosslinking process as well as the peaks that are seen in the sample that was not crosslinked. The following results compare the uncrosslinked samples to the crosslinked and microcrystalline cellulose (MCC) loaded samples. For the neat chitosan sample, the characteristic peaks were noticeable at 1648 cm^{-1} , 1563 cm^{-1} and 1152 cm^{-1} and these peaks correspond to the amide 1 (C=O stretching), amide 2 (NH₂ deformation) and glycosidic linkages respectively [18].

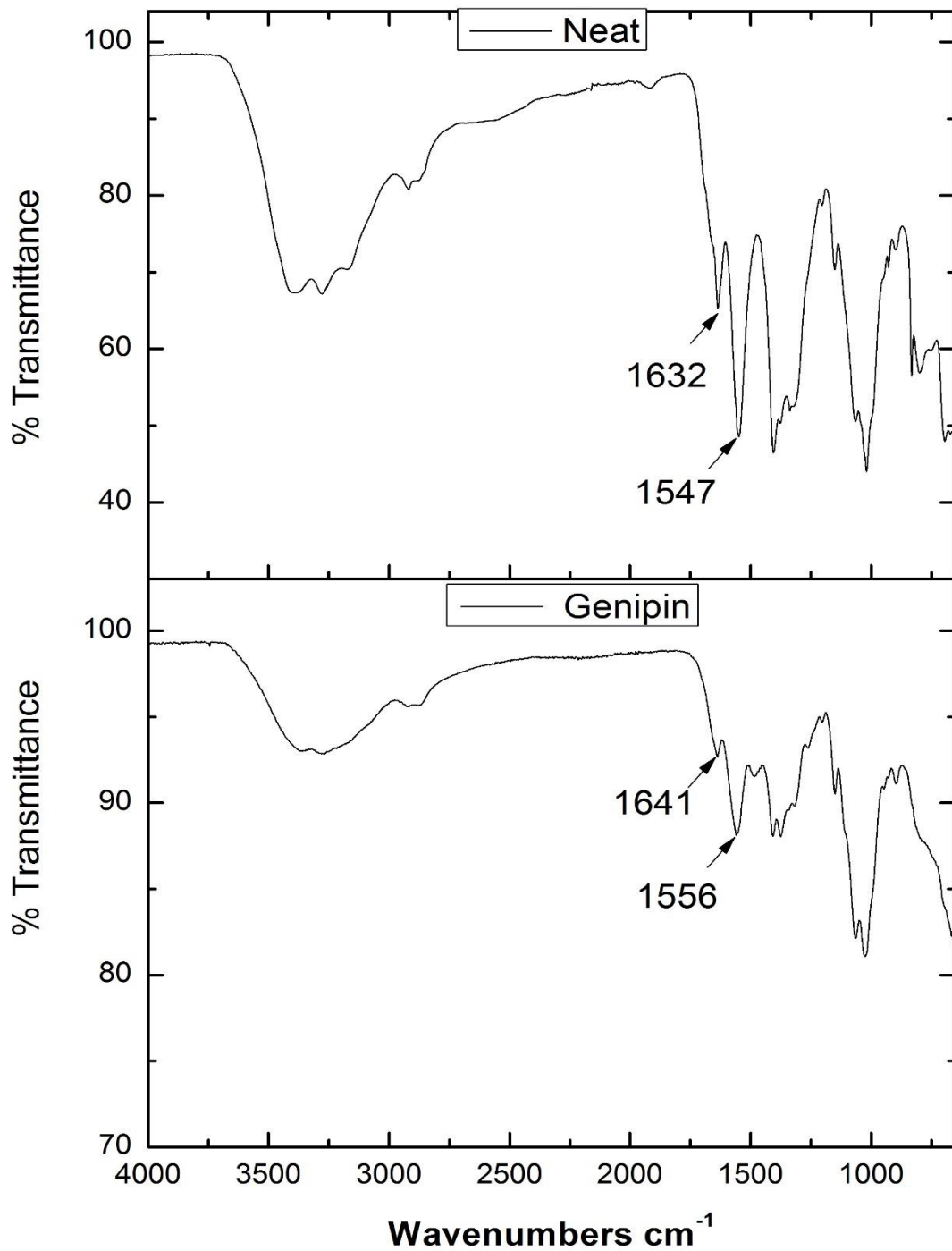


Figure 4.7: FTIR spectra for the neat uncrosslinked chitosan and genipin crosslinked samples

Figure 4.7 shows the characteristic peaks of uncrosslinked chitosan sample labelled clean and of the genipin crosslinked samples. The spectrum shows characteristic peaks for the clean sample with broad peak from 3000 cm^{-1} to 3700 cm^{-1} with three distinct peaks representative of amine and hydroxyl group stretching vibrations. The broad peaks are as a result of the hydrogen bonds between these groups. The peaks that are at 1632 cm^{-1} were characteristic of primary amine groups that were observed at 1641 cm^{-1} for the genipin crosslinked sample. There is a shift observed to a higher wavenumber which is indicative of the interaction between the chitosan and the genipin. The decrease in the intensity for the crosslinked samples representative of the carbonyl group is indicative of crosslinking procedure that involves the carbonyl groups in the chitosan and the amine groups in the genipin. The peak observed at 1547 cm^{-1} is indicative of the primary amine groups which has also shifted to a higher wavenumber due to its interaction with the genipin and is 1556 cm^{-1} in the genipin crosslinked spectrum. The decrease in the intensity of the peak is also indicative of the crosslinking of the samples. The peak that was observed at 1052 cm^{-1} was indicative of the glycosidic linkages and hence the transmittance of this peak was not affected as the amide region of the spectrum. The peaks that were observed at 1020 cm^{-1} are indicative of the C-N stretching vibrations. For the genipin crosslinked sponges, there is a decrease in the transmittance peak at 1550 cm^{-1} which is due to amide II N-H bending vibration groups that are a result of the crosslinking. The appearance of the shoulder at the peak at 1700 cm^{-1} wavenumbers in the spectrum indicates the ester linkages that were formed due to the crosslinking. The shift occurring from 1632 cm^{-1} with a decrease in the peak intensity suggests that there was an interaction with genipin that results in a ring opening reaction due to the nucleophilic attack by the amino groups on the chitosan. This shift also suggests the formation of a heterocyclic amine after the crosslinking procedure. An increase in the genipin concentration also had an effect on the FTIR spectra with the peak 1641 cm^{-1} being affected the most. This is evidenced by the sample crosslinked with 3mg genipin having a peak comparable to the peak at 1556 cm^{-1} as seen in Figure A. 1.

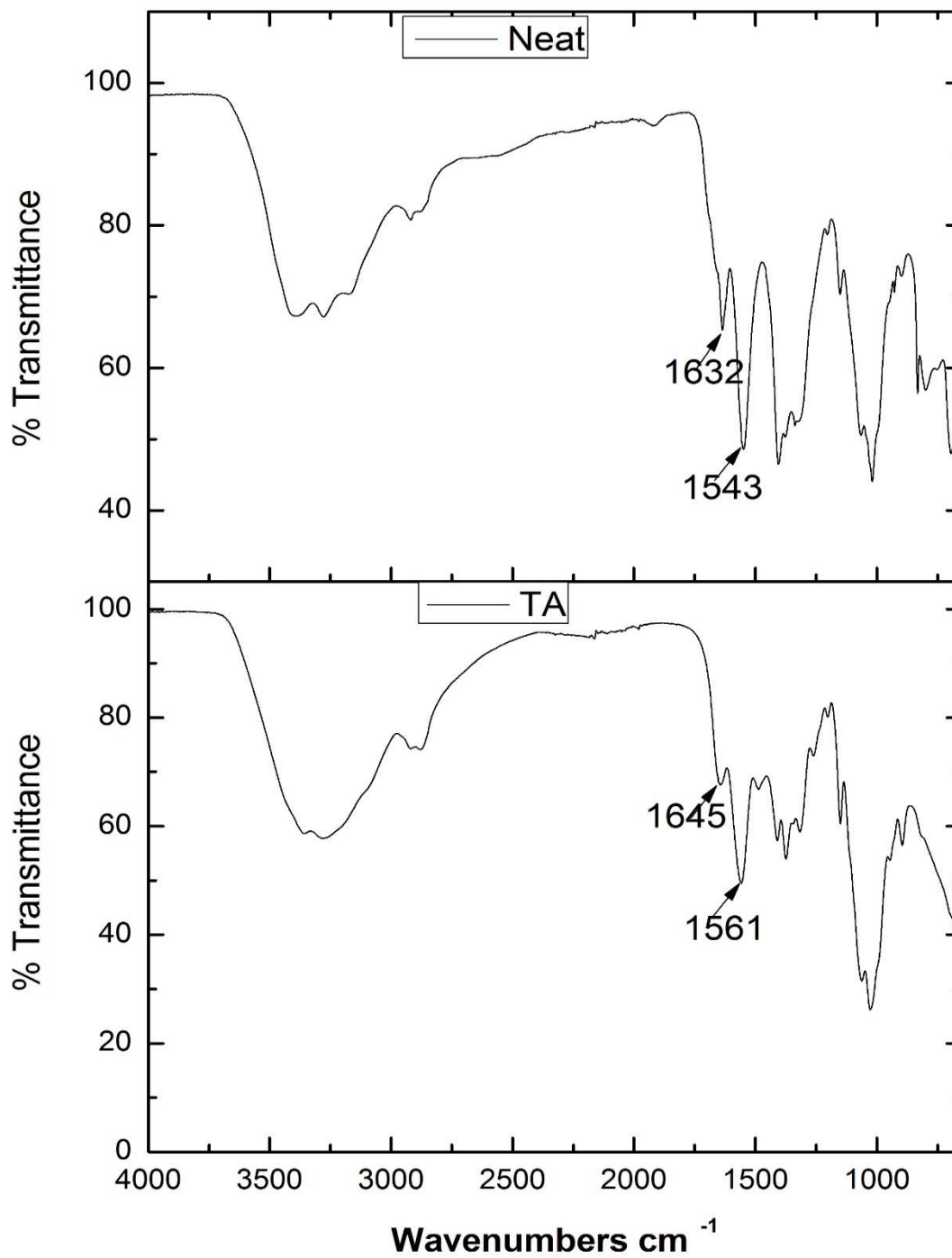


Figure 4.8: FTIR spectra of uncrosslinked and tannic acid crosslinked chitosan samples namely, Neat and TA respectively

The FTIR spectra above show the samples that were crosslinked with tannic acid labelled TA and the uncrosslinked sample labelled “Neat”. From the spectra it is clear that the peaks observed for the neat sample between 3000 and 3700 cm^{-1} had three distinct peaks at 3389, 3276 and 3170 which are representative of the hydroxyl and amine group stretching vibrations overlaps [4]. The samples crosslinked with TA have a broader peak between 3000 and 3700 cm^{-1} wavenumbers and the distinct peaks visible for the uncrosslinked sample are no longer present with two slight bumps visible at 3275 and 3354 cm^{-1} . This is indicative of the hydrogen bonding due to the large number of hydroxyl groups on the tannic acid and the crosslinking that has occurred. The peaks occurring at 1632 cm^{-1} are representative of the C=O stretching of the amide groups and the peak occurring at 1543 cm^{-1} is representative of the primary amine bending. The peak at 1645 cm^{-1} is indicative of crosslinking due to asymmetric angular deformation of the $-\text{NH}_3^+$ group on the chitosan [19]. The peak at 1561 cm^{-1} can be attributed to secondary amine bonds (amide II) that are a result of the crosslinking.

4.4 Scanning electron microscopy (SEM) analysis

To monitor the morphological properties of the resultant sponges, SEM was done to analyse the microstructures that were present on the samples. An understanding of the properties of the resultant sponges' morphologies can assist in the elucidation of the relationship between the crosslinking agents and the results obtained in further analysis. The morphologies of these samples are discussed in this section along with the effect each of the crosslinking agents had on the sponges in comparison to the neat sample. The effects of any other parameters used in the synthesis that resulted in a morphological change are also discussed.

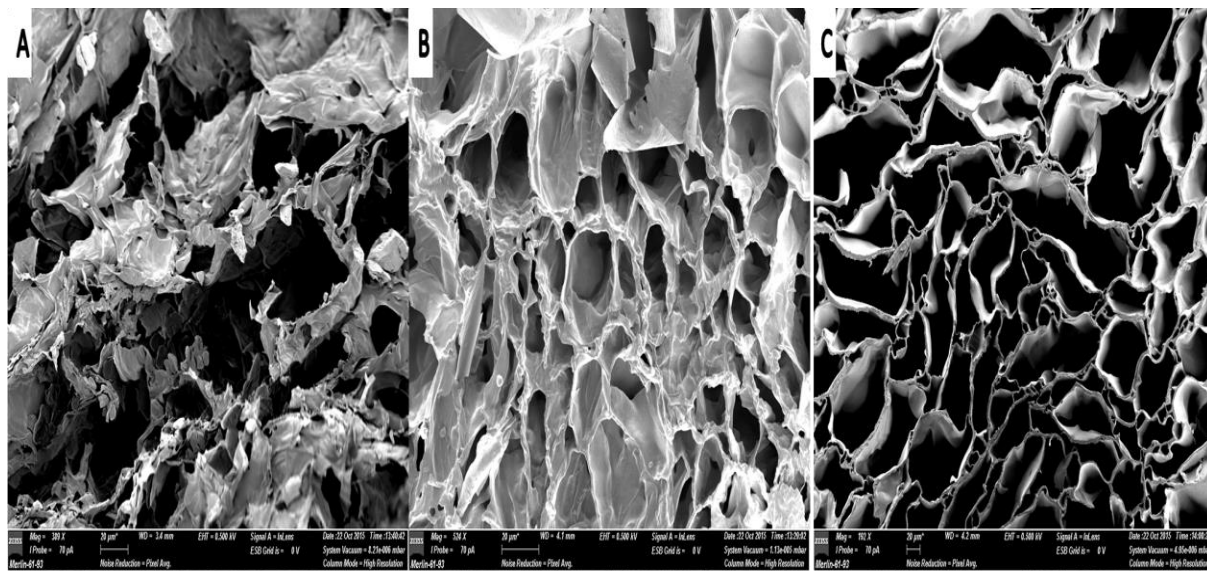


Figure 4.9: Comparison of the morphologies for A, the uncrosslinked sample, B, genipin crosslinked sample and C, tannic acid crosslinked sample

From Figure 4.9 above, we can see that there are visible differences between the samples depending on whether they are crosslinked and the crosslinking agent used. Sample A was not crosslinked and the sample does not show a distinct porous structure. The sample also shows that the uncrosslinked chitosan is not stable due to the lack of a continuous and connected structure. Sample B is the genipin crosslinked sponge that shows a connected porous structure. Sample C is the tannic acid crosslinked sample and shows a continuously connected porous structure. Of the three samples, the TA crosslinked sample has the largest pore size and a more open structure. The samples in the images for the crosslinked samples are the sample crosslinked with 10 mg genipin and the sample crosslinked with 80 mg tannic acid.

The samples that are highlighted in the following images show the SEM results of the samples that were uncrosslinked and were either placed in the oven or synthesized at room temperature before being frozen in liquid nitrogen and subsequent lyophilisation. The focus on the following images is the effects that the thermal treatment had on the resultant sponges before the freeze-drying step was carried out.

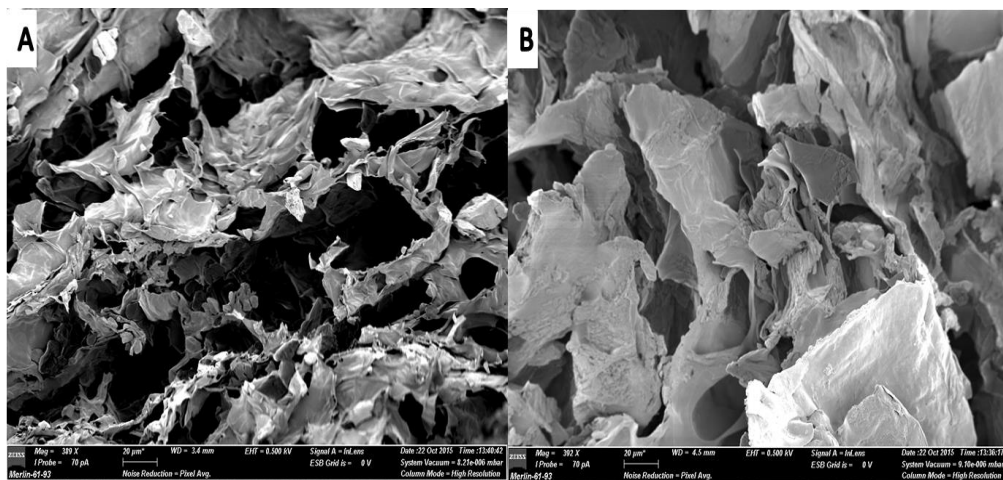


Figure 4.10: SEM images for uncrosslinked samples with A no thermal treatment and B is thermally treated

The samples marked A and B were uncrosslinked and were taken from two samples, with sample A synthesised at room temperature and with sample B synthesized by placing in the oven at 60 °C with the tannic acid and genipin crosslinked samples. These samples did not show any discernible porous structure that was interconnected as the samples were not able to maintain the porosity and due to the static interaction between the molecular chains which would result in the loss of the porosity. This collapse in the structure was due most likely to the inability of the chain entanglements and the hydrogen bonds between the chitosan polymeric chains being unable to maintain the structural integrity during the synthesis process [20].

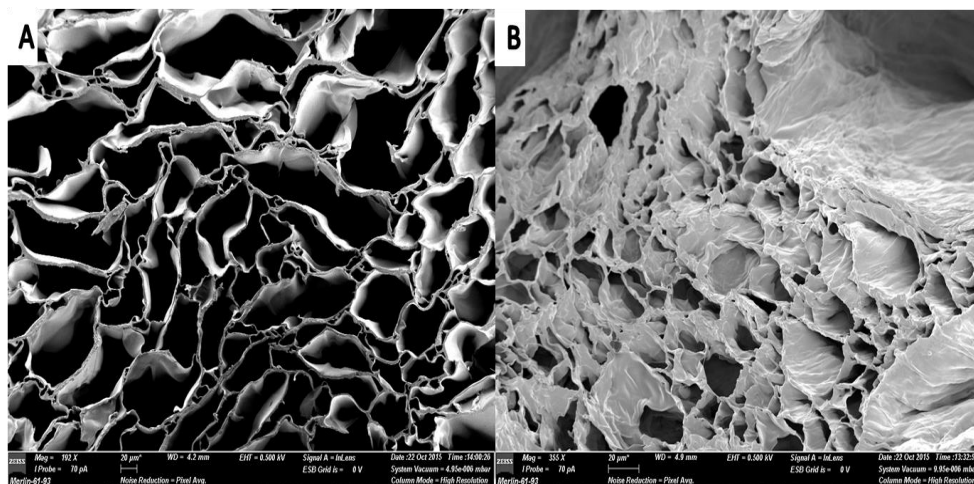


Figure 4.11: SEM images for tannic acid crosslinked samples A, synthesized at room temperature and B synthesized at 60°C.

The figure above shows the morphologies of the tannic acid crosslinked samples that were synthesised at room temperature and at 60 °C marked A) and B) respectively. A porous structure can be seen for the samples chosen above and the effect the temperature had is clearly visible. The samples that were synthesised at room temperature show that the porosity was well pronounced in the samples that were crosslinked at room temperature whereas the porosity for the samples that were subjected to thermal treatment, the porosity is not as pronounced. For the TA crosslinked samples, the porosity of the samples increased with an increase in the crosslinking agent concentration. This can be attributed to a faster reaction occurring between the chitosan and the TA resulting in the sponges becoming rigid and the bubbles not distributing themselves throughout the sample but rather fusing together [7].

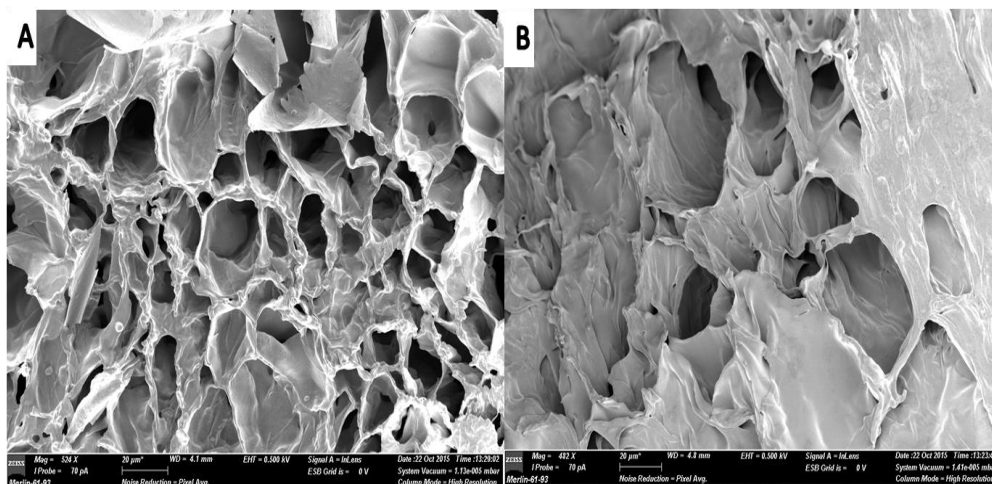


Figure 4.12: SEM images for genipin crosslinked samples A, before peptide treatment and B, after peptide treatment and oven drying.

The samples shown in Figure 4.12 above show the porous structure obtained for the samples that were crosslinked using genipin. The sample marked A) shows the sample that had been placed in the oven for 5 hours, as the samples that were left to crosslink at room temperature had lost all the bubbles before the lyophilisation process could be carried out. In comparison to the samples that were synthesized at room temperature for the tannic acid, the porosity is less well defined, but is interconnected nonetheless. The image marked B) shows the resultant morphology of the sponge after the samples had been treated with an antimicrobial peptide and oven dried. From the above image, the effect of the treatment on the morphology shows that the porous structure is affected by the oven drying and/or a combination of the peptide addition and the subsequent oven drying.

4.5 Confocal microscopy results

The incorporation of the microcrystalline cellulose into the chitosan sponges was monitored using confocal microscopy (CM). This was done to determine if the MCC had been dispersed in the chitosan matrix and had not aggregated.

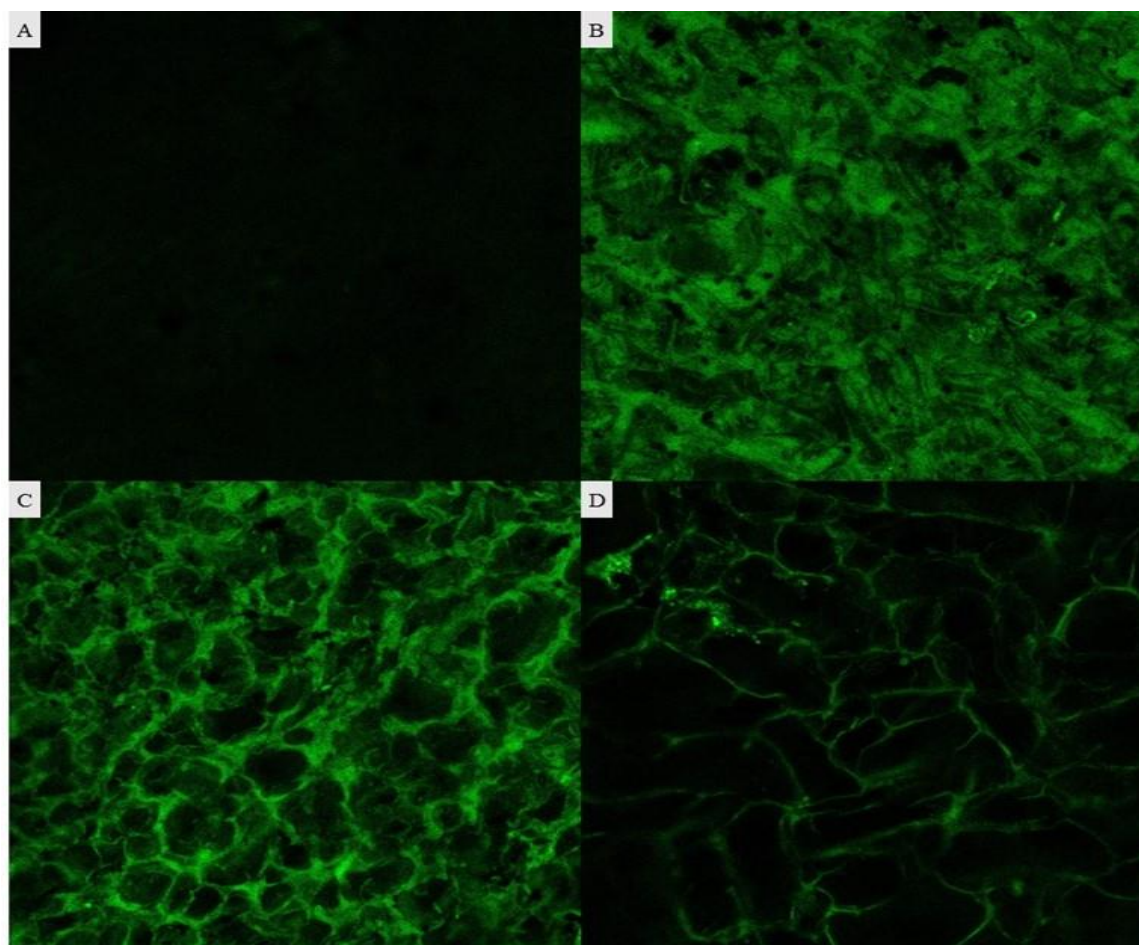


Figure 4.13: Confocal microscopy image showing A; Neat sample without labelled MCC, B; Chi/MCC sample with labelled MCC, C; Gen/MCC sample with labelled MCC and D; TA/MCC sample with labelled MCC

From the images obtained from the confocal microscopy analysis, the fluorescence labelled MCC can be seen and was distributed homogeneously in the samples B), C) and D). The porosity of the sponges can be seen in the image with the fluorescence labelled MCC shown in the crosslinked samples C) and D). For sample A, the image does not show any fluorescence as it did not contain labelled MCC and this was confirmation of having successfully labelled the MCC which was incorporated in the sponges using the fluorescence labelling dye fluorescein isothiocyanate (FITC). The purpose of this was to show that any of the properties obtained for the subsequent analysis tests using the MCC loaded samples was not as a result of poor distribution of the MCC. All the samples contained homogeneously distributed MCC and as such any variation or anomalies

were not due to the MCC loadings but rather other factors. The results in this section also agree with the results obtained using the SEM analysis.

4.6 Thermal gravimetric analysis results

Thermal gravimetric analysis (TGA) was done on the samples to determine the specific thermal ranges in which important occurrences appear. The region of importance from literature was the range in which the chitosan melts and the region the chitosan starts to degrade and to monitor how the crosslinking would affect these areas. The degradation of the chitosan sponges is affected by the crosslinking procedures to the imparted stability of the structure.

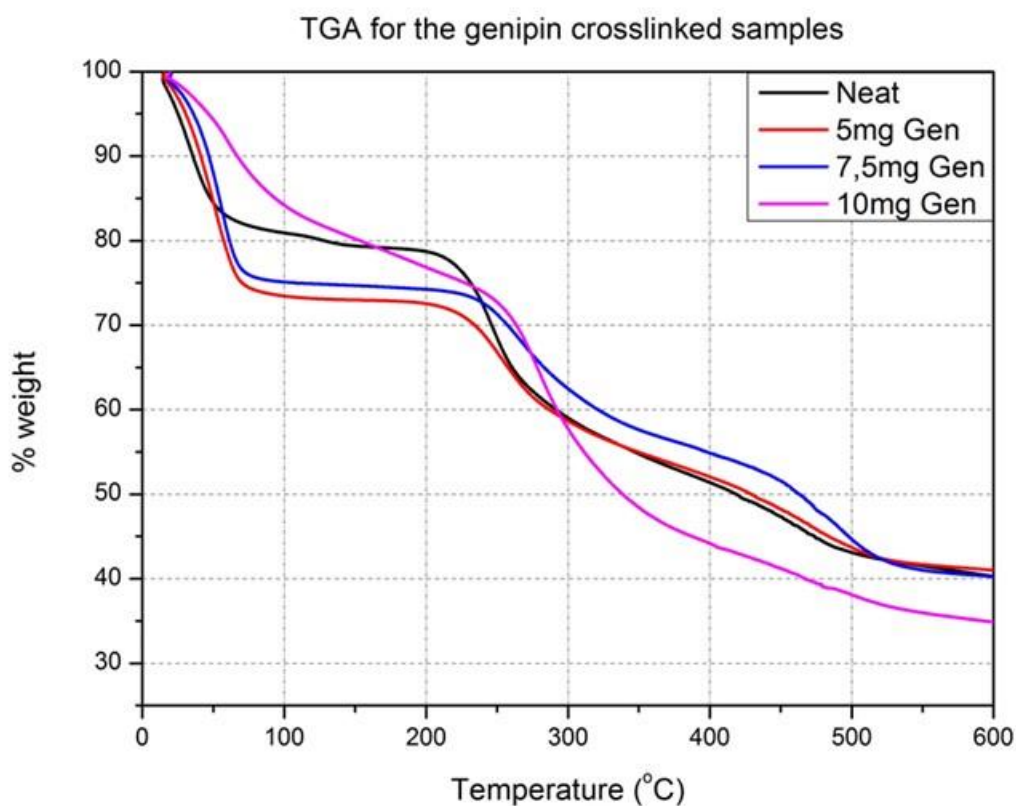


Figure 4.14: TGA graph above shows the neat uncrosslinked sample and the samples crosslinked with 5, 7.5 and 10mg of genipin.

The thermograms shown in Figure 4.14 show the effect the genipin had on the thermal properties of the resultant sponges in comparison to the samples that were not crosslinked. From the graph, we can see that the samples that were crosslinked with 5mg and 7.5mg genipin, namely 5mg Gen and 7.5mg Gen, did not exhibit any transitional phases in the temperature range 60 - 200°C. This goes to show that the transition in the clean sample at around 120°C was no longer occurring and was due to the crosslinking. The sample crosslinked with 10mg genipin, namely 10mg Gen, shows a gradual drop in the % weight of the sample from the beginning of the experimental run with significant thermal transitions occurring at 60 and 230°C. These results were not definitive as to the actual procedures occurring but indicated a positive result as to the crosslinking of the chitosan as the thermal activities in the clean sample were not visible for the crosslinked samples. Further analysis would have to be carried out to determine the exact nature of these thermal activities.

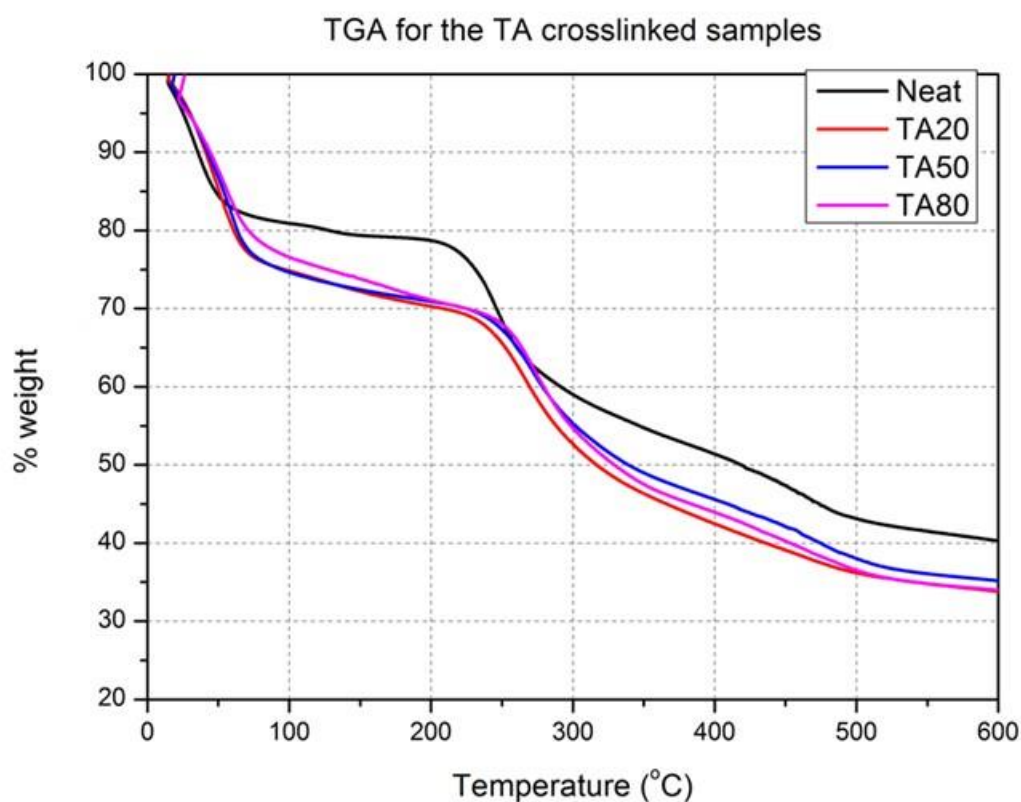


Figure 4.15: TGA thermogram of the neat uncrosslinked sample and the samples crosslinked with 20, 50 and 80 mg of tannic acid labelled TA20, TA50 and TA80 respectively.

The TGA graph in Figure 4.15 shows that the tannic acid crosslinked samples had greater water degradation than the uncrosslinked sample and this can be attributed to the crosslinked sponges having a more defined structure as seen in the SEM images in the previous section. As was mentioned in the previous section, the porosity of the samples increases with an increase in the crosslinking agent concentration due to the higher crosslinking agent concentration resulting in the larger pores. This is as a result of the crosslinking agent reacting much faster as the concentration is increased. The fusion of the bubbles due to the quick acting action results in the availability of a larger area for the water to be trapped within the structure of the sponges. The crosslinking agents also contain hydroxyl groups on their structure and these are also capable of interacting with water molecules thereby resulting in the larger drop because of this trapped water. It can also be seen that there is a slight increase in the onset temperature for the degradation step of the sponges that occurs at about 200°C for the uncrosslinked sample and occurs at around 230 – 260°C for the samples that are crosslinked with TA. These results show that the degradation temperature increases with an increase in the concentration of the crosslinking agent, namely, tannic acid. This increase in the degradation temperature illustrates that the material is crosslinked and is harder to degrade.

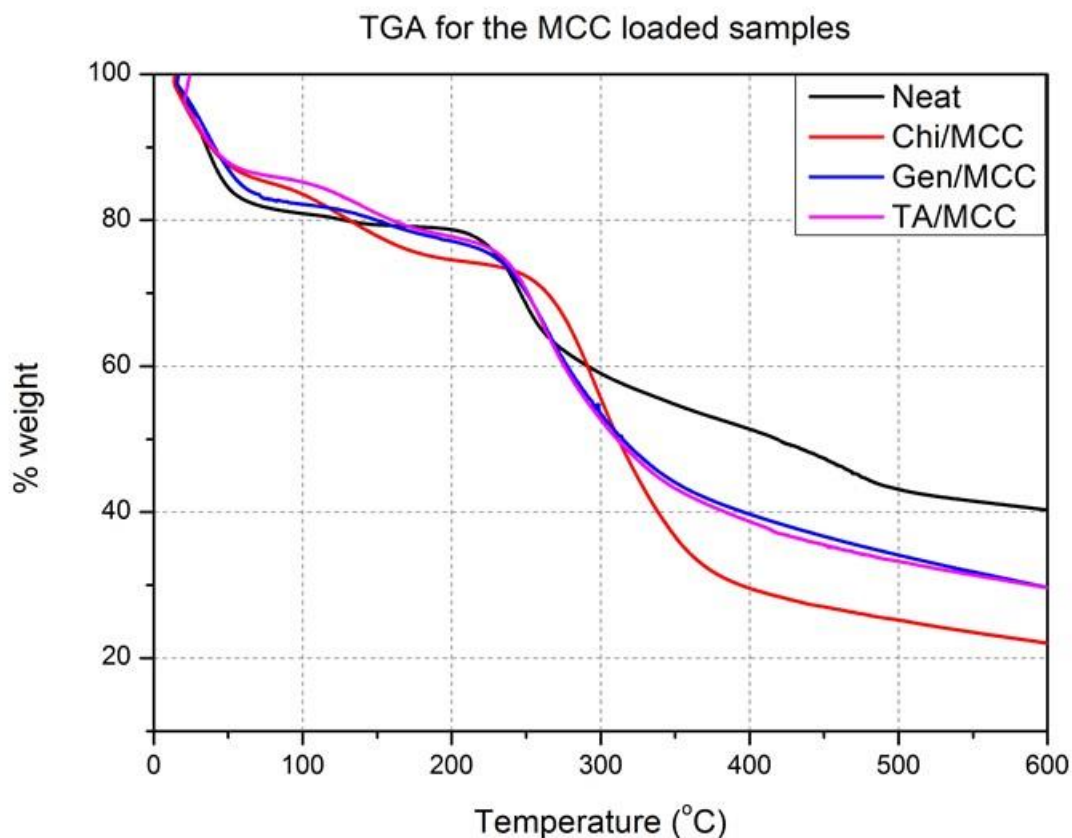


Figure 4.16: TGA thermogram of the neat uncrosslinked sample, uncrosslinked sample loaded with MCC, the genipin crosslinked sample loaded with MCC and the tannic acid crosslinked sample loaded with MCC labelled Neat, Chi/MCC, Gen/MCC and TA/MCC respectively.

The graph in Figure 4.16 shows the results obtained for the samples that contained microcrystalline cellulose and the properties imparted on the samples as a result of the inclusion. The samples showed more thermal activity in the region from about 60 – 200°C. This was the region of importance as it has been mentioned in literature that chitosan undergoes melting within this region [2]. From the above thermogram, the addition of the MCC to the dry sample results in the MCC acting as a filler for the dry sample due to the decrease in the water loss region in comparison to the neat chitosan sample. Another weight drop is seen for the chi/mcc sample as well as the TA/MCC sample from 100-150°C. This degradation could be the melting or the degradation of the chitosan with the MCC having a larger influence on the effect.

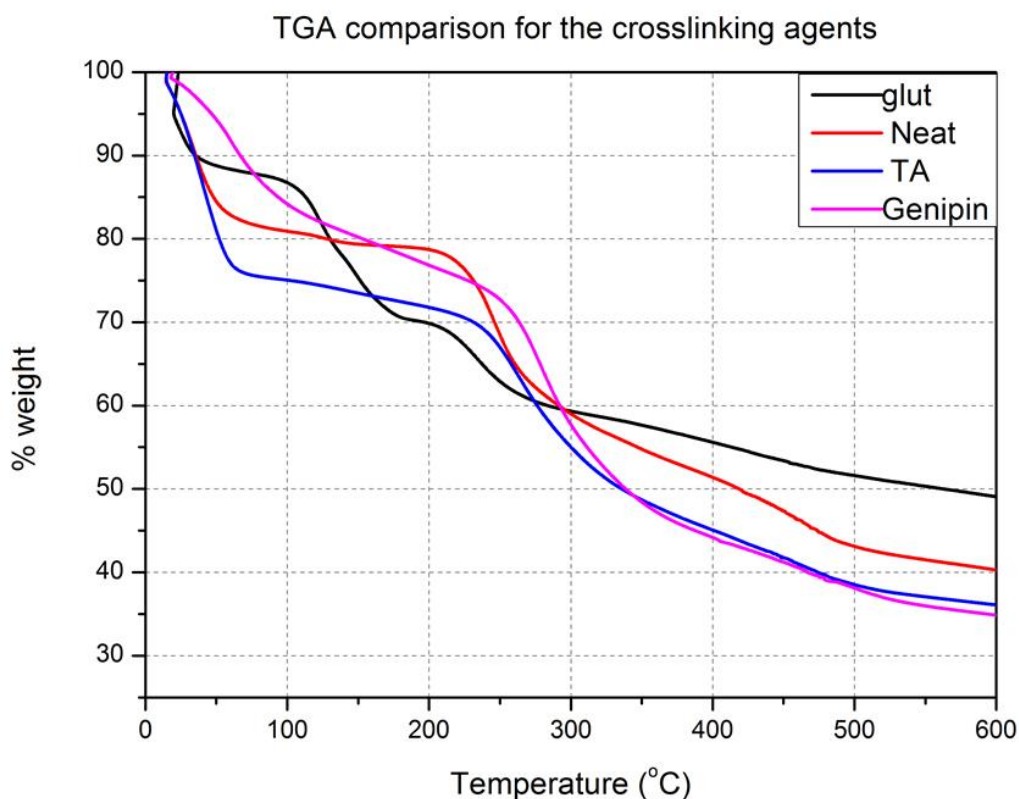


Figure 4.17: TGA thermogram comparing the neat uncrosslinked sample, glut; the glutaraldehyde crosslinked sample, TA; the tannic acid crosslinked sample and the genipin crosslinked sample.

The thermograms comparing the crosslinking agents that were used, that is, genipin, tannic acid and glutaraldehyde with respect to the uncrosslinked sample are shown in Figure 4.17 above. From the graph we can see that the sample that was crosslinked with glutaraldehyde had the most thermal activity. The results obtained above showed that the degradation step occurred after the 200° and there were multiple thermal occurrences at temperatures below that and as such the differential scanning calorimetry had to be carried out in order to discern the nature of the activity. The samples that were synthesized and contained glutaraldehyde showed the highest residual percentage weight and this was due to the effectivity of the crosslinking in comparison to the other crosslinking agents.

4.7 Differential scanning calorimetry results

DSC was done in order to differentiate the thermal activities that had occurred in the TGA analysis and to distinguish how they were related to the crosslinking of the chitosan sponges. The peak to look out for was the peak at 50 – 60 °C which corresponds to the relaxation of the complex and the reorganisation of the chitosan molecules present in the sample [13]. This reorganisation is due to the change in the hydrogen bond strength between the polymeric chains due to the residual water in the sample starting to move and due to volumetric expansion of this water as a result of the water being degraded from the sample [13, 21]. The peaks at this temperature were also noticed to only occur for the first heating of the sample and not in the second heating due to the residual water not being a factor after reaching temperatures in excess of 150 °C. The degradation of the chitosan is also known to occur between 114.5 and 124.1 °C [22]. At the elevated temperatures of up to 150°C, the degradation is as a result of the weakening of the hydrogen bonds between the polymer chains of the chitosan which reduces the intermolecular interactions. This results in the chain mobility increasing and the probability of scission of the glycosidic bonds also occurs in this temperature range. The glass transition temperature (T_g) for chitosan has been reported as a range of values due to the difficulty in obtaining the actual value [23]. This is largely due to the difficulty in the preparation of the samples and their tendency to be hygroscopic [23]. There have been various reports as to the T_g of chitosan ranging from 150 – 200 °C as a result of the complexity of the determination [23]. *Sakurai et al.* indicated that the peak that appeared at 150 °C was due to α -relaxation and was most likely due to the secondary molecular motion due to the chitosan going through a pseudo-stable state. As such, this region was of importance in the determination of the effects of the crosslinking that had been done.

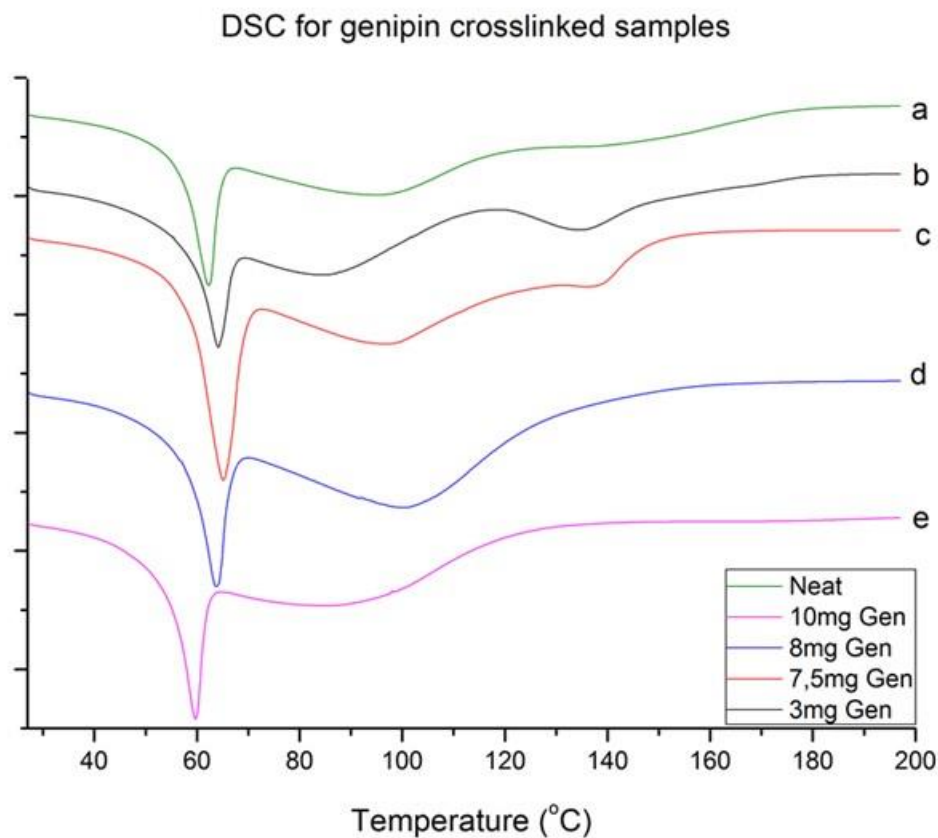


Figure 4.18: DSC thermograms of a) un-crosslinked chitosan sponge, b) 3 mg genipin crosslinked sample, c) 7.5 mg genipin crosslinked sample, d) 8 mg genipin crosslinked sample and e) 10 mg genipin crosslinked sample

From Figure 4.18 above, we can see that there were visible trends and differences in the samples with an increase in the crosslinking agent concentration. For the sample without any crosslinking agent, labelled neat, there are three endothermic events that occur with a sharp peak at 60 °C, and a broad endothermic peak that goes from 65 – 110 °C and another broad endothermic peak from 120 – 140 °C. The endothermic peak from 65 – 110 °C was for the water from the sample and the peak from 120 – 140 °C is for the degradation of the sample. With the addition of 3 mg of genipin, the broad peak at 120 – 140 °C becomes a bit more defined and sharper than the one in the clean sample. With the 7.5 mg sample, the distinction between the two curves is not as distinct as the sample with 3 mg genipin and this could be due to the water content in this sample being higher.

For the 8 mg sample, the only peaks remaining are the 60 °C endothermic peak and the broad endothermic peak due to the water trapped in the sample that occurs from 70 – 120 °C. The degradation peak, due to α -relaxation, of the chitosan is not visible at around 140 – 150 °C. With an increase in the genipin concentration to 10 mg, the degradation peak is also not visible and this is indicative of the fact that after 8 mg, the genipin crosslinked samples do not degrade and/or go through an α -relaxation but rather are more stable at this temperature where the neat sample had an endothermic peak. There is a general trend in the graph that shows that the peak for the water trapped in the sample moves to lower temperature indicating that there is less water in the sample which is indicative of smaller pores in the samples due to the crosslinking. The absence of the second peak that was seen in the clean chitosan sample also shows that the sample was successfully crosslinked and did not go through a degradation phase in the temperature range shown. The lower crosslinking agent concentration samples did however show that the chitosan still underwent melting and this is due to the concentration being so low the effect of the crosslinking was not able to prevent the melting from taking place.

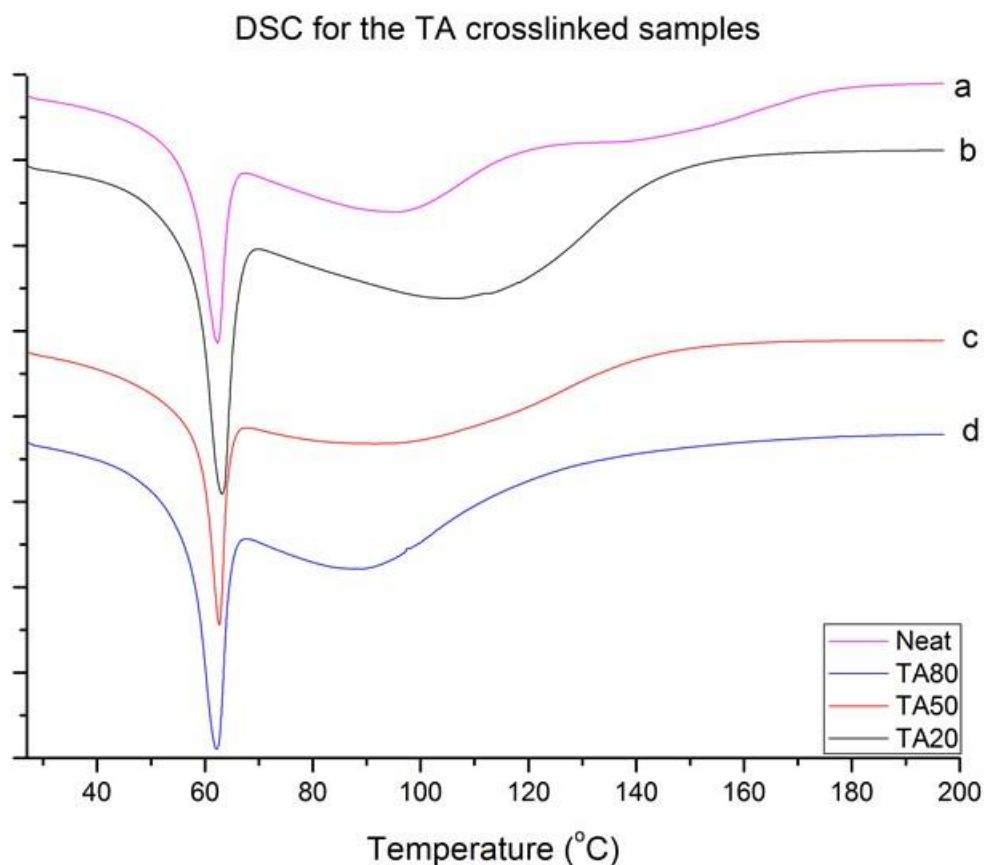


Figure 4.19: DSC thermogram of a) neat un-crosslinked chitosan sponge, b) 20mg tannic acid (TA20) crosslinked sample, c) 50mg (TA50) crosslinked sample and d) 80mg (TA80) crosslinked sample

Figure 4.19 shows the DSC thermograms for the tannic acid crosslinked sponges in comparison to the clean chitosan sample. On addition of just 20 mg of tannic acid the third peak from 118 – 170 °C that is visible in the neat chitosan sample is no longer visible and could be a part of the broader peak from 80 – 140 °C. The water degradation peak is however broader. On addition of 50 mg of TA, the broad peak from 65 – 135 °C is much less defined and does not reach the same temperature as the 20 mg TA sample did. The highest value for the broad peak for the 50 mg TA sample is also less than the value for the second peak in the clean sample. At a concentration of 4 wt% represented by 80 mg, the peak is at a value less than 100 °C and is much narrower. The peak at 60 °C is sharp for all the peaks and is similar in all the samples which indicates that the peaks appearing at this temperature are a result of the polymeric backbone and the interactions with the

backbone polymer. The graph shows that there is a decrease in the broad peak associated with the water trapped in the samples and this shows that as the chitosan was crosslinked, the pores within the samples became smaller and less water was trapped as a result. The second melting peak present in the clean sample is also not available indicating that the crosslinking of the sample resulted in a more thermally stable structure up for the temperature range shown.

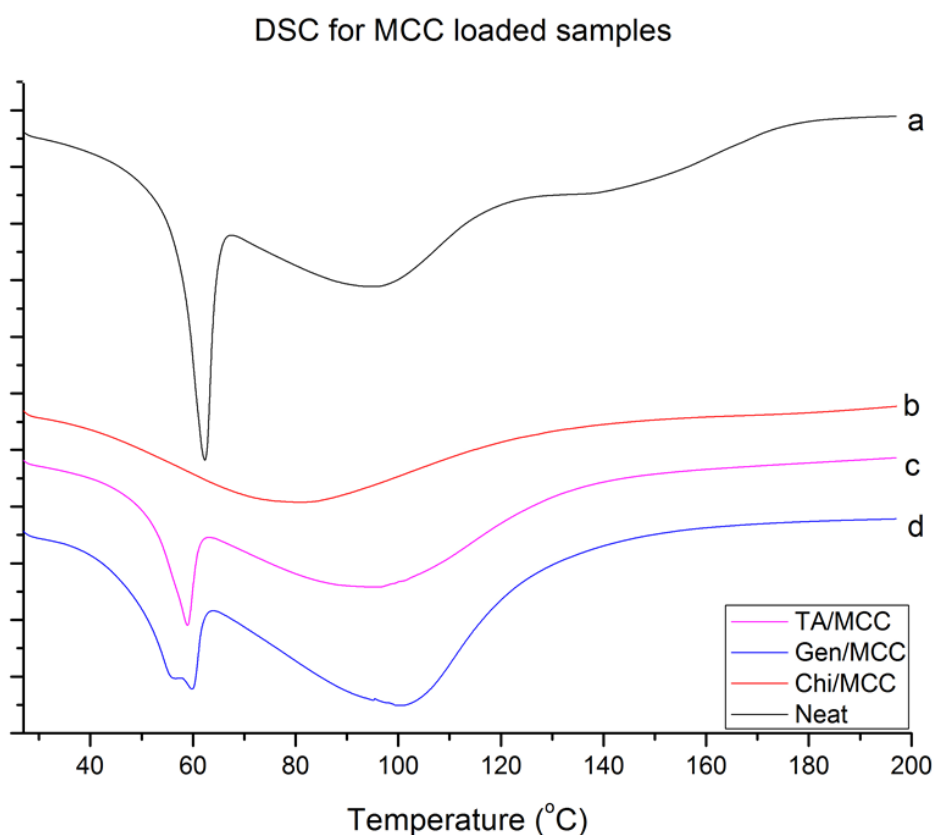


Figure 4.20: DSC thermogram of MCC loaded samples with a) neat uncrosslinked sample with no MCC, b) Chi/MCC sample, c) the TA/MCC sample and d) the Gen/MCC sample.

The above graph shows the DSC thermogram of the samples that had MCC loaded in them. We can see that once the MCC was added to the samples, the peak at the 60 °C temperature is not present for the Chi/MCC sample. There is a presence of a broad peak indicating the presence of

water in the sample. On crosslinking, the sample crosslinked with tannic acid shows the peak at 60 °C indicating that the tannic acid has an effect on the chitosan as it is able to maintain the structural properties of the chitosan responsible for the peak at 60 °C. This is also true for the genipin crosslinked sample, however, there is a shoulder on the peak at 60 °C which could be due to the MCC interacting with the genipin and the absence of a peak in the Chi/MCC indicating that the peak at 60 °C for the chitosan component is similar to that of the MCC and when they are in the same matrix they cancel each other out. The broad peak seen in the Chi/MCC sample shows that the MCC prevent the chitosan molecules from moving and thus limits flexibility [13]. This shows that the MCC is capable of adding to the mechanical properties of the chitosan due to the limited flexibility imparted by its addition.

4.8 Conclusion

Genipin and tannic acid were both successfully used to crosslink chitosan and to subsequently synthesize sponges using the bubbling technique. The synthesis of the sponges required variations in temperature and time for the crosslinking procedure to occur. Microcrystalline cellulose was incorporated in the sponges and the distribution was homogeneous as shown by confocal microscopy. The morphological properties of the synthesized sponges were influenced by the crosslinking agent used, the concentration of the crosslinking agent and the conditions used during the synthesis. These parameters played a big role in the resultant porosities as seen in the SEM images.

The temperature used during the synthesis of the sponges had an adverse effect on the resultant sponges and their morphology with the genipin crosslinked samples being affected positively in that the reaction time was reduced and the synthesis time was also reduced. The porosity could also be maintained for the samples that were synthesized at 60 °C in comparison to the samples that were synthesized at room temperature. For the TA samples, the temperature had an effect on reducing the crosslinking time from 7 hours to 5 hours.

The thermal properties of the sponges were also affected by the crosslinking and the addition of MCC to the sponges. The degradation of the samples in the temperature range from about 140 –

200 °C was decreased with a minimal addition of the crosslinking agents and at higher crosslinking agent concentration, they were not there implying a more stable sponge.

4.9 References

1. Muzzarelli R, El Mehtedi M, Bottegoni C, Aquili A, Gigante A. Genipin-Crosslinked Chitosan Gels and Scaffolds for Tissue Engineering and Regeneration of Cartilage and Bone. *Mar Drugs* . Multidisciplinary Digital Publishing Institute; **2015**;13(12):7314–38.
2. Garnica-Palafox IM, Sánchez-Arévalo FM. Influence of natural and synthetic crosslinking reagents on the structural and mechanical properties of chitosan-based hybrid hydrogels. *Carbohydr Polym*. **2016**;151.
3. Morgado PI, Lisboa PF, Ribeiro MP, Miguel SP, Simões PC, Correia IJ, et al. Poly(vinyl alcohol)/chitosan asymmetrical membranes: Highly controlled morphology toward the ideal wound dressing. *J Memb Sci* . Elsevier; **2014**;469:262–71.
4. Rivero S, García MA, Pinotti A. Crosslinking capacity of tannic acid in plasticized chitosan films. *Carbohydr Polym*. **2010**;82(2):270–6.
5. Yao CK, Liao J Der, Chung CW, Sung WI, Chang NJ. Porous chitosan scaffold cross-linked by chemical and natural procedure applied to investigate cell regeneration. *Appl Surf Sci* . Elsevier B.V.; **2012**;262:218–21.
6. Lai HL, Abu’Khalil A, Craig DQM. The preparation and characterisation of drug-loaded alginate and chitosan sponges. *Int J Pharm*. **2003**;251(1–2):175–81.
7. Chen C, Liu L, Huang T, Wang Q, Fang Y. Bubble template fabrication of chitosan/poly(vinyl alcohol) sponges for wound dressing applications. *Int J Biol Macromol* . Elsevier B.V.; **2013**;62:188–93.
8. Sung HW, Liang IL, Chen CN, Huang RN, Liang HF. Stability of a biological tissue fixed with a naturally occurring crosslinking agent (genipin). *J Biomed Mater Res*. **2001**;55(4):538–46.
9. Kreuter J. Nanoparticles and microparticles for drug and vaccine delivery. *J Anat*. **1996**;189 (Pt 3):503–5.
10. Nwe N, Chandkrachang S, Stevens WF, Maw T, Tan TK, Khor E, et al. Production of fungal chitosan by solid state and submerged fermentation. *Carbohydr Polym*. **2002**;49(2):235–7.
11. Delmar K, Bianco-Peled H. The dramatic effect of small pH changes on the properties of chitosan hydrogels crosslinked with genipin. *Carbohydr Polym*. **2015**;127:28–37.
12. Kumari R, Dutta PK. Physicochemical and biological activity study of genipin-crosslinked chitosan scaffolds prepared by using supercritical carbon dioxide for tissue engineering applications. *Int J Biol Macromol*. **2010**;46(2):261–6.

13. Bégin A, Van Calsteren MR. Antimicrobial films produced from chitosan. *Int J Biol Macromol*. **1999**;26(1):63–7.
14. Mori T, Okumura M, Matsuura M, Ueno K, Tokura S, Okamoto Y, et al. Effects of chitin and its derivatives on the proliferation and cytokine production of fibroblasts in vitro. *Biomaterials*. **1997**;18(13):947–51.
15. Seol Y-J, Lee J-Y, Park Y-J, Lee Y-M, Young-Ku, Rhyu I-C, et al. Chitosan sponges as tissue engineering scaffolds for bone formation. *Biotechnol Lett*. **2004**;26:1037–41.
16. Zhang Y, Zhang M. Three-dimensional macroporous calcium phosphate bioceramics with nested chitosan sponges for load-bearing bone implants. *J Biomed Mater Res*. **2002**;61(1):1–8.
17. Busilacchi A, Gigante A, Mattioli-Belmonte M, Manzotti S, Muzzarelli RAA. Chitosan stabilizes platelet growth factors and modulates stem cell differentiation toward tissue regeneration. *Carbohydr Polym* . Elsevier Ltd.; **2013**;98(1):665–76.
18. Silva SS, Motta A, Rodrigues MT, Pinheiro AFM, Gomes ME, Mano JF, et al. Novel genipin-cross-linked chitosan/silk fibroin sponges for cartilage engineering strategies. *Biomacromolecules*. **2008**;9(10):2764–74.
19. Silva MC, Andrade CT. Evaluating conditions for the formation of chitosan/gelatin microparticles. *Polímeros* . ABPol; **2009** ;19(2):133–7.
20. Kuo YC, Ku IN. Cartilage regeneration by novel polyethylene oxide/chitin/chitosan scaffolds. *Biomacromolecules*. **2008**;9(10):2662–9.
21. Mucha M, Pawlak A. Thermal analysis of chitosan and its blends. **2005**;427:69–76.
22. Archana D, Dutta J, Dutta PK. Evaluation of chitosan nano dressing for wound healing: Characterization, in vitro and in vivo studies. *Int J Biol Macromol* . Elsevier B.V.; **2013**;57:193–203.
23. Dong Y, Ruan Y, Wang H, Zhao Y, Bi D. Studies on glass transition temperature of chitosan with four techniques. *J Appl Polym Sci*. Wiley Subscription Services, Inc., A Wiley Company; **2004**;93(4):1553–8.

5 Chapter 5: Absorption and mechanical results

5.1 Introduction

Multiple factors are known to be responsible for the absorption properties of polymeric materials. Chitosan is a polyelectrolyte and this plays a vital role in the ability to absorb water [1]. An increase in the crosslinking agent concentration results in a reduction of these polyelectronic sites thereby reducing the hydrophilicity. However, other factors are also involved in the absorption of water and exudates and those include the porosity of the samples and the nature of the crosslinking agents. *Chen et al* indicated that an increase in glutaraldehyde concentration for the crosslinking of chitosan led to a decrease in the water absorption rate and was due to an increase in the crosslinking density [2].

The glutaraldehyde molecule is significantly smaller than the genipin and TA molecules and as such the crosslinking bridges would be smaller and more compact than the genipin and TA and this could result in this reduction in absorption. The main focus in this chapter was to determine the effect of the TA and genipin crosslinking agents on the absorption properties. For this purpose absorption tests were done and the results will be discussed in the following section.

The modification of the naturally occurring polymer, chitosan, is done for the betterment of the mechanical properties and to prevent the material synthesized from the polymer from degrading quickly [3]. The focus of the mechanical tests is to determine the effect of crosslinking the chitosan based sponges with tannic acid and genipin. Further analysis is based on the effect differing the crosslinking agent content has on these properties. Porous materials are required to have good/adequate mechanical strength to support cellular growth during the tissue development stage in the healing process [4]. The porosity of the sponges is advantageous for tissue growth but the strength is expected to be adequate to allow for a uniform regeneration [4].

5.2 Absorbance results analysis

The ability of the samples to absorb exudate is of importance as it is one of the reasons for using a sponge in the synthesis of a scaffold for the use as a wound dressing. As such, the results that were obtained from the absorbance tests are summarised in the following table and analysed.

Table 5.1: Absorbance results

Sample	Test 1	Test 2	Test 3	Average absorbance	Standard error
	Absorbance	Absorbance	Absorbance		
Neat	485.05	489.62	496.54	490.40	5.78
Chi/MCC	522.08	531.52	547.18	533.59	12.68
Gen/MCC	344.65	326.14	349.93	340.24	12.49
TA/MCC	582.75	601.22	594.89	592.95	9.39
TA20	480.86	478.00	446.92	468.60	18.82
TA40	463.26	474.23	486.46	474.65	11.61
TA50	598.22	599.10	600.99	599.43	1.41
TA80	608.69	614.33	623.90	615.64	7.69
TA125	656.97	647.72	646.51	650.40	5.72
TA200	672.36	684.81	687.23	681.46	7.98
Gen 5mg	257.09	260.08	233.23	250.13	14.71
Gen 7.5mg	300.90	312.74	306.85	306.83	5.92
Gen 10mg	579.05	578.42	583.62	580.36	2.84

From the above results, the following graph could be obtained to clearly show the effect the crosslinking agents had on the absorbance properties.

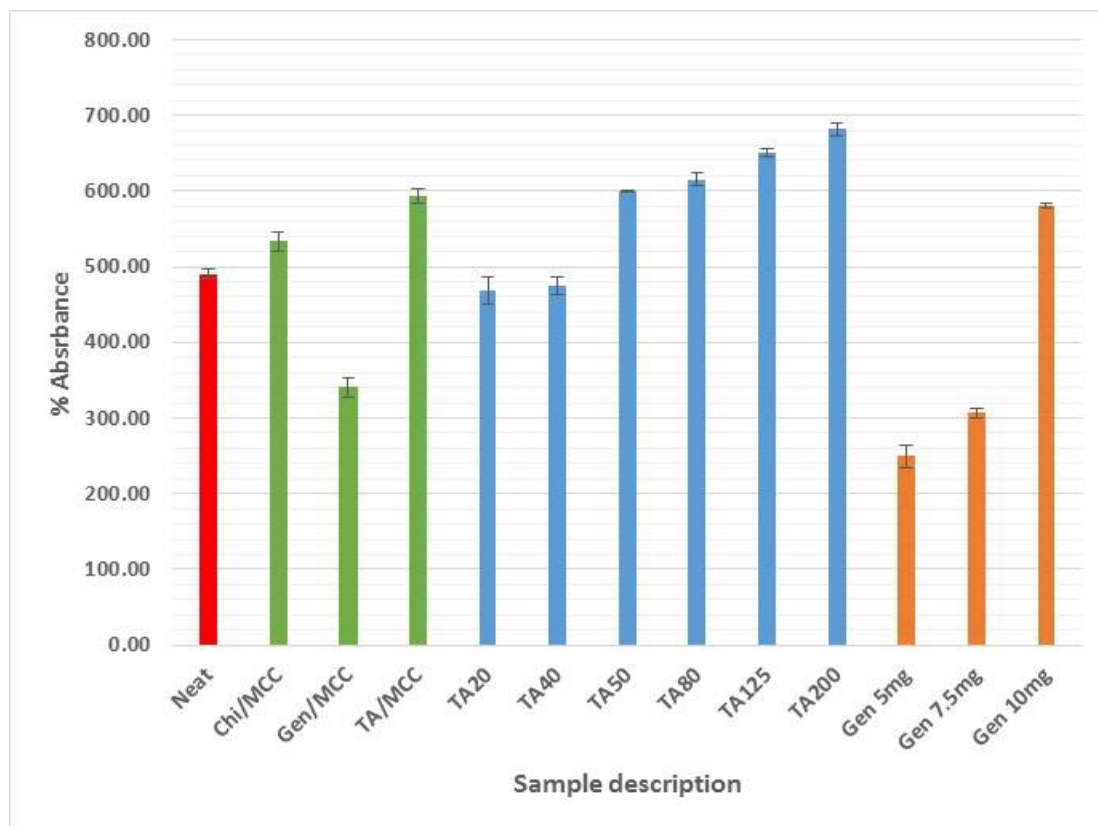


Figure 5.1 : Comparison of the absorbance properties

It has been reported that glutaraldehyde is the most studied synthetic chemical for crosslinking chitosan and as such, reference to the advancements made in the wound treatment field can be made [3, 5]. Crosslinking with glutaraldehyde has shown that there is a decrease in the absorbance properties and was due to the glutaraldehyde causing a rigid structure. The absorbance in glutaraldehyde crosslinked chitosan sponges was therefore largely due to the chitosan and the porous structure [6]. For the samples that were crosslinked with genipin, the concentrations that were below 7.5 mg showed that this was also true for the genipin crosslinked samples. This can also be attributed to the decrease in the ability of the molecular chains in the polymeric chains as they had formed new bonds. This is evidenced by the reduction in the peak intensity for the samples that were crosslinked with genipin in the FTIR spectrum in Figure 4.7 [7]. The Gen/MCC sample showed a decrease in the absorbance in comparison to the neat sample and this was indicative of the rigid structure that was formed. The sample was crosslinked with 3.5 mg of genipin which was lower than the samples crosslinked 7.5 mg genipin, but was higher than the 5 mg genipin

crosslinked sample. This shows that the MCC had a positive effect on the absorbance as it was higher, with an absorbance of 340%, than the 7.5 mg crosslinked sample with an absorbance of 300%. For the samples with 10 mg genipin, the absorbance was however higher than that of the clean sample. This can be attributed to the structure of the sponge that is crosslinked with the higher concentration of genipin having larger pores due to the faster crosslinking action. This was also true for the samples that were crosslinked with the tannic acid, as the lower crosslinking agent concentration samples, the absorbance was less than that of the clean samples and increased with TA concentration increase. *Rivero et al* reported that the increase in the tannic acid concentration had no effect on the absorbance of chitosan films that were crosslinked using tannic acid [5]. This shows that the porosity of the samples was the main reason for the increase in the absorbance seen in the graph. This porosity, however, could also result in the tannic acid's hydrophilic nature to come to the fore as there is a larger surface area in comparison to a film and could have a greater effect on the absorbance in the sponges. Therefore, the increase in the absorbance for the tannic acid crosslinked samples can also be attributed to this hydrophilic nature of the TA as it has many hydroxyl moieties in its structure. The FTIR results that are shown in Figure 4.8 show that there is an increase in the transmittance peaks in the $3000 - 3400 \text{ cm}^{-1}$ range which indicates an increase in the hydrogen bonds. TA is also very bulky in comparison to the genipin molecule and as such could result in there being a larger free volume which would also affect the absorbance properties.

5.3 Mechanical properties

The mechanical properties for the sponges are an important factor in that they give us an indication of the parameters that might need changing to mould a product that will suit the end use. As such, the compressional tests were performed on the samples to distinguish the effects imparted by the various materials used in the synthesis of the sponges. The compressional tests were used to determine the mechanical properties for sponges and were also capable of showing the importance of each component in the composite [8]. The compressional test results in this section were obtained by placing a weight on the samples and measuring the compression after an hour. Readings of the compression after the hour were taken down to calculate the stress experienced by the sponges and give an idea of the resultant mechanical properties.

The following graphs, Figure 5.2 and Figure 5.3, show the results for the samples that were uncrosslinked, the samples crosslinked with glutaraldehyde, TA and the samples crosslinked with genipin. The glutaraldehyde (glut) sample was used as a reference as there is an abundance of literature on the improvement of mechanical properties when used to crosslink chitosan and as such was used to compare the properties imparted at 3 % crosslinking density [2]. Neat chitosan samples were also subjected to the compression and this was then used as a reference to determine the effect the crosslinking had on the mechanical properties.

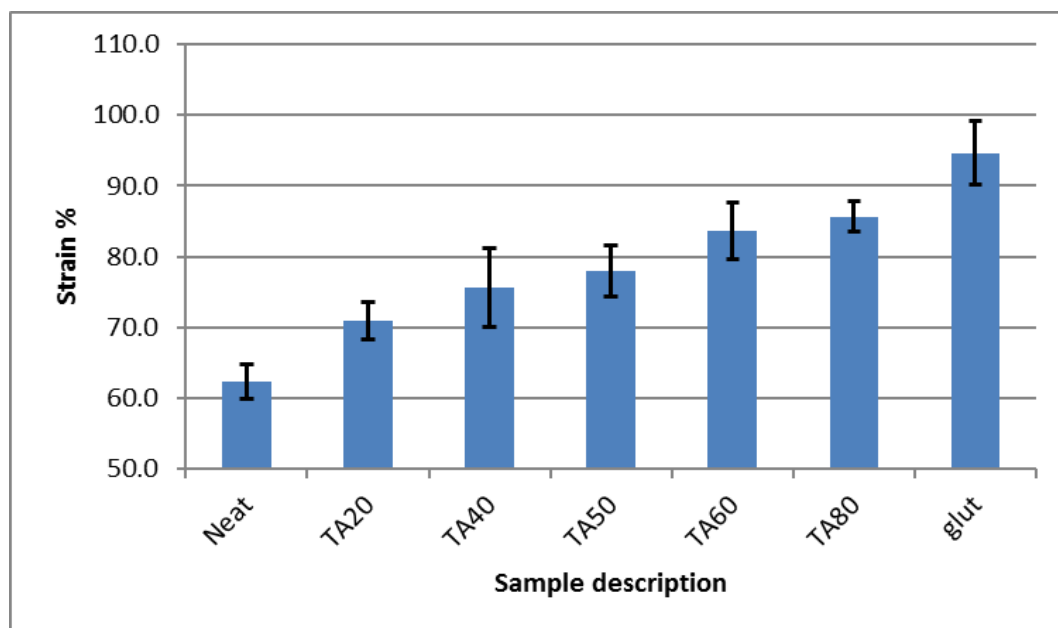


Figure 5.2: Compressional test results showing Strain % for TA crosslinked samples

The strain experienced by the samples showed a clear trend with regard to increasing tannic acid concentration as can be seen in the graph in Figure 5.2. The uncrosslinked sample had undergone the most compression and as such had a percentage strain average of 63 %. This was due to the uncrosslinked sample having a weaker structure in comparison to the TA crosslinked samples. The TA had a positive effect on the strain due to the compression for the crosslinked samples being less for all the crosslinked samples in comparison to the uncrosslinked samples. The trend seen in the graph is that there is an increase in the mechanical properties with an increase in the TA concentration as evidenced by increase in the strain percentage. The samples crosslinked with glutaraldehyde had the highest strain percentage of all the samples in the graph with a 95% strain.

The closest to this value was the TA80 sample with 87%. This was less than the glutaraldehyde sample but was far much better than the uncrosslinked sample.

The samples that were crosslinked with genipin, seen in Figure 5.3, showed a similar trend in that the increase in the concentration of the genipin resulted in an increase in the resistance to the compression as seen in the increment of the strain percentage. The addition of 1 mg genipin was significant enough to raise the strain percentage to an average of 68% in comparison to the uncrosslinked sample which had 63%. This shows that the genipin was indeed crosslinking the sample as this resulted in better mechanical properties. The increment in the strain percentage for these low concentrations of the genipin shows how effective using such low concentrations have on the mechanical properties.

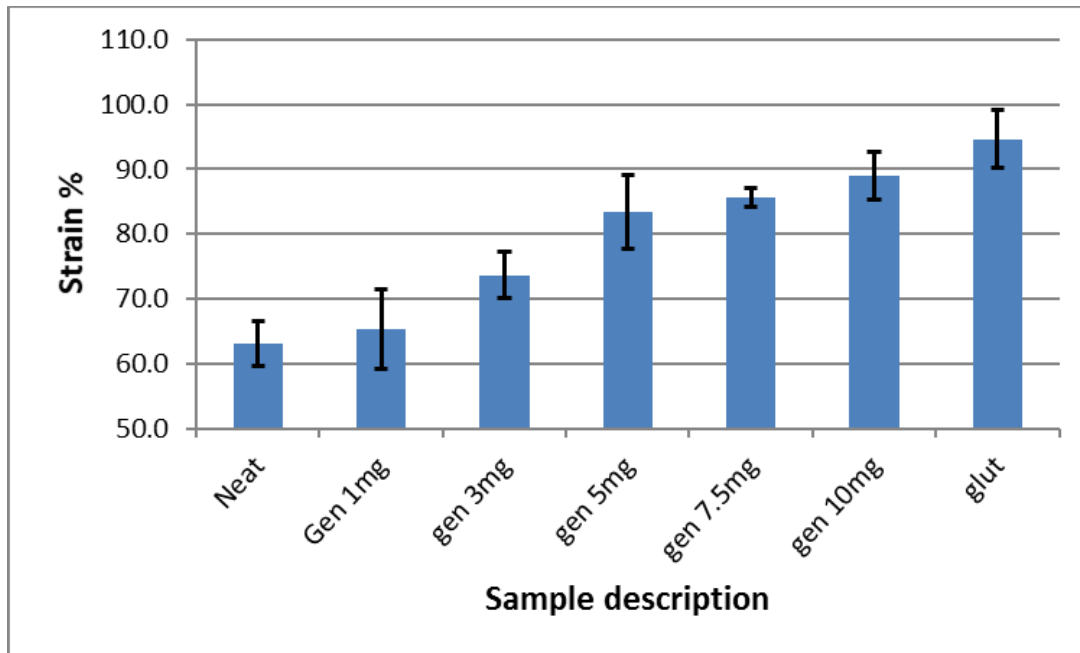


Figure 5.3 : Compression results showing strain (%) for genipin crosslinked samples

The compressive modulus is an important part of determining the mechanical properties as it gives the ratio of the stress applied to the material and how much it compresses [8]. The method that we used, however, was rudimentary and was mainly for determining if there was any significant difference in the ability to resist compression between the different samples with different concentrations.

5.4 Conclusions

The absorbance properties for the sponges were improved with an increase in both the TA and genipin concentrations. This shows that the porosity of the sponges was influenced by the increase in the crosslinking agent concentration. This was due to the fusion of the air bubbles in the matrix that led to larger pores which would result in a more accessible area within the sponge and increase the absorbance. The crosslinking agents are also capable of enhancing the hydrophilic properties, although the polyelectronic sites are reduced, due to TA having a large number of hydroxyl groups that can counter this reduction.

The mechanical properties with regard to the compressional stability were also analysed. The analysis showed that the clean chitosan sample did have a relatively good resistance to compression but this was improved by the crosslinking. The samples that were crosslinked had higher strain percentages implying they could better resist compression. The use of TA and genipin had good results but these were however less than those obtained for glutaraldehyde at the concentrations studied. The glutaraldehyde sample had a 95% strain percentage whilst the TA crosslinked samples with the highest resistance to compression had an 87% strain and the genipin crosslinked sample with the highest resistance had 89% strain.

5.5 References

1. Dimida S, Demitri C, De Benedictis VM, Scalera F, Gervaso F, Sannino A. Genipin-cross-linked chitosan-based hydrogels: Reaction kinetics and structure-related characteristics. *J Appl Polym Sci* . **2015**;132(28)
2. Chen C, Liu L, Huang T, Wang Q, Fang Y. Bubble template fabrication of chitosan/poly(vinyl alcohol) sponges for wound dressing applications. *Int J Biol Macromol* . Elsevier B.V.; **2013**;62:188–93.
3. Sung H-W, Huang R-N, Huang LLH, Tsai C-C. In vitro evaluation of cytotoxicity of a naturally occurring cross-linking reagent for biological tissue fixation. *J Biomater Sci Polym Ed*. Taylor & Francis Group ; **1999** ;10(1):63–78.
4. Sionkowska A, Płanecka A. Preparation and characterization of silk fibroin/chitosan composite sponges for tissue engineering. *J Mol Liq*. **2013**;178:5–14.
5. Rivero S, García MA, Pinotti A. Crosslinking capacity of tannic acid in plasticized chitosan films. *Carbohydr Polym*. **2010**;82(2):270–6.
6. Vimala K, Mohan YM, Sivudu KS, Varaprasad K, Ravindra S, Reddy NN, et al. Fabrication of porous chitosan films impregnated with silver nanoparticles: A facile approach for superior antibacterial application. *Colloids Surfaces B Biointerfaces*. **2010**;76(1):248–58.
7. Garnica-Palafox IM, Sánchez-Arévalo FM. Influence of natural and synthetic crosslinking reagents on the structural and mechanical properties of chitosan-based hybrid hydrogels. *Carbohydr Polym*. **2016**;151.
8. Sionkowska A, Kaczmarek B, Lewandowska K. Modification of collagen and chitosan mixtures by the addition of tannic acid. *J Mol Liq* . Elsevier B.V.; **2014**;199:318–23.

6 Chapter 6: Antimicrobial results

6.1 Introduction

Chitosan has essential properties that include its antimicrobial efficacy which gives it the ability to prevent bacteria from growing [1-5]. The efficacy of chitosan has however been reported to be limited and a variety of methods can be applied to try and increase the antimicrobial efficacy of the chitosan composites [6]. As such, the chitosan composites could be boosted by incorporating other polymeric materials that are antimicrobial within the chitosan matrix that is to be used as a wound dressing material. This can also be overcome by modifying the surface of the chitosan by attaching antimicrobial agents so as to make areas in contact with the affected areas have a higher efficacy or by incorporating silver nanoparticles and other drugs to boost the efficacy [3].

In this section, the effect of crosslinking with genipin and tannic acid had on the chitosan based sponges, was investigated in order to determine if the inherent antimicrobial properties were affected or if there was any additional efficacy imparted and/or enhanced on the sponges. The effects of incorporating an antimicrobial peptide, namely Gramicidin S (GS), were monitored along with the effects of incorporating microcrystalline cellulose (MCC), a reinforcing agent, within the sponge would have on the final antimicrobial properties of the sponges. The MCC was a viable choice in the reinforcement and the peptide attachment possibilities as it is also used as a diluent in tablets, that is, it is used as a therapeutic enhancement of the active ingredient [5]. This would help increase and/or bring the GS effects to the foreground once incorporated into the sponge. The GS has been used in recent research and had successfully shown that cellulose had positive attachment of the peptide which would also possibly be beneficial in the enhancement of the antimicrobial results [7]. In this study, the MCC was added to the sponges to further enhance the mechanical properties and to possibly assist with the attachment of the GS.

6.2 Antimicrobial results

The synthesized sponges, after attachment of the peptides as indicated in Section 3.7.8, were dried using two methods, that is, in the oven at 40°C and by the lyophilisation method. The lyophilisation method was time consuming and as such the method of drying the sponges in the oven was used

to dry the sponges faster. Both the drying methods were successful in drying the samples but had different properties depending on the method used. As such, the results obtained for both the drying procedures were analysed to determine if the temperature used to dry the sponges had any effect on the resultant antimicrobial properties. The results in the following section were obtained from the samples that were dried in the oven after peptide attachment unless otherwise stated. It is important to note that the percentage inhibition can go over 100% which would indicate prevention of growth and killing the bacteria.

Antimicrobial activity for genipin (oven dried)

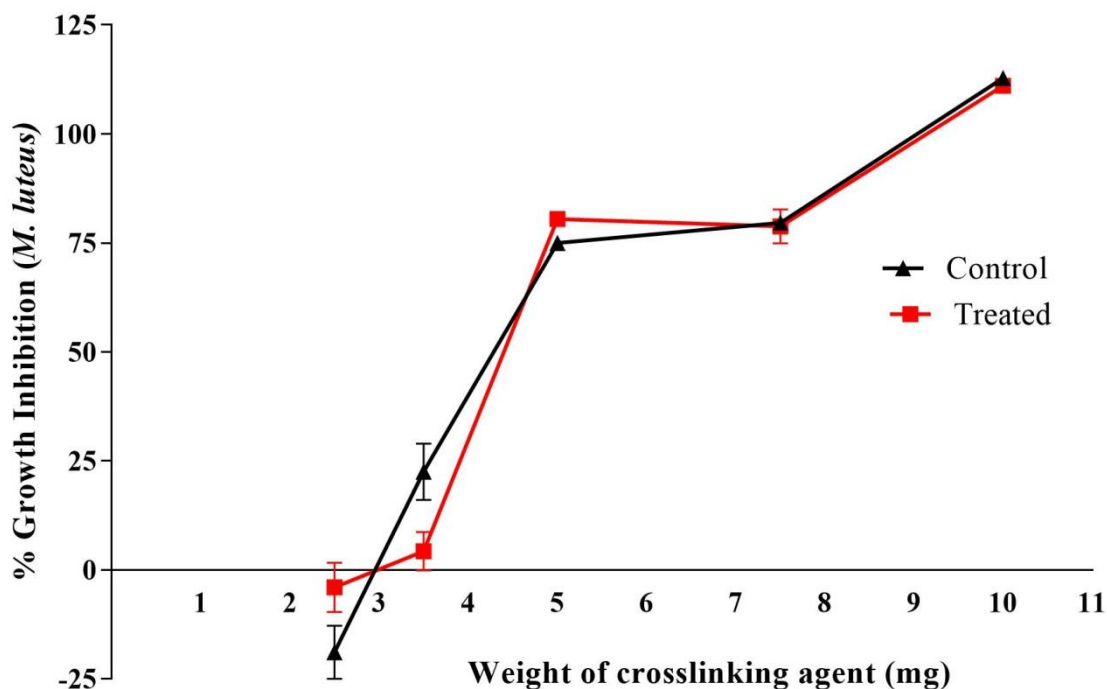


Figure 6.1: Antimicrobial activity for the control and GS treated genipin crosslinked sponges

The above graph shows the effect the genipin concentration used in the crosslinking procedure, had on the antibacterial efficacy of the sponge. The graph clearly shows that there was an increase in the antimicrobial efficacy of the crosslinked sponges, labelled control, that were crosslinked with genipin. From the graph we can also see that when the genipin concentration was increased, the percentage growth inhibition of the samples also increased indicating that the crosslinking procedure had a positive effect on the antimicrobial properties of the chitosan.

The results labelled as treated in the graph were for the samples that had GS incorporated in the sponges. From the graph, the effect of the GS loaded on the sponges is miniscule in terms of the resultant antimicrobial efficacy as they are similar to the untreated samples. At each of the genipin concentrations, there were minor differences which could be due to the bacterial behaviour and not the antimicrobial nature of the components. The trend imparted by the GS was however not clear as to whether it was higher than the samples that were not treated or lower as there is

alternation between the selected samples. This is seen with the treated samples being higher in percentage growth inhibition for the samples crosslinked with 2.5 mg (0.125 wt%) and the 5 mg (0.25 wt%) genipin and lower for the samples crosslinked with 3.5 mg (0.175 wt%) and the 10 mg (0.5 wt%) genipin. there was a slight dip in the antimicrobial efficacy for the sample crosslinked with 7.5 mg (0.375 wt%) genipin. The general trend for the genipin crosslinked samples was that there was an increase in the efficacy with an increase in the genipin concentration.

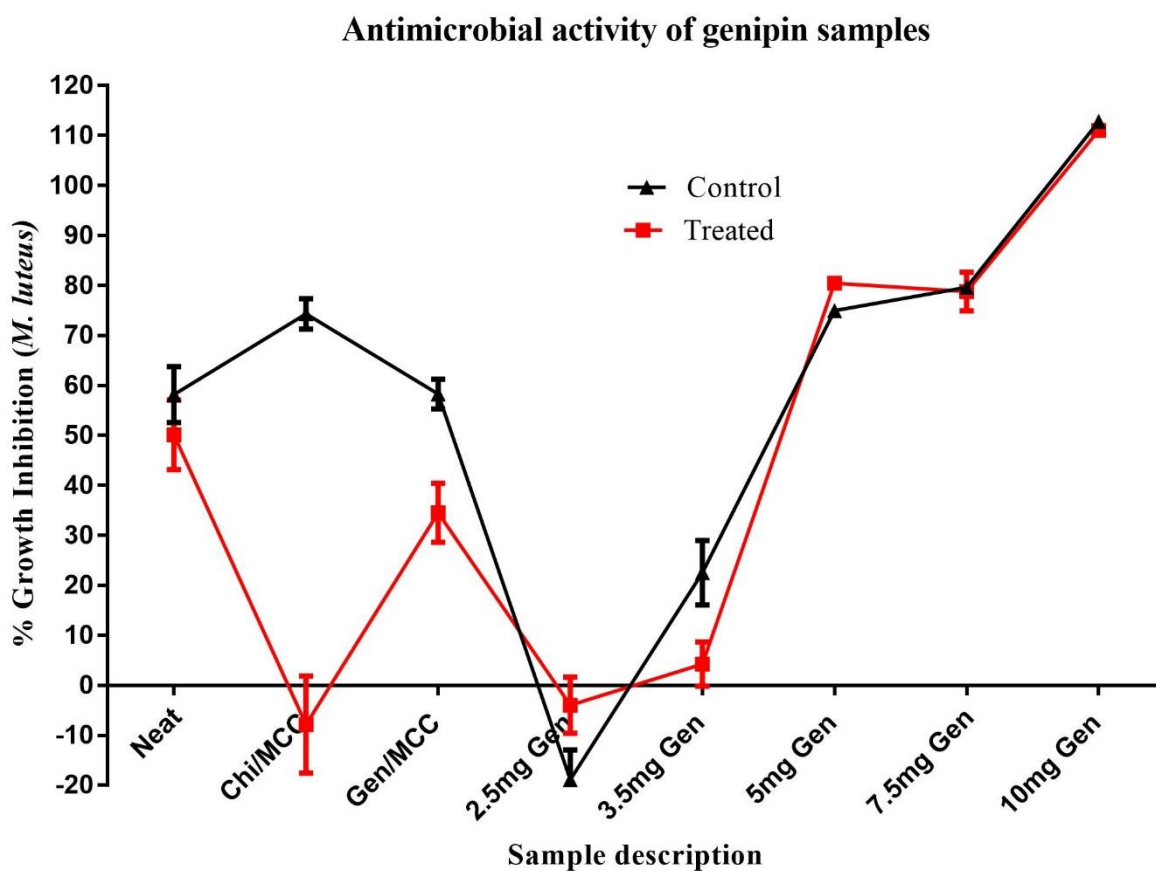


Figure 6.2: Antimicrobial activity for the genipin crosslinked samples, MCC loaded samples and the neat uncrosslinked samples

The graph above, Figure 6.2, illustrates the effect of the uncrosslinked samples, the samples that had MCC incorporated in them and the samples that were crosslinked with genipin. The samples that were not crosslinked, labelled “Neat” in the graph, show that there was no significant effect to the growth inhibition when compared to the samples that were treated with the GS. There is a

slight drop in the percentage growth inhibition that suggests some interaction with the sponges, but was less significant as it was within the error region.

The samples that had MCC incorporated showed that when they were not treated with GS, the growth inhibition increased whereas the samples that were treated with GS showed a large drop in comparison to the untreated MCC loaded control sample. The decrease in the efficacy suggests that the GS was interacting with the Chi/MCC sponge in such a way that the active sites for both the GS and the Chi/MCC complex were blocked off and allowed the bacteria to grow. This could be due to the ionic nature of the GS, chitosan and the MCC interacting in such a way that the antimicrobial properties are lost. The mechanism in which the GS interacts with the membranes of the bacteria is such that the peptide disrupts the lipid bilayer which results in simultaneous augmentation of its permeability that causes cell death [8, 9].

The above results also show that when the crosslinking of the chitosan sponges, with as low as 5 mg, which is 0.25 % (w/w) genipin to chitosan concentration, led to a significant increase in the antimicrobial properties of the sponges. This goes to show that the crosslinking process in the synthesis of the sponges creates a structure that has a higher efficacy than the lower concentration and uncrosslinked samples.

Antimicrobial activity for tannic acid (oven dried)

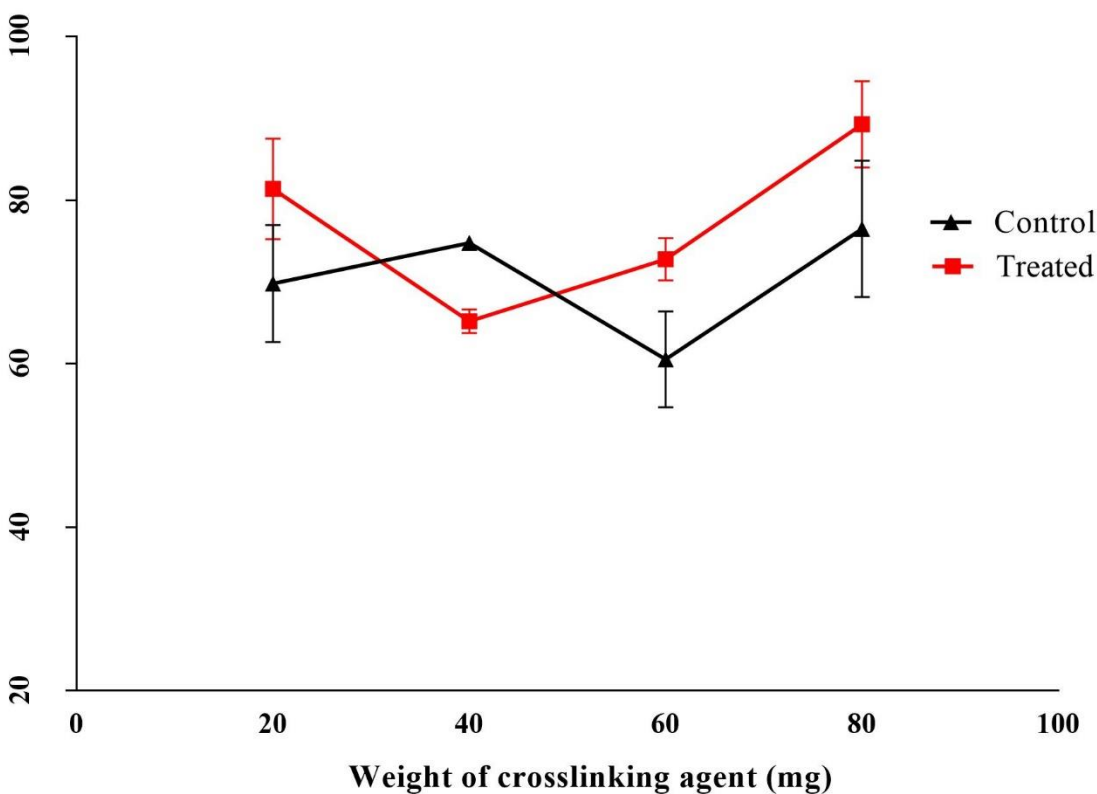


Figure 6.3: Graph of the antimicrobial properties for the tannic acid crosslinked samples

For the samples that were crosslinked using tannic acid (TA), the above graph was obtained. The effect that was as a result of the increment in the TA did not show any distinct trend but rather showed that the efficacy ranged between 50 % and 90 % for all the samples. An increase in the TA concentration did not show any recognisable trend. The samples that were treated with GS showed that with the lower concentration sample, namely 20 mg TA (1 wt%), the efficacy was higher and dropped at 40 mg (2 wt%) concentration and then rose again for the 60 mg (3 wt%) sample and was highest for the 80 mg (4 wt%) sample. The reason for this behaviour could be that the lower crosslinking agent concentration sample had smaller pores and this resulted in the GS settling on the surface of the sample and imparting some of the growth inhibition seen for the 20 mg sample. The sample crosslinked with 40 mg of TA showed a decrease in the growth inhibition in comparison to the 40mg sample which could indicate that the interaction between the GS and the sponge was more pronounced and resulted in a decrease in the efficacy. The sample with 60

mg TA also had a lower percentage growth inhibition and as such shows that there was negative interaction between the GS and the sponge. As the concentration increased to 80 mg, it seems as though the TA in the sample played a larger role in the percentage growth inhibition as there is a higher inhibition in comparison to all the other samples.

The samples that were not treated, however, showed that the samples with the 20 mg TA concentration had a lower growth inhibition in comparison to the treated sample which implied that the GS was the determining factor for these samples' efficacy. The sample with 40 mg was however lower for the GS treated samples which indicated that the GS interaction with the sponges resulted in a decrease of active sites to prevent growth. There was a decrease and an increase for the samples with 60 mg and 80 mg TA respectively. This anomaly indicated that there might be some interaction with the different TA concentrations or that the differences averaged out and meant that there was generally no effect to the antimicrobial properties imparted by the crosslinking.

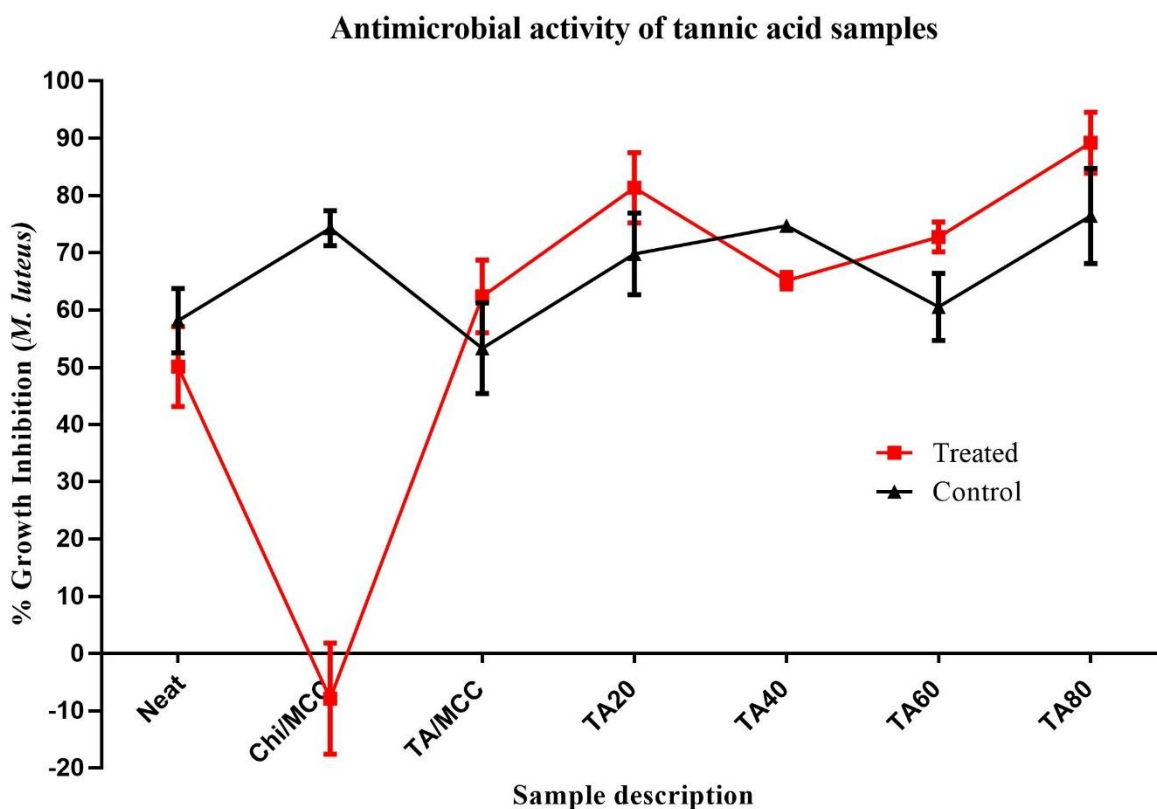


Figure 6.4: Graph of antimicrobial properties of tannic acid crosslinked samples

The effects that resulted from the addition of MCC to the tannic acid crosslinked samples can be seen in Figure 6.4 above. For the control samples, the addition of MCC resulted in an increase in the percentage growth inhibition of the bacteria in comparison to the clean samples. When the samples that were loaded with MCC were crosslinked using TA, the percentage growth inhibition decreased. This shows that there might be an interaction between the TA, the MCC and the chitosan which resulted in the samples having similar percentage growth inhibition to those of the clean samples.

For the samples that had MCC loaded, had been crosslinked with TA (labelled TA/MCC) and treated with the GS, the growth inhibition was higher than that of the clean sample which indicated that the GS and the TA had a positive effect on the antimicrobial efficacy of the sponges. The antimicrobial efficacy of the treated sponges was also higher than that of the untreated sample indicating that the GS was imparting some of the antimicrobial properties observed. This could be as a result of the crosslinking with TA allowing the GS to contribute to the antimicrobial properties of the sponges.

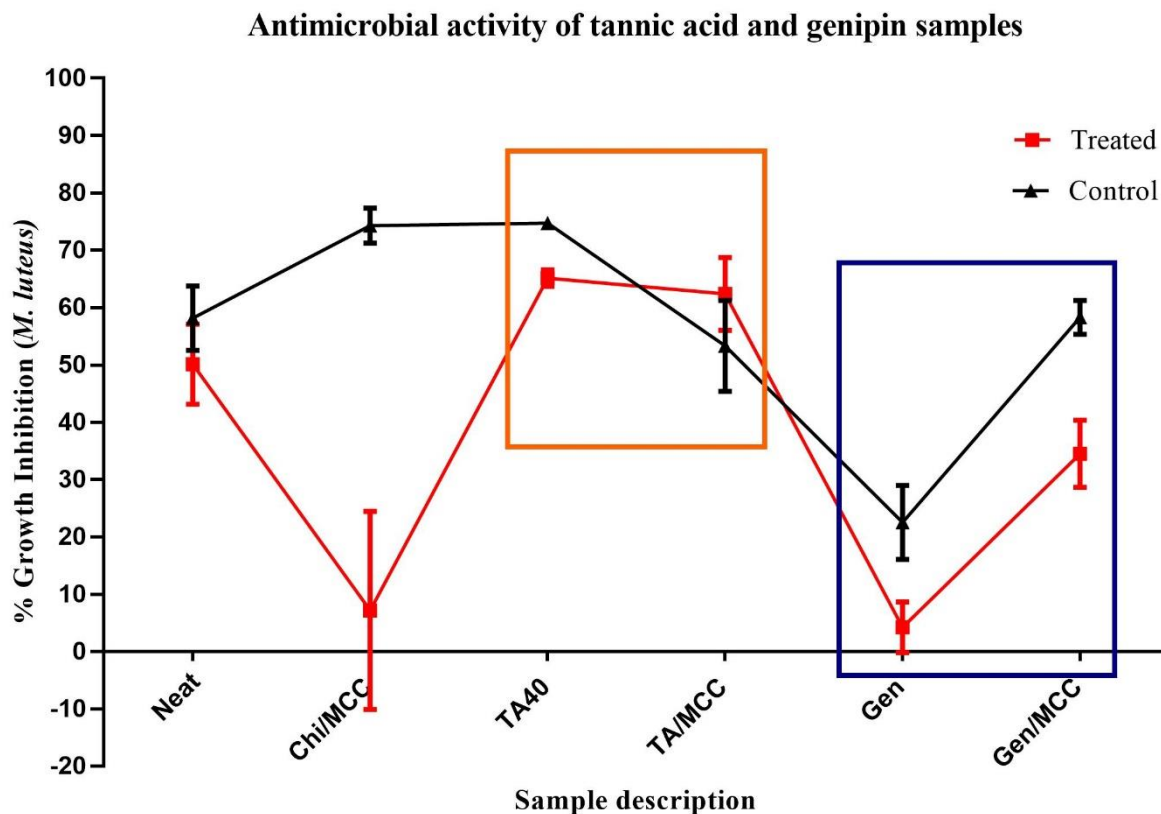


Figure 6.5: A comparison of the effect of MCC on the sponges both crosslinked and uncrosslinked.

To directly compare the effect of the MCC on the resultant sponges, results from the samples that had the same crosslinking agent concentration were plotted in the Figure 6.5 above. The large drop in the percentage growth inhibition for the sample that was loaded with MCC was presumably due to the interaction between the different components. The distribution of the MCC in the samples, as seen in **Error! Reference source not found.**, was homogeneous therefore the interaction with the peptides was not in question. The concentration of the MCC was high in the sample, 10 wt%, so as to ensure all the sections of the samples had MCC present in the MCC loaded sponges to eliminate the chances of considering a GS untreated area. This goes to show that the interaction between the peptide and the chitosan loaded with MCC resulted in the poor performance of the percentage growth inhibition.

The samples in the orange box were crosslinked using 40 mg TA, which is 2 wt%, and from the results we can see that for the samples that were not treated with GS, the bacterial growth inhibition of the sponge dropped. This could be the result of the interaction between the different components

of the sponges interacting in such a way that the antimicrobial properties are reduced. There is a strong possibility that the MCC and the TA could have hydrogen bonding between the large amount of hydroxyl moieties present in their structures and the cationic nature of the chitosan would result in a decrease in the active sites. There is a clear indication that the MCC and the TA resulted in higher antimicrobial efficacy when used individually as seen in the increase from the clean to the TA40 samples and Chi/MCC samples respectively. When both the MCC and the TA were used to synthesize a sample, the percentage growth inhibition decreased and implies that the MCC and TA interacted in a negative way towards the antimicrobial properties. The samples that were treated with GS showed a relatively similar percentage growth inhibition in both the samples with and without MCC, that is, TA/MCC and TA40 respectively.

For the samples that were crosslinked using genipin, the microbial growth inhibition was decreased significantly for the samples that did not contain MCC in comparison to the clean sample. The treated sample showing the largest drop in the growth inhibition indicating a negative effect from crosslinking with the lower concentration of the genipin as illustrated in Figure 6.2. The samples in the blue box in Figure 6.5 refer to the genipin crosslinked samples of the sponges and show that the addition of the MCC to the sponges resulted in a higher inhibition. This was the case for both the treated and untreated samples as they both showed an increase in the percentage inhibition in comparison to the sample without MCC. The indication from the graph was that the values obtained for the samples Gen/MCC are more or less the average of the values of the Chi/MCC and Gen samples for the untreated sponges.

For the treated samples, however, the sum of the Chi/MCC and the Gen samples resulted in the percentage inhibition of the Gen/MCC sample. This shows that the GS was playing a part in the antimicrobial efficacy values in a positive way for the combination of the MCC and the low concentration genipin samples. At this stage, we could not determine, however, if the increment was because of the peptide or because of all the components working together. What is clear is that the Gramicidin S played a role in the increment of the antimicrobial nature of the sponge due to the increment seen in comparison to the untreated samples.

The following results were obtained for the samples that were dried using the freeze drying method. The results obtained for both the crosslinking agents when using the freeze drying method

were different from the results obtained for the samples that had been dried in the oven. This implies that temperature has a significant influence on the antimicrobial properties.

Antimicrobial activity for genipin (freeze dried)

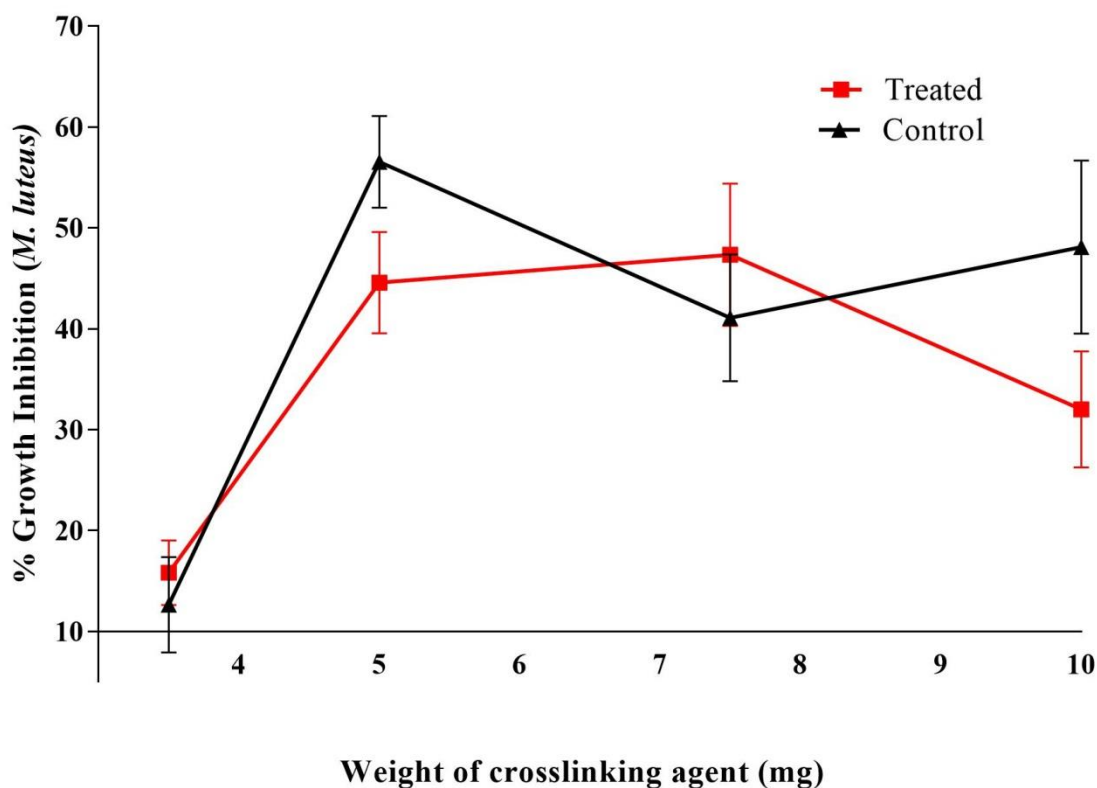


Figure 6.6: Graph of antimicrobial activity of freeze-dried genipin crosslinked samples

The results that are shown in Figure 6.6 were obtained for the genipin crosslinked samples that had been freeze-dried after the peptide attachment. From the results in Figure 6.1, we can see that there is a distinct difference in the antimicrobial properties imparted on the sponges from the lyophilisation procedure. For the samples that were oven dried, at 5 mg (0.25 wt%) concentration of genipin, the percentage growth inhibition had an average of 80 % whereas in the case of the freeze-dried samples, the inhibition was at 60 %. The microbial inhibition also decreased with an increase in the genipin concentration for the samples that were freeze-dried. This shows that there is an adverse effect on the antimicrobial properties and these effects are due to the thermal activity that takes place during the interaction with the peptides for the genipin crosslinked samples during

the drying process in the oven. The similarities that are observed are the lack of a distinct and clear difference between the samples that were treated with the peptide and the samples that had not been treated.

The graph above, Figure 6.6 also shows a similar trend to that observed for the TA sponges that had been dried in the oven as seen in Figure 6.3. The graphs show that with an increase in the crosslinking agent concentration, there was either an increase or decrease occurring simultaneously for the untreated control samples.

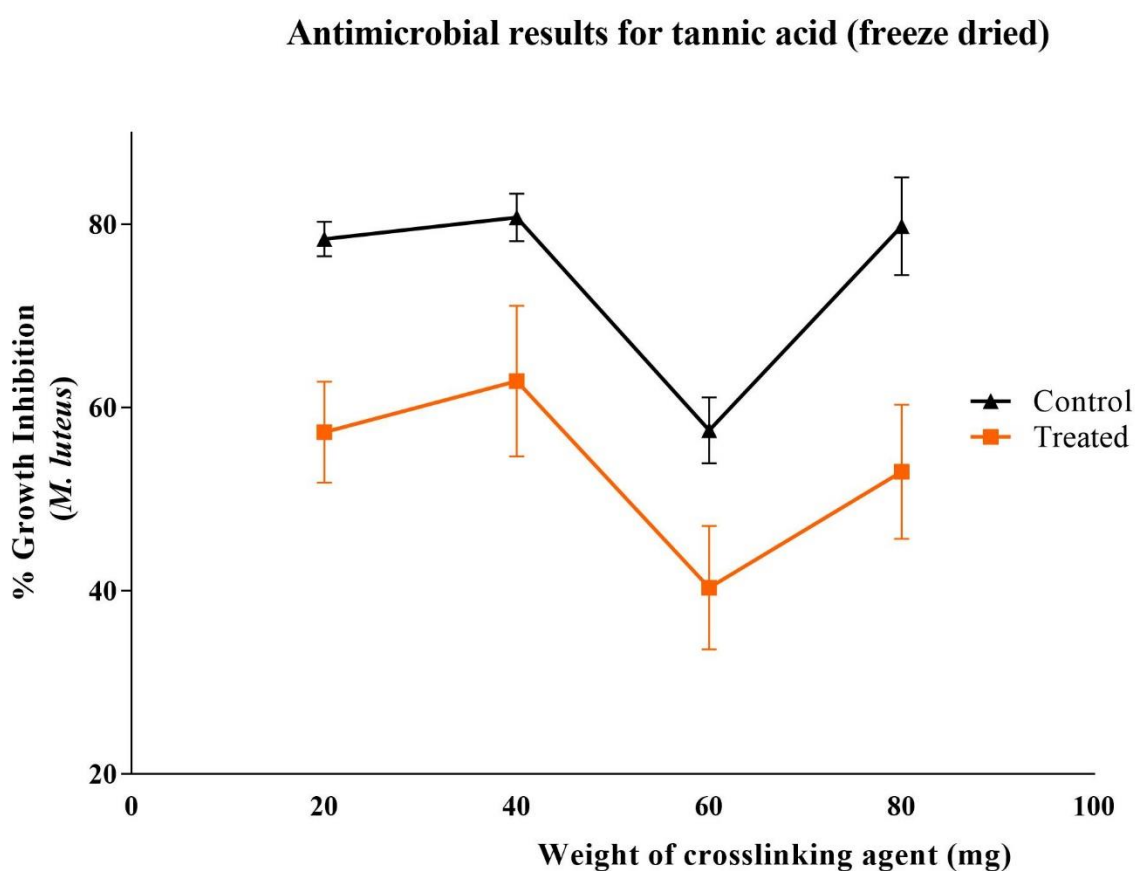


Figure 6.7: Graph of antimicrobial activity for freeze-dried TA crosslinked samples

The above graph, Figure 6.7, show the results obtained for the samples that were crosslinked using TA and from this graph we can see that there is a slight increase in the antimicrobial properties with an increase in the tannic acid concentration for the untreated control samples. The results also show values that are higher than those obtained for the samples that were dried in the oven that are

shown in Figure 6.3. This shows that TA had a positive effect on the antimicrobial properties for the TA crosslinked samples that were dried using the freeze-drying method. These results indicate that the heat from drying the sample in the oven had a detrimental effect on the antimicrobial properties which could be due to degradation of the complex.

There is a clear distinction between the treated and the untreated samples in Figure 6.7 above. The samples that were treated with the antimicrobial peptide showed reduced efficacy as they had a lower growth inhibition percentage in comparison to the control samples. The treated samples show an increase from 20 mg to 40 mg and a decrease at 60 mg and an increase again to 80mg. This shows that the TA crosslinked samples and the GS interaction in the sponges had an effect on the properties and these effects resulted in unpredictable outcomes and the exact effect not known. The samples that were untreated showed a slight increase in the percentage growth inhibition but were significantly higher than the clean sample that had not been treated with the GS as seen in Figure 6.4.

6.3 Conclusions

This section was aimed at determining the effect of the crosslinking, the incorporation of MCC and the attachment of antimicrobial peptides on the antimicrobial properties of the chitosan sponges. It was observed that the genipin crosslinking of the samples had varying effects on the percentage growth inhibition depending on the method used to dry the samples. When the samples were dried in the oven, the antimicrobial efficacy of the samples increased with an increase in the crosslinking agent concentration. This showed that the genipin also imparted some of the antimicrobial properties of the resultant sponges at higher crosslinking agent content. The samples that were crosslinked with genipin and dried in the freeze-drier after peptide treatment showed that the antimicrobial efficacy was generally similar with some unpredictability in the efficacy.

The samples that were crosslinked using the TA showed that the samples that were freeze-dried had a higher inhibition in comparison to the samples that were oven dried. This shows that the oven drying procedure had an adverse effect on the antimicrobial properties and the better method was freeze-drying after the peptide attachment. The samples that were oven dried and crosslinked

with the TA exhibited similar properties to the samples that were crosslinked with genipin and freeze-dried after the attachment of the GS in that they were mostly unpredictable.

The samples that had MCC incorporated showed that there was an increase in the percentage growth inhibition for the samples that were not treated with the GS. The samples that were treated with GS had a lower percentage growth of 7 % growth inhibition than the untreated samples which had 74 % growth inhibition implying that there was some blockage of the active sites in the sponges. When the samples were crosslinked with TA, the antimicrobial efficacy did increase compared to the untreated samples and this increase in the percentage growth inhibition could be due to the crosslinking reducing the interaction between the uncrosslinked MCC incorporated samples with the bacteria. For the genipin crosslinked samples, the treated samples had a lower percentage inhibition compared to the untreated samples.

6.4 References

1. Anitha A, Divya Rani VV, Krishna R, Sreeja V, Selvamurugan N, Nair SV, et al. Synthesis, characterization, cytotoxicity and antibacterial studies of chitosan, O-carboxymethyl and N,O-carboxymethyl chitosan nanoparticles. *Carbohydr Polym.* **2009**;78(4):672–7.
2. Koide SS. Chitin-chitosan: Properties, benefits and risks. *Nutr Res.* 1998;18(6):1091–101.
3. Chen C, Liu L, Huang T, Wang Q, Fang Y. Bubble template fabrication of chitosan/poly(vinyl alcohol) sponges for wound dressing applications. *Int J Biol Macromol* . Elsevier B.V.; **2013**;62:188–93.
4. Radhakumary C, Antonty M, Sreenivasan K. Drug loaded thermoresponsive and cytocompatible chitosan based hydrogel as a potential wound dressing. *Carbohydr Polym* [Internet]. Elsevier Ltd.; **2011**;83(2):705–13.
5. Ravi Kumar MN. A review of chitin and chitosan applications. *React Funct Polym* [Internet]. **2000**;46(1):1–27.
6. Pranoto Y, Rakshit SK, Salokhe VM. Enhancing antimicrobial activity of chitosan films by incorporating garlic oil, potassium sorbate and nisin. *LWT - Food Sci Technol.* **2005**;38(8):859–65.
7. Hilpert K, Elliott M, Jenssen H, Kindrachuk J, Fjell CD, Körner J, et al. Screening and Characterization of Surface-Tethered Cationic Peptides for Antimicrobial Activity. *Chem Biol.* **2009**;16(1):58–69.
8. Andreu D, Cativiela C. Therapeutic Index of Gramicidin S is Strongly Modulated by D - Phenylalanine Analogues at the. **2009**;664–74.
9. Staudegger E, Prenner EJ, Kriechbaum M, Mcelhaney RN, Lohner K. X-ray studies on the interaction of the antimicrobial peptide gramicidin S with microbial lipid extracts : evidence for cubic phase formation. **2000**;1468.

7 Chapter 7: Conclusions and recommendations

7.1 Conclusions

In this study, chitosan based sponges were synthesized and characterised both with and without modifications aimed at bettering the mechanical properties. The modifications that were applied were crosslinking with genipin, glutaraldehyde and tannic acid (TA); and the incorporation of microcrystalline cellulose (MCC).

7.1.1 Synthesis of chitosan based sponges and modifications

The synthesis of chitosan based sponges reinforced by crosslinking with two natural crosslinking agents' tannic acid, genipin and a synthetic crosslinking agent glutaraldehyde (glut) was achieved using the bubbling method and freeze-drying. The synthesis method was optimised for both crosslinking agents as they required different synthesis parameters namely, temperature, time, crosslinking agent concentration, incorporation of microcrystalline cellulose, the treatment with antimicrobial peptides and the maintenance of the porous structure of the sponges. The optimum conditions were achieved to enable the synthesis of continuously porous structures. The influence of these parameters on the sponge properties differed and these differences were analysed in comparison to the neat uncrosslinked sample.

7.1.2 Morphological properties

The use of crosslinking agents resulted in porous structures that had pores that increased in size with an increase in the crosslinking agent concentration. This was as a result of the crosslinking process restricting the movement of bubbles within the matrix and fusing the bubbles that resulted in large pores. For the samples crosslinked with genipin, the synthesis at 60°C yielded the best sponges with a porous structure. The tannic acid samples had a better structure when synthesized at room temperature. The incorporation of MCC affected the morphology of the samples as it resulted in an uneven surface for the sponges. Scanning electron microscopy (SEM) was used to determine these morphological properties. The distribution of the MCC in the samples was, however, homogeneous as was seen in the images obtained using confocal microscopy. This technique gives a depth image that shows that the distribution was not just homogeneous at the surface but throughout the samples.

7.1.3 Sponge characteristics

The successful crosslinking of the chitosan was confirmed by FTIR which was used to show the characteristic peaks representing the groups affected by the crosslinking. The technique was also capable of showing the differences in the concentrations of the crosslinking agents as seen in Appendix A. The crosslinking was also confirmed using the redissolution method and showed that the samples that were crosslinked did not redissolve. The thermal properties for the sponges were improved as the degradation of the neat chitosan sponges occurred at a lower temperature of 200°C whereas the crosslinked samples started degrading at 230°C as shown by TGA analysis. This was also confirmation that the crosslinking process was successful.

The absorbance properties of the chitosan sponges, both crosslinked and uncrosslinked, were then analysed. This showed that the absorbance properties were improved for the samples crosslinked with TA. For the samples crosslinked with genipin, it was only at higher genipin concentrations that the absorbance properties were higher than those of the uncrosslinked samples. This can be attributed to the larger pore sizes seen for the samples with higher genipin content used for the crosslinking. The samples that had MCC incorporated showed that there was an increase in the absorption for all the samples used in comparison to samples with the same crosslinking agent concentration but with no MCC.

The compressional resistance of the sponges was measured and showed that there was an increase in the strain percentage for the samples that were crosslinked in comparison to the uncrosslinked samples. The focus in this part was to compare a synthetic crosslinking agent namely glutaraldehyde, in comparison to the two natural crosslinking agents genipin and tannic acid. The results showed that the sponges crosslinked with glut had higher percentage strain compared to the TA and genipin crosslinked samples.

7.1.4 Antimicrobial properties

This section was aimed at determining the effect the crosslinking and the modifications that had been applied had on the inherent chitosan antimicrobial properties. This was achieved with the alamar assay which confirmed the pros and cons of the synthesis methods. For the genipin crosslinked samples, the antimicrobial efficacy increased with an increase in concentration for the

samples dried in the oven. The samples that were freeze – dried did not show a significant trend other than the initial increase from low genipin concentrations. This was the case for both the samples treated with Gramicidin S (GS) and the control samples. For the TA samples, the samples that were freeze – dried showed a clear distinction between the GS treated samples and the untreated samples in that the GS had a negative effect on the antimicrobial efficacy. For the TA samples that were dried in the oven, the percentage growth inhibition remained relatively the same for both the sample without any clear trend.

The incorporation of MCC to the uncrosslinked chitosan sample resulted in an increase in the antimicrobial efficacy for the samples that were not treated with GS. The samples treated with GS, however, had a large drop in the percentage inhibition in comparison to both the neat sample and the untreated sample indicating a negative interaction with the GS. For the samples with MCC and crosslinked with TA, the GS treated samples had higher antimicrobial properties compared to the untreated samples which indicated a positive interaction with the GS. The samples that were crosslinked with genipin and had MCC showed higher percentage growth inhibition in comparison to the samples that did not have MCC for both the treated and untreated samples.

The overall conclusions drawn from the study was that the crosslinking of chitosan if carefully controlled could yield desirable properties. The crosslinking was capable of bettering the mechanical properties of the sponges by increasing the strain percentage. The morphology of the sponges was more controlled and the porosity much more defined for the crosslinked samples. The absorbance properties of the sponges were increased due to an increase in the porosity and was a function of the crosslinking agent concentration. The antimicrobial properties of chitosan sponges were improved by the crosslinking procedures and was dependant on the concentrations of the crosslinking agents with the higher concentrations having better efficacy.

7.2 Recommendations

Recommendations for further studies include

- The determination of the effect of the pore sizes at the same crosslinking agent concentrations on the antimicrobial properties

- The determination of the time temperature relationship during the synthesis of the sponges on the antimicrobial properties for the samples treated with GS
- Determination of the antimicrobial properties with different antimicrobial properties
- The effect of using multiple antimicrobial polymers on the mechanical and antimicrobial properties
- Determination of the possibility to use the sponges in wounds
- The use of differing MCC loading on the antimicrobial properties
- The effect of incorporating the antimicrobial peptides during the synthesis on the physical and chemical properties of the sponges

8 Appendix A

FTIR comparisons for the different genipin and TA content

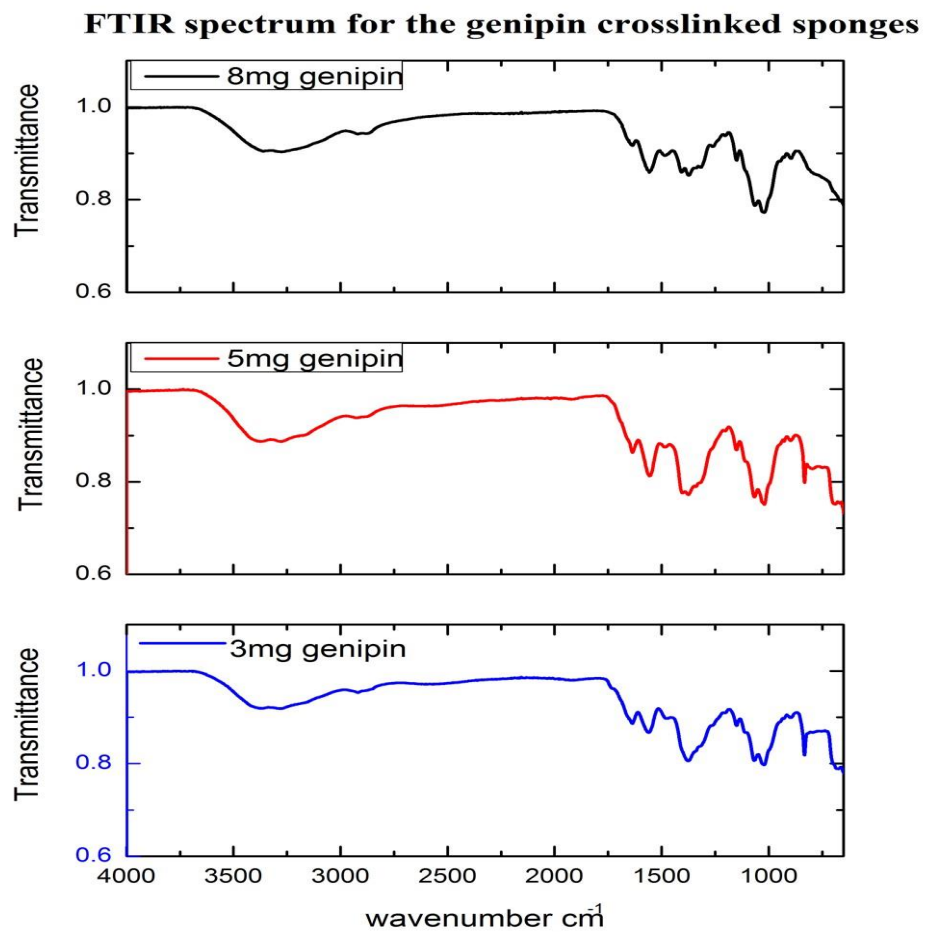


Figure A. 1: FTIR spectra of chitosan sponges crosslinked with 3,5 and 8mg genipin

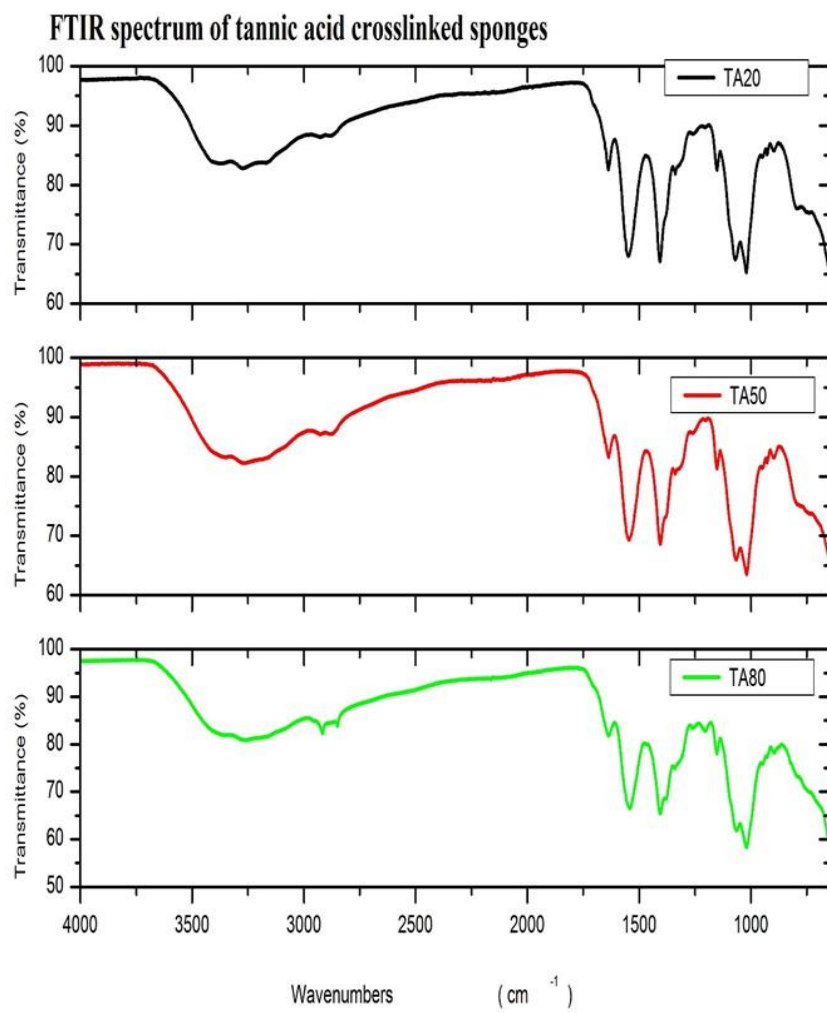


Figure A. 2: FTIR spectrum of chitosan sponges crosslinked with 20, 50 and 80 mg TA

9 Appendix B

SEM images of the sponges and a comparison of the different crosslinking agent content

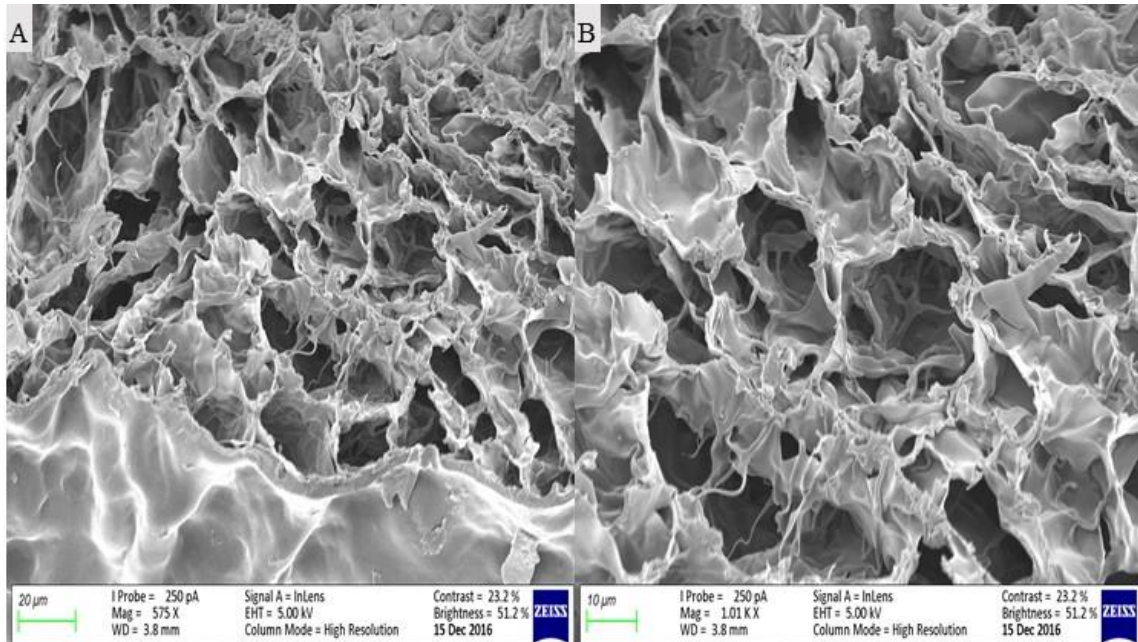


Figure B. 1: SEM images of glutaraldehyde crosslinked sponges at two magnifications

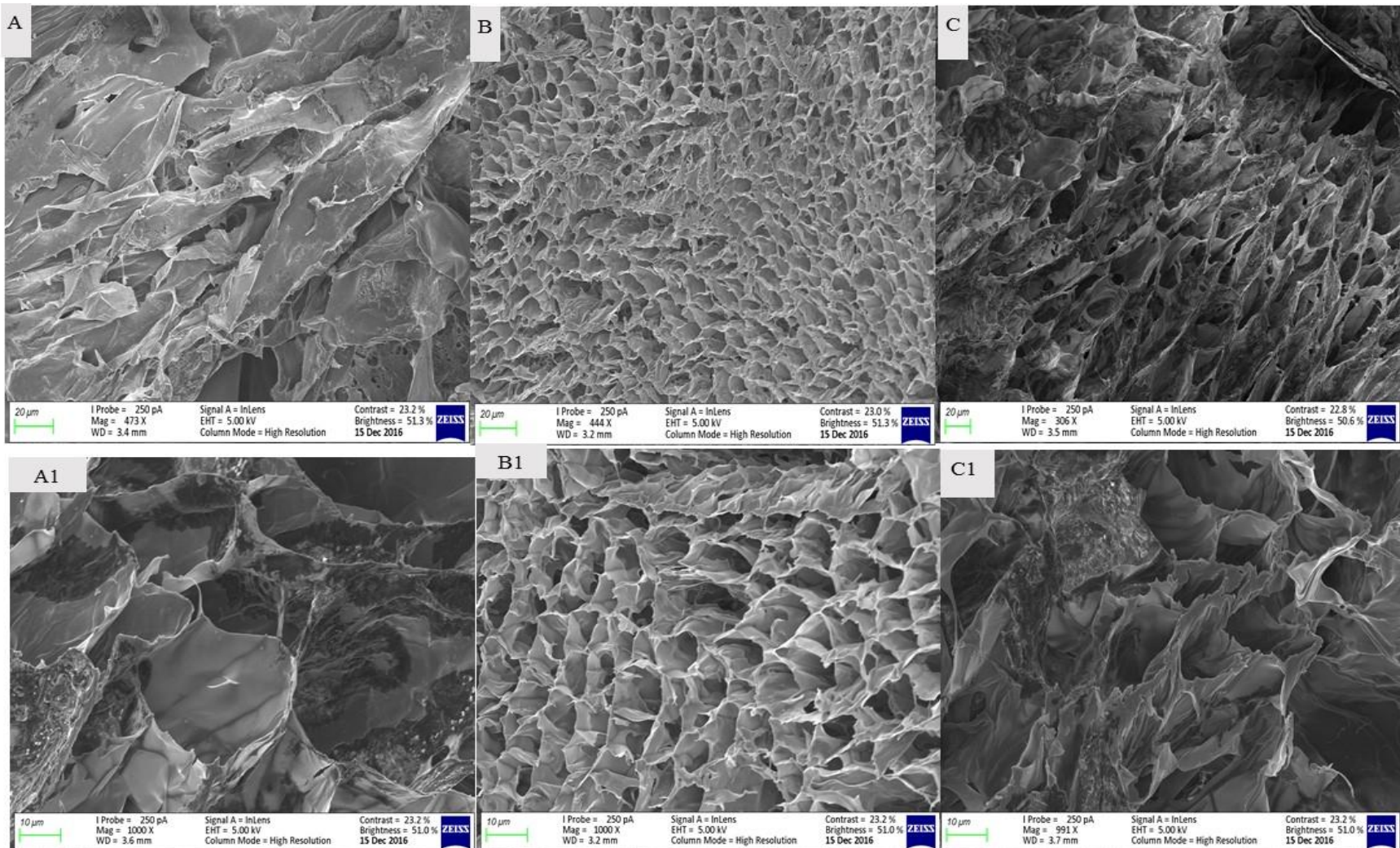


Figure B. 2: SEM images of genipin crosslinked samples with A and A1 – 3mg genipin sample; B and B1 – 5mg sample; and C and C1 – 10mg sample at different magnifications

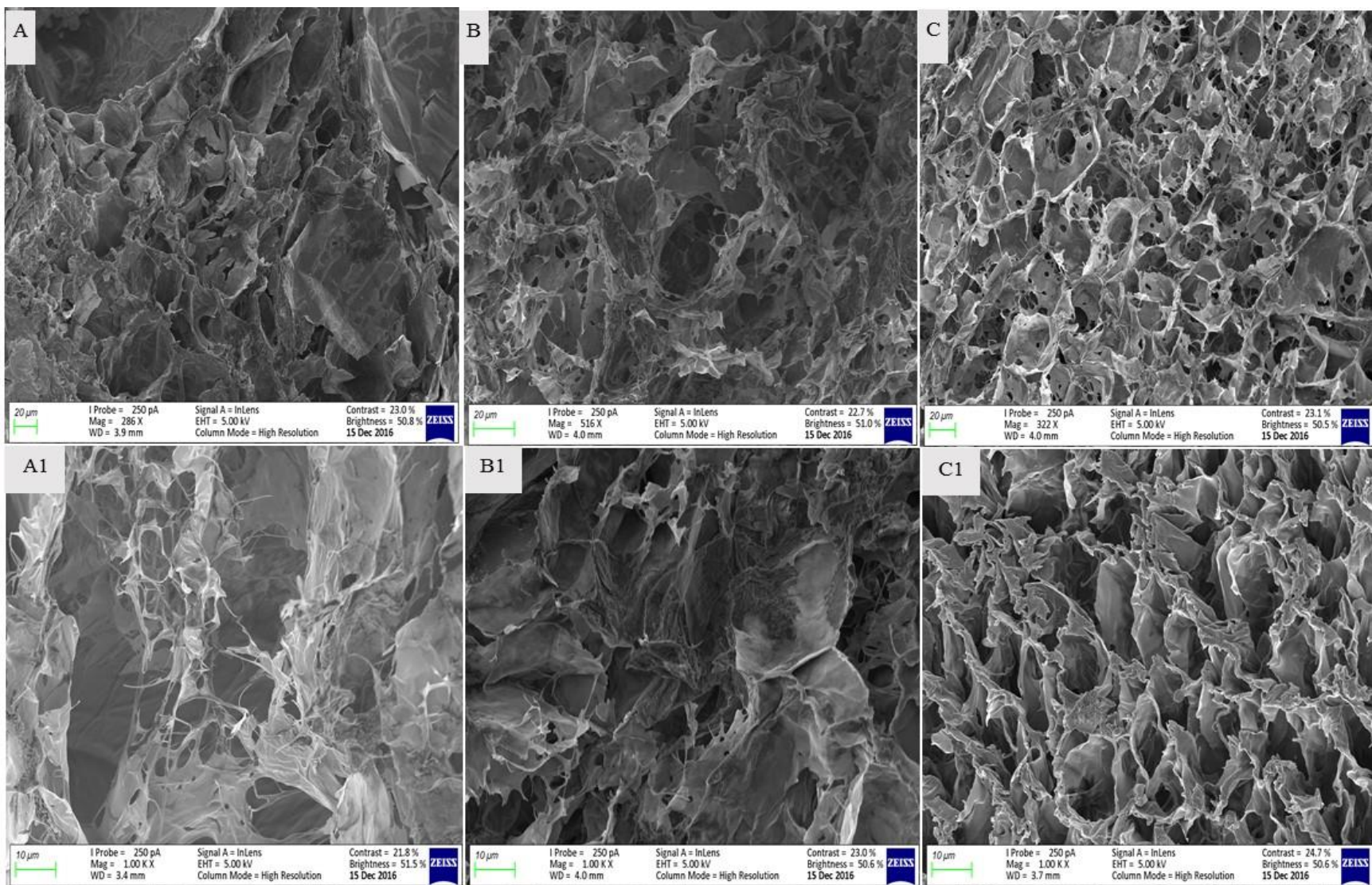


Figure B. 3: SEM images of TA crosslinked sponges with A and A1 – TA80 sample; B and B1 – TA50 sample; and C and C1 – TA20 sample at different magnifications

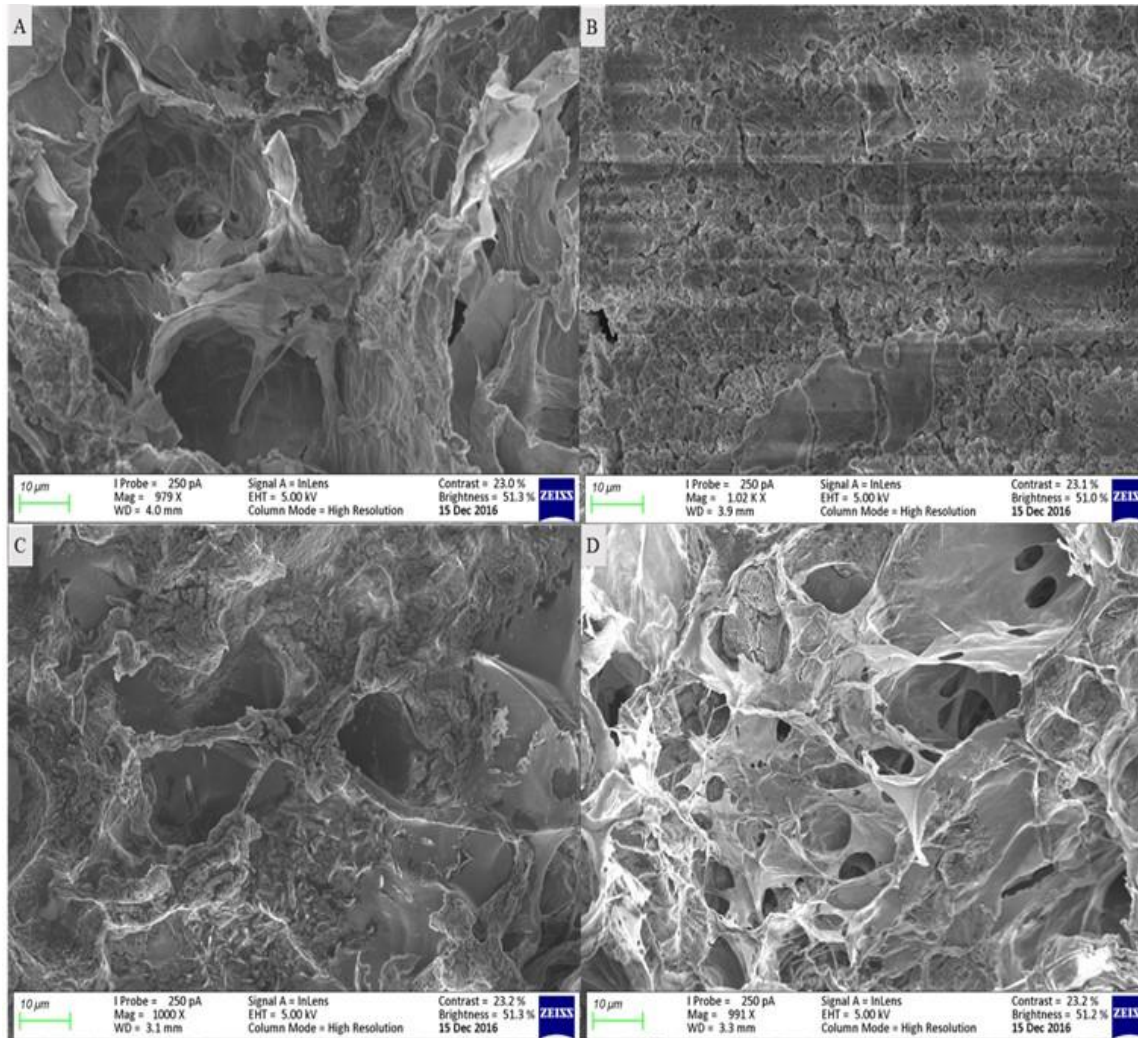


Figure B. 4: SEM images of MCC loaded samples

10 Appendix C

Confocal microscopy images

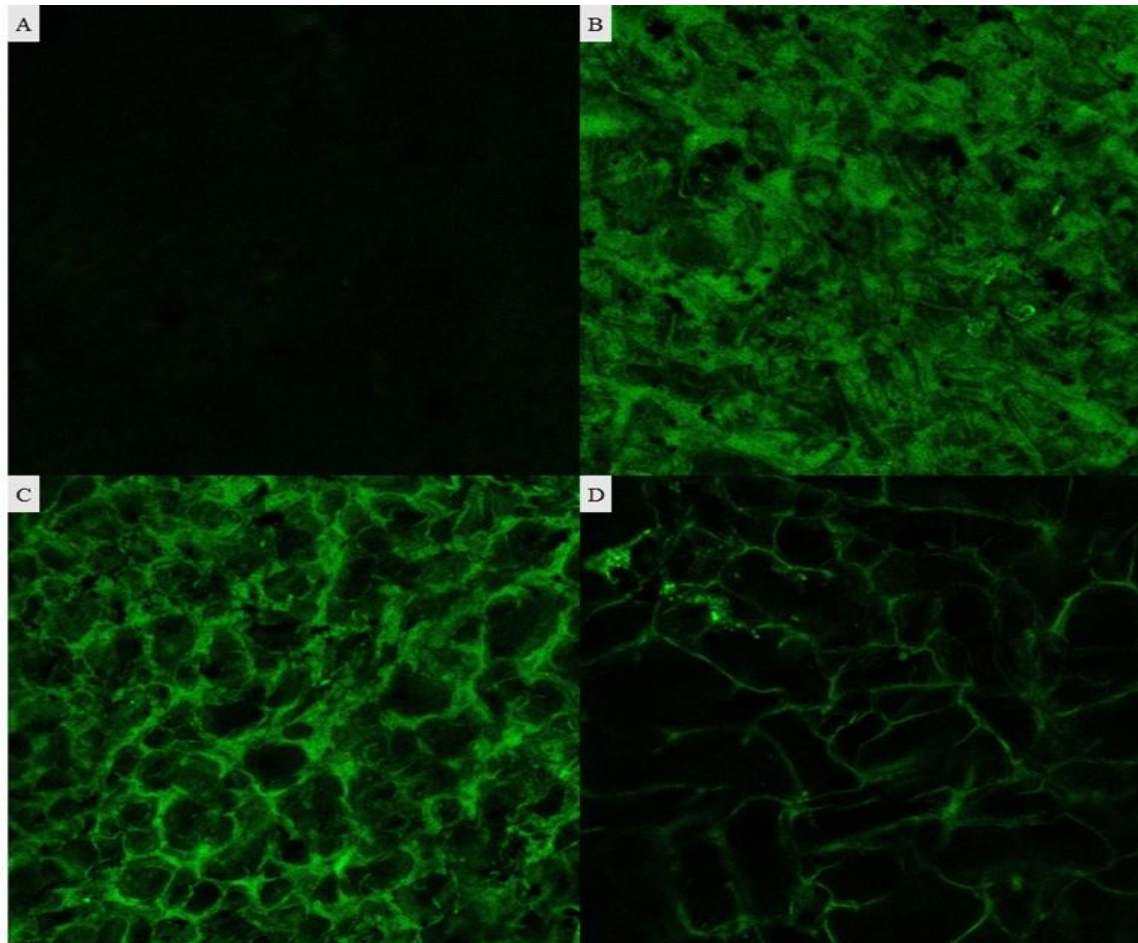


Figure C. 1: Confocal Microscopy images of A – chitosan sponges without fluorescent MCC; B – uncrosslinked sample with fluorescent MCC; C – genipin crosslinked sample with fluorescent MCC; and D – TA crosslinked sample with fluorescent MCC

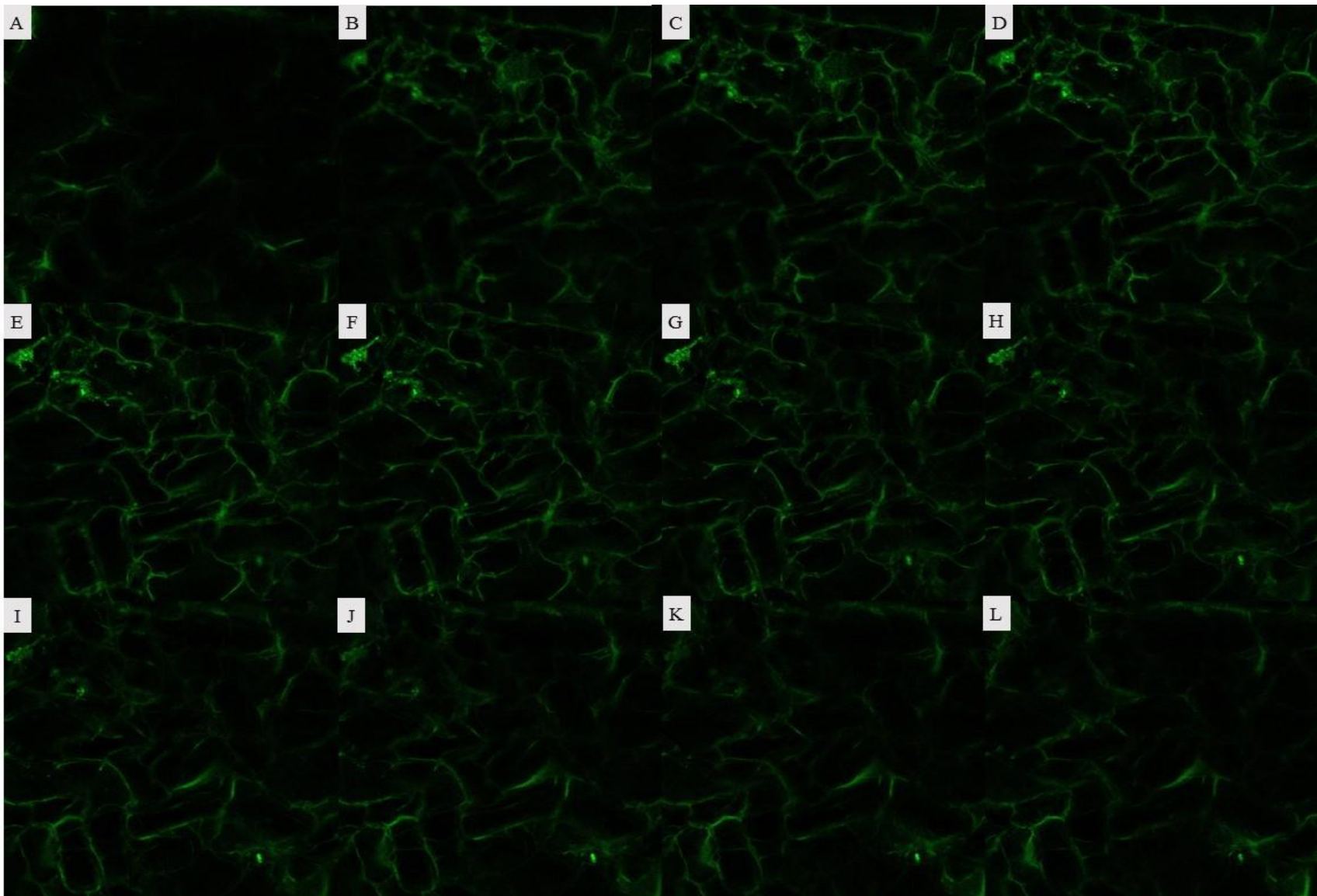


Figure C. 2: Confocal microscopy images showing the depth profile of fluorescent MCC loaded TA crosslinked chitosan sponges

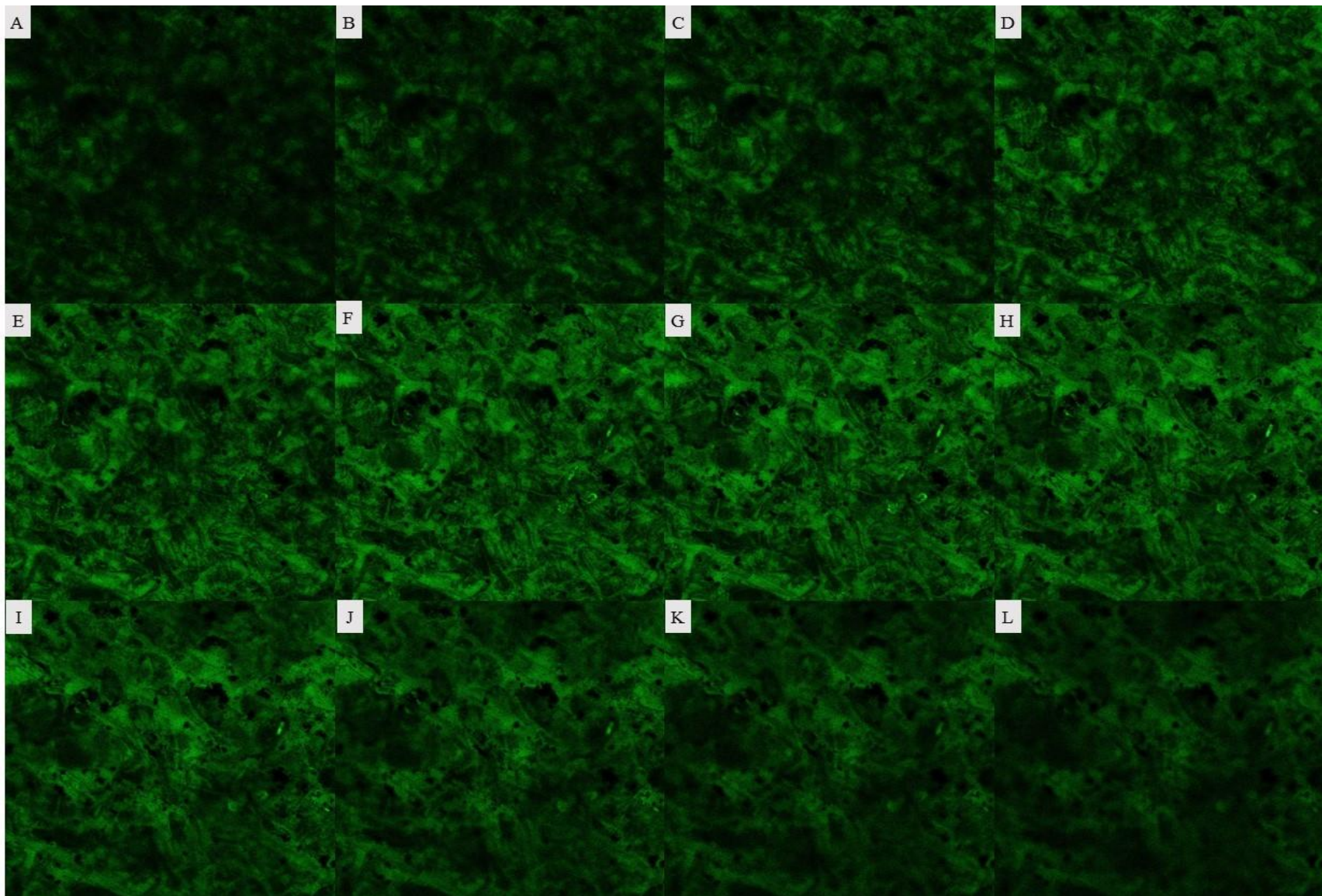


Figure C. 3: Confocal microscopy images showing the depth profile of MCC loaded uncrosslinked chitosan sponges

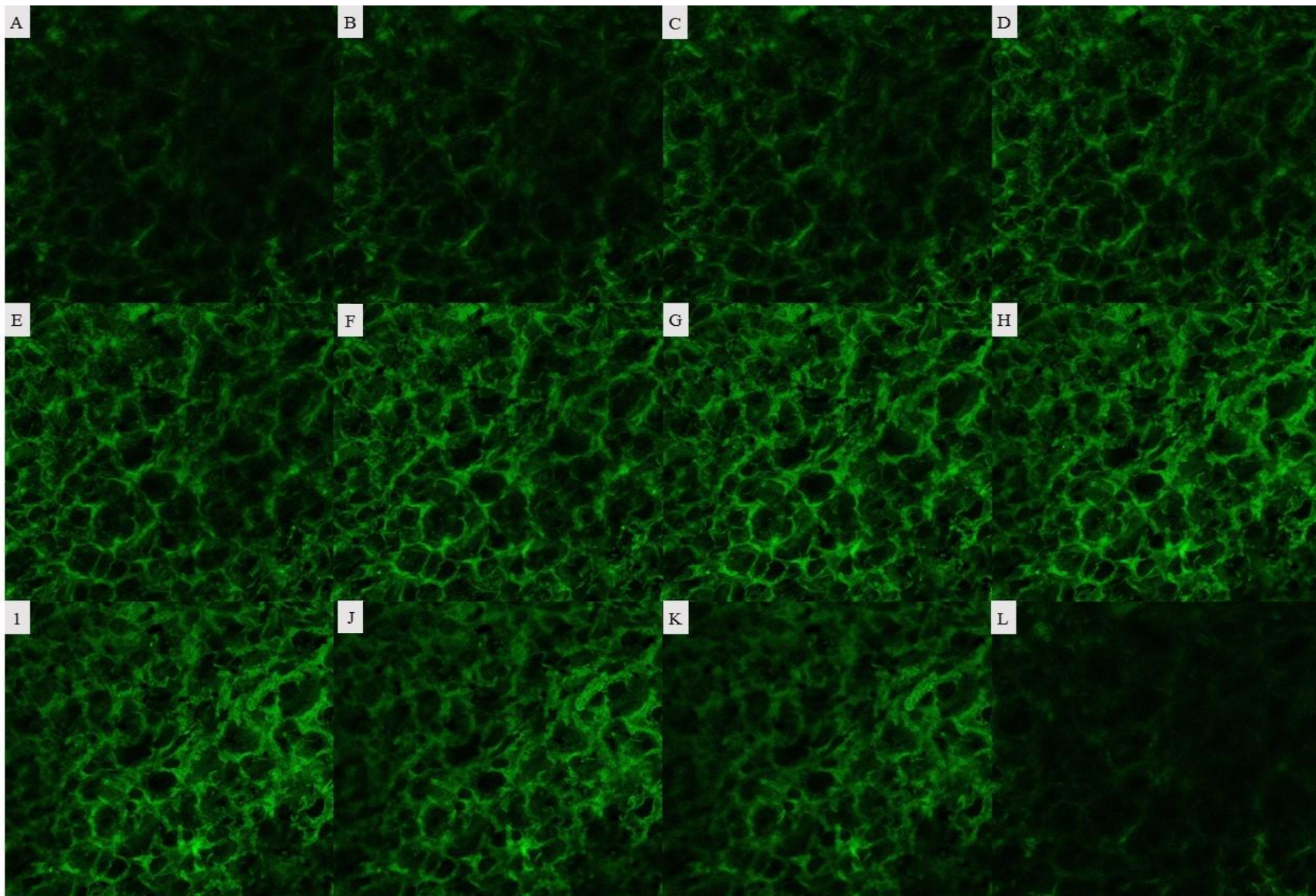


Figure C. 4: Confocal microscopy images showing the depth profile of genipin crosslinked sample loaded with fluorescent MCC

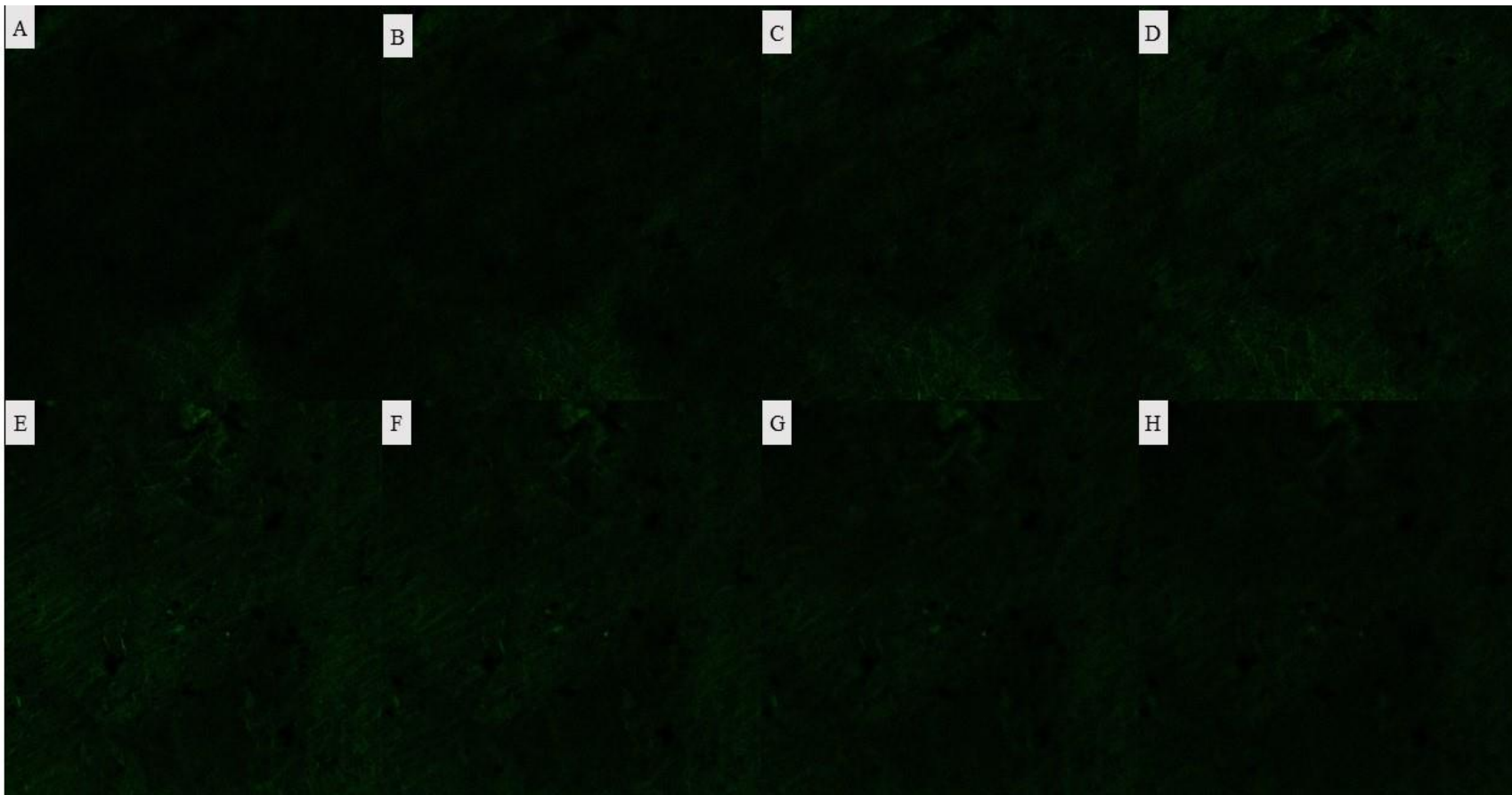


Figure C. 5: Confocal microscopy images showing the depth profile of chitosan samples without labelled MCC

11 Appendix D

Absorbance results

The following table comprises of all the results used in the calculation for the absorbance as well as the average and standard deviation for these results

Table D 1: Absorbance results

Sample	Test 1			Test 2			Test 3			Average absorbance	Standard error
	Dry weight	Wet weight	Absorbance	Dry weight	Wet weight	Absorbance	Dry weight	Wet weight	Absorbance		
Neat	101.7	595.0	485.1	100.2	590.8	489.6	101.1	603.1	496.5	490.4	5.78
Chi/MCC	100.1	622.7	522.1	100.9	637.2	531.5	101.1	654.3	547.2	533.6	12.68
Gen/MCC	100.2	430.1	329.9	100.0	456.0	356.0	99.8	434.7	334.9	340.2	13.84
TA/MCC	100.2	715.7	615.5	100.6	682.7	582.1	100.3	681.5	581.2	593.0	19.54
TA 20	97.2	564.6	480.9	99.1	572.8	478.0	100.8	551.3	446.9	468.6	18.82
TA 40	101.8	573.4	463.3	100.5	577.1	474.2	101.2	593.5	486.5	474.7	11.61
TA 50	100.9	704.5	598.2	100.1	699.8	599.1	101.5	711.5	601.0	599.4	1.41
TA 80	101.3	717.9	608.7	101.2	722.9	614.3	100.0	723.9	623.9	615.6	7.69
TA 125	100.5	589.9	487.0	101.1	577.0	470.7	100.1	587.1	486.5	481.4	9.25
TA 200	101.3	782.4	672.4	100.7	790.3	684.8	100.2	788.8	687.2	681.5	7.98
Gen 5mg	100.2	357.8	257.1	101.2	364.4	260.1	100.2	333.9	233.2	250.1	14.71
Gen 7.5mg	99.9	400.5	300.9	99.7	411.5	312.7	100.8	410.1	306.8	306.8	5.92
Gen 10mg	103.1	700.1	579.0	100.1	679.1	578.4	99.5	680.2	583.6	580.4	2.84

Table D 2: Mechanical properties results

Sample description	Test 1			Test 2			Test 3			Average strain %	Standard deviation
	Initial (cm)	Final (cm)	Strain %	Initial (cm)	Final (cm)	Strain %	Initial (cm)	Final (cm)	Strain %		
Neat	1	0.59	59	1	0.65	65	1	0.65	65	63.0	3.46
Gen 1mg	1	0.60	60	1	0.64	64	1	0.72	72	65.3	6.11
gen 3mg	1	0.74	74	1	0.70	70	1	0.77	77	73.7	3.51
gen 5mg	1	0.85	85	1	0.88	88	1	0.77	77	83.3	5.69
gen 7.5mg	1	0.87	87	1	0.84	84	1	0.86	86	85.7	1.53
gen 10mg	1	0.92	92	1	0.85	85	1	0.9	90	89.0	3.61
glut	1	0.99	99	1	0.95	95	1	0.9	90	94.7	4.51
Neat	1	0.62	62	1	0.65	65	1	0.6	60	62.3	2.52
TA20	1	0.70	70	1	0.74	74	1	0.69	69	71.0	2.65
TA40	1	0.82	82	1	0.72	72	1	0.73	73	75.7	5.51
TA50	1	0.82	82	1	0.75	75	1	0.77	77	78.0	3.61
TA60	1	0.88	88	1	0.80	80	1	0.83	83	83.7	4.04
TA80	1	0.85	85	1	0.84	84	1	0.88	88	85.7	2.08
glut	1	0.99	99	1	0.95	95	1	0.9	90	94.7	4.51

12 Appendix E

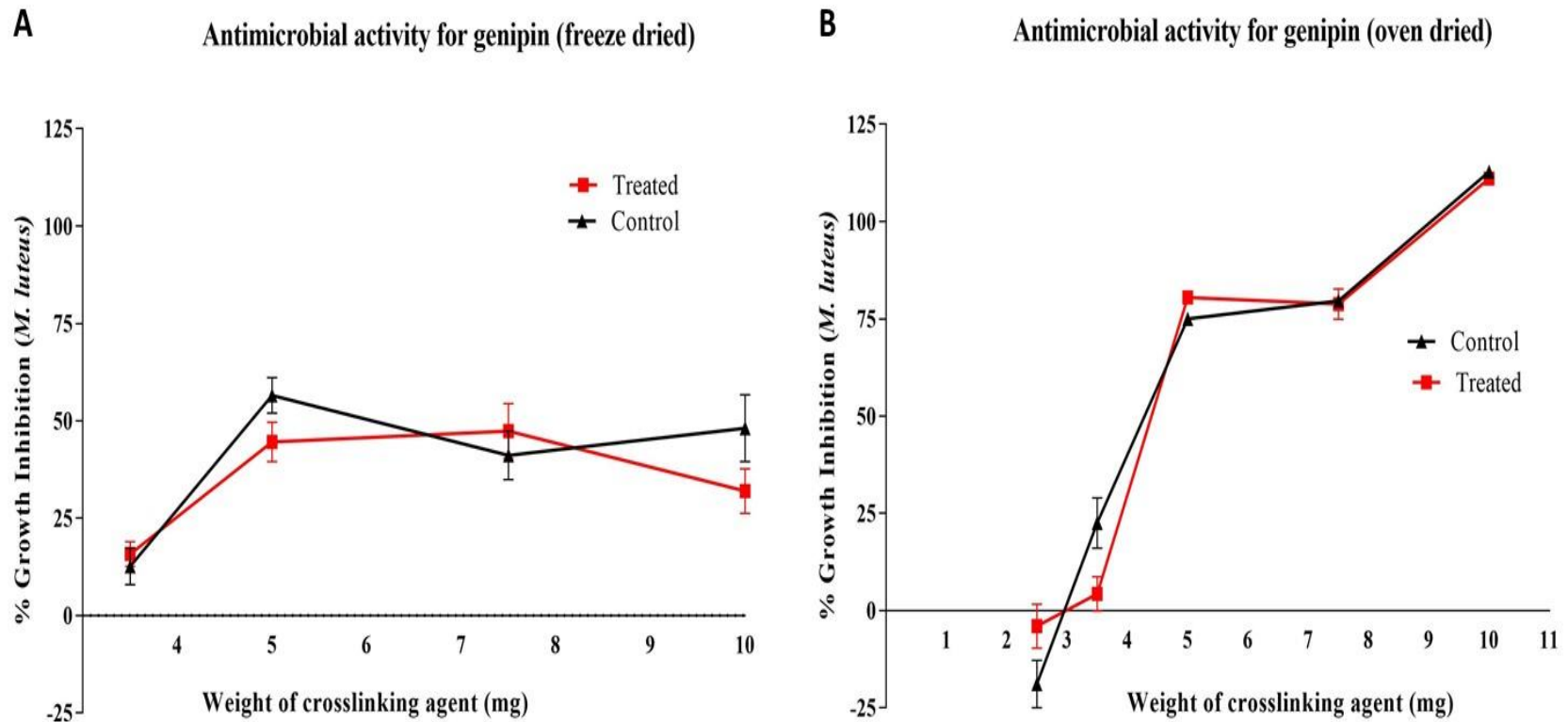


Figure E. 1: Comparison of the antimicrobial properties for the genipin crosslinked samples with A) the freeze – dried samples and B) the oven dried samples

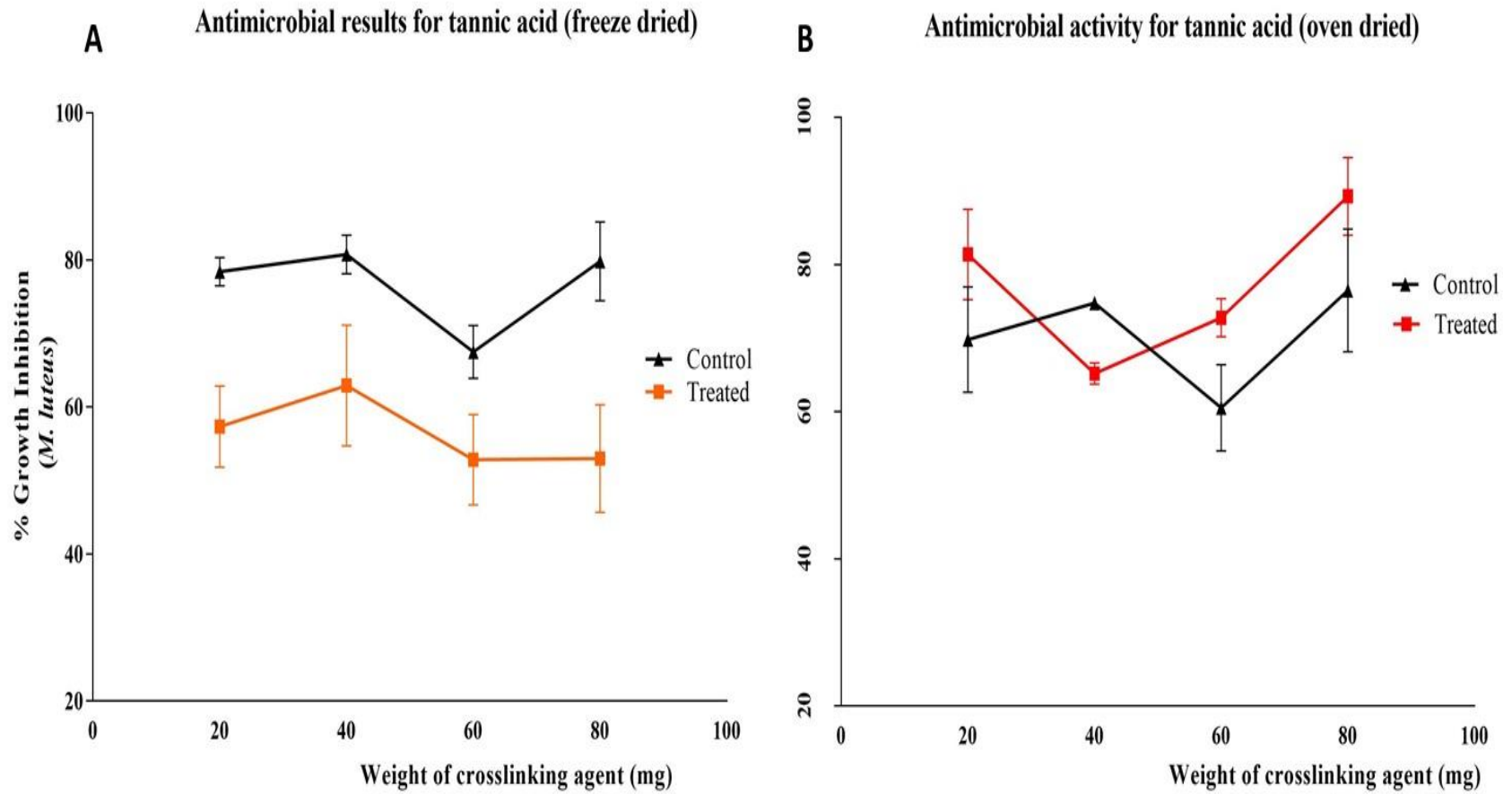


Figure E. 2: Comparison of the antimicrobial properties for the TA crosslinked samples with A) the freeze – dried samples and B) the oven dried samples.